

PARAMETRIC AND OPTIMAL DESIGN OF MODULAR MACHINE TOOLS

A Dissertation

Presented to

The Faculty of the Graduate School

University of Missouri – Columbia

In Partial Fulfillment

Of the Requirements for the Degree

Doctor of Philosophy

By

Donald Harby

Dr. Yuyi Lin, Dissertation Supervisor

December 2007

The undersigned, appointed by the dean of the Graduate School, have examined the dissertation entitled

**PARAMETRIC AND OPTIMAL DESIGN OF MODULAR MACHINE
TOOLS**

presented by Donald Harby,

a candidate for the degree of doctor of philosophy,

and hereby certify that, in their opinion, it is worthy of acceptance.

Professor Yuyi Lin

Professor Douglas Smith

Professor Robert Winholtz

Professor A. Sherif El-Gizawy

Professor Luis Occena

ACKNOWLEDGMENTS

The author is deeply indebted to his advisor, Dr. Yuyi Lin, for his invaluable direction and assistance. He further extends many thanks to the members of his doctoral committee, Dr. Douglas Smith, Dr. Sherif El-Gizawy, Dr. Robert Winholtz, and Dr. Luis Occena, for their time and effort in reading the manuscript and their many helpful suggestions.

The author would also like to express his appreciation to Dr. Douglas Smith, for the GAANN fellowship, without this support this project would not have been possible. The author would also like to express his appreciation to Dr. Robert Kallenbach for the use of the computer hardware and software and his valuable input on the topic of Neural Networks.

Finally and most importantly, the author wishes to acknowledge the support and encouragement of my parents, as well as my wife and children, Denee, Weston, and Wyatt, for their loving support and personal sacrifices. The author would like to dedicate this work to them.

TABLE OF CONTENTS

LIST OF FIGURES	v
LIST OF TABLES	viii
CHAPTER 1 INTRODUCTION	1
1.1 Background, Motivation and Purpose	1
1.2 Literature Review	4
1.2.1 Discrete Optimization	4
1.2.2 Heuristic Discrete Optimization Methods in Mechanical Structures.....	6
1.2.3 Particle Swarm Optimization	8
1.2.4 Surrogate Modeling	10
1.2.5 Structural Optimization	12
1.3 Objective	15
CHAPTER 2 THEORETICAL BACKGROUND.....	17
2.1 Finite Element Analysis.....	17
2.2 High-Speed FEA Approximation	26
2.3 Basic NN Structure	27
2.4 NN Test.....	33
2.6 NN training.....	45

2.7 General Comments and Results from NN test.....	51
2.7 Optimization Algorithms	52
2.8 Branch and Bound Discrete Optimization	54
2.9 Hybrid Continuous Optimization.....	61
CHAPTER 3 DISCREET OPTIMIZATION OF MMT STRUCTURES	66
3.1 Application of DSO, FEA, and NN.....	66
3.2 Traditional Topology Optimization.....	74
3.3 Large Scale MMT Base Optimization.....	83
CHAPTER 4 CONCLUSTION AND FUTURE WORK	87
4.1 Conclusion	87
4.2 Future Research	88
REFERENCES	90
APPENDIX	98
Appendix A: MATLAB FEA Functions.....	98
Appendix B: MATLAB Program Used to Test FEA Approximation	102
Appendix C: MATLAB Program For DSO of Typical MMT Base Side.....	116
Appendix D: MATLAB Program – Material Distribution Topology Optimization	131
Appendix E: MATLAB Program PSO of MMT Base 3D	136
Appendix F: MATLAB Program Used to Generate AutoLISP Program.....	149
Appendix G: Sample AutoLISP Code Generated from MATLAB	151
VITA	157

LIST OF FIGURES

Figure 1 Typical MMT structure (ASME B5.43M)	2
Figure 2. Typical grounded structure	14
Figure 3. Standard steel S and C profiles	15
Figure 4. General Beam	18
Figure 5.	20
(a) The free-body diagram	20
(b) the first element.....	20
Figure 6. A typical neuron.....	28
Figure 7. Transfer functions.....	29
Figure 8. A typical 2 layer feed forward neural network.....	30
Figure 9. Neural network training flowchart	31
Figure 10. Typical radial bias neuron.....	32
Figure 11. Test cantilever beam	33
Figure 12. Simple beam nodal deflection.	35
Figure 13. Modified simple beam nodal deflection.....	36
Figure 14. NN training with no previous weights and biases.	37
Figure 15. Training using previous weights and biases.	38
Figure 16 Side of typical MMT base structure	39
Figure 17. Training time with no previous weights and biases.....	41
Figure 18. Modified structure topography	42
Figure 19. Time to retrain NN	44

Figure 20. Training history for traingda	47
Figure 21. Training history for trainrp	48
Figure 22. Training history for trainscg	49
Figure 23. Training history for trainlm	50
Figure 24. Structural Bracket Example	55
Figure 25. Branch and Bound Tree for the Structural Bracket Example	57
Figure 26. Tree for typical MMT base side	60
Figure 27. Branch and bound flowchart for MMT base side	60
Figure 28. Typical topology and cross section	61
Figure 29. Particle swarm optimizer flowchart	65
Figure 30. Parallel NN training and branch and bound	69
Figure 31. Optimal topology for first load condition	70
Figure 32. Optimal design for second load location	71
Figure 33. Optimal design for third load location	72
Figure 34. Optimal design for fourth load location	73
Figure 35. Optimal topology using material density method	74
Figure 36. Optimal topology using material distrubution method	79
Figure 37. Discrete optimization using NN with lateral load	81
Figure 38. Discrete optimization using the material density method and 25% volume	82
Figure 39. Discrete optimization using the material density method and 30% volume	82

Figure 40. Discrete optimization using the material density method and 40% volume.....	82
Figure 41. Discrete optimization using the material density method and 50% volume.....	83
Figure 42. The optimal topology with applied loads.....	85
Figure 43. Program generated 3D model	86

LIST OF TABLES

Table 1. Standard steel cross sections.....	14
Table 2. Simple cantilever beam example displacements and CPU times	34
Table 3. Modified simple cantilever beam example displacements and CPU times	36
Table 4. Nodal displacement and CPU time.....	40
Table 5. Standard steel shapes	40
Table 6. Displacements and CPU times for structure with new topology	43
Table 7. Standard steel shapes	43
Table 8. Optimization results for first load condition.....	70
Table 9. Optimization results for second load condition	72
Table 10. Optimization results for third load condition	72
Table 11. Optimization results for forth load condition.....	73
Table 12. Element sections and CPU times for 3D MMT base	84

CHAPTER 1

INTRODUCTION

1.1 Background, Motivation and Purpose

Current manufacturing enterprises are faced with more competition than ever. To survive and flourish in the global market manufacturers are constantly looking for ways to increase production rate and lower cost. Machine tools are used in many modern manufacturing processes. Design and selection of machine tools has a great impact on the productivity and cost of many manufacturing processes. During the past several decades a significant amount of research has been conducted in the area of machine tool design, with the goal to develop more efficient and lower cost tools for manufacturing.

Over the years machine tools designed for manufacturing have developed into two classes. The first is general purpose machine tools designed for a large range of operations. Examples of these are standard milling machines or lathes. The design and operation of these standard machines is a very mature subject and little research is left to be done. The other class of machine tools are those designed for a very specific part of a process. These machine tools are sometimes referred to as dedicated machine tools. These types of machine tools are usually used in high speed or high volume production. The machining of automotive engine blocks is an example. Many interesting areas of these specific machine tools can be investigated and improved. This approach is

generally very effective; however, it is not without disadvantages. If the product design is changed even slightly, the machine tool may have to be scrapped and a new machine tool designed and built. Another problem is that the lead-time to design and build such a machine can be very long. An approach to overcome these problems is to produce a re-configurable or modular machine tool (MMT). Using this approach custom machine tools could be designed and built quickly from existing modular components (Figure 1).

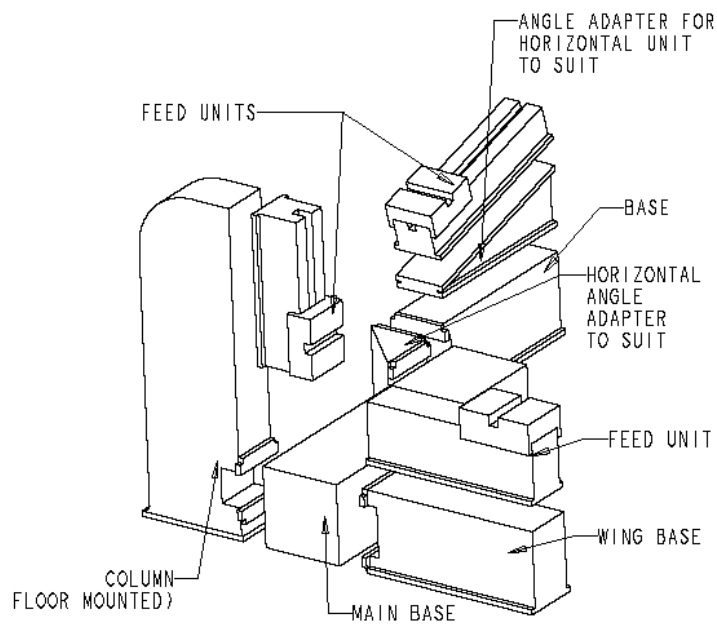


Figure 1. Typical MMT structure (ASME B5.43M)

There already exist standards for MMT components (ASME B.43M)[1]. Typically, these MMT components are made of large steel castings or fabrications. Stress, strain, deflection, and rigidity are not an issue with these components so very little design effort is put into MMT components. A better approach would be to

fabricate these components from stock pieces of standard steel shapes such as standard steel C or L cross sections. Many standard MMT components could be quickly assembled from a library of stock components. Due to the rapidly increasing cost of steel in recent years it would cost much less than cast components. Also, a significant reduction in cost could be realized by combining modern optimization and analysis techniques. An automated method of selecting elements and designing MMT could be developed. The idea of using an inventory of standard steel cross-section components coupled with optimization and analysis leads to a very interesting discrete structural optimization (DSO) problem.

With the fast advances of computer technology, much progress has been made in DSO research. However, the roots of DSO come from the early non-linear integer programming research initiatives of the US military, specifically, the work of the Rand Corporation in the 1950's and 60's[2]. The conclusion of most of this early work on integer and discrete optimization was that the problems required exponential-time solutions or 2^n operations to solve [3]. This led to the idea that only small scale problems could be solved. With the rapid increase in computer speed many new approaches to DSO have been proposed. Some of these areas of research include partial enumeration, genetic algorithms (GA) and simulated annealing (SA) [4, 5, 6, 7, 8, 9, and 10]. Many of these areas of DSO are still very immature and should be areas of current research [11]. Many of these techniques have less than exponential-time solutions.

Even if the difficulties of discrete optimization are overcome, many other areas of DSO, as applied to MMT, need further investigation. Most of the current research effort has been directed to truss structures or structures with pinned joints. The stress, strain or displacement constraints in these types of models can easily be solved using analytical methods. This is fine for most civil engineering problems, i.e., bridges or buildings; however, for MMT this needs to be extended to frame and 3D solid components. When the model is extended to frame or 3D solid components, it is the current accepted practice to use finite element analysis or methods (FEA or FEM). The use of FEA with DSO has one major disadvantage in that they are often computationally costly. Because of the large number of FEA calls in DSO, one of the most important potential areas of research is finding faster FEA algorithms or alternatives to FEA [11].

1.2 Literature Review

A review of the literature pertaining to discrete structural optimization as related to this study can be divided into five sections; discrete optimization in general, heuristic discrete optimization methods in mechanical structures, particle swarm optimization, surrogate modeling, and structural optimization.

1.2.1 Discrete Optimization

Discrete optimization has been an important area of research over the last few decades. A wide variety of algorithms have been developed and applied to

many areas of mathematics and engineering [12]. Even with extensive research an efficient and general method of discrete optimization seems difficult to obtain.

In the 1950's and early 1960's many methods were tested on discrete optimization problems. It was generally accepted that most methods except full enumeration failed to produce a global optimum. But, full enumeration was impractical to solve anything but trial problems [13]. Land and Doig used non-linear programming relaxation to determine bounds of a discrete problem. This first general method for integer programming problems was found to be too difficult to efficiently implement on computers [14]. Dakin then modified this method to be efficiently implemented on computers [15]. Algorithms of this type, those that obtain bounds from relaxation methods and then use the bounds to prune, are generally referred to as branch and bound algorithms. Little et al. was the first to use the branch and bound term when applying this type of algorithm to the traveling salesman problem [16]. Edmonds developed a general purpose branch and bound algorithm for discrete optimization and he proved it would solve discrete problems in polynomial time [17]. Most of this early research was focused on linear well behaved convex problems. Linear programming was the most accepted relaxation method. However, some later work showed that the branch and bound method could be extended to non-linear systems by using non-linear relaxation methods [18]. Over the years other methods of discrete optimization have been developed. Many of these methods rely on random or heuristic searches. Roth developed a method of combining random and partial

searches [19]. Initial random starting points are generated, then partial searches were used to find the local optimum. The process is then repeated in an attempt to find a global optimum. This method was tested successfully on large problems with modest computational cost. A method that used common features or details of many discrete optimization problems as a library of optimization methods was developed by Goldstein and Lesk [20]. This method was adapted to many problems, however, it was not as good as some heuristic methods. In a general review of numerical optimization methods More et.al. found the bulk of the research prior to 1979 had been based on relaxation methods of linear programming [21]. They also concluded there was room for further research in discrete optimization, especially using heuristic methods. Most of the previous research on discrete optimization was based on branch and bound or random search methods and had been oriented toward special problems and very few general purpose methods existed [22]. In a recent survey of discrete optimization Shcherbina concluded that there is doubt that general discrete optimization problems could be solved efficiently and that the branch and bound method may be the most practical [23].

1.2.2 Heuristic Discrete Optimization Methods in Mechanical Structures

Over the years many methods have been developed to solve discrete optimization problems in mechanical structures. One of the most popular approaches in recent years has been the use of heuristic methods. These

methods include not only genetic algorithms (GA) and simulated annealing (SA) but a few lesser known approaches.

The comparison of GA and SA to full enumeration and branch and bound has been studied by several researchers. Balling used a SA method to optimize steel frames using a set of standard discrete shapes [24]. This research used realistic three dimensional test problems and the results were compared to a modified linear branch and bound method. The results using the SA method were shown to be similar to the branch and bound method. Kocer and Arora compared full enumeration, SA, and GA on standard discrete prefabricated steel sections [25]. The cross-section shape and steel grades were considered as discrete variables. In this research the GA method found the optimal solution in all cases and was the most efficient in terms of CPU time. Huang and Arora compared GA, SA, and full enumeration and concluded, by the use of examples, that GA and SA could be used to find the global optima [25].

Although the GA and SA methods have received much of attention in recent years with respect to discrete optimization they have a few areas with unanswered questions. For instance, will they always produce global optima and can they be implemented and tuned to solve discrete structural optimization problems? Using a practical structural system and a GA based method Rajeev and Krishnamoorthy efficiently solved a discrete variable problem with constraints [26]. They showed that even though the GA is not well suited for constrained problems a penalty-based transformation can be implemented. They

also showed the GA method is suitable for a parallel computing environment. Near optimal solutions in reasonable computing times were obtained on large design space layout and sizing problems of steel roof trusses using a GA by Koumousis et al. [27]. They also reported that no clear rules exist for tuning of the GA parameters and the estimate of the parameters is delicate. Using the uniform building code as constraints Camp et al. developed a GA based method for optimizing two-dimensional steel frame structures [28]. The method was tested on 30 designs. The method always produced structures satisfying the code standards while minimizing the weight but the solution was not guaranteed to be global. Lu and Kota successfully applied a GA method to a mixed discrete topology and continuous sizing problem [29]. A new heuristic method based loosely on the harmonics of music is the harmony search (HS) method. This method is simple and mathematically less complex than the GA. Its convergence capability was shown to be better than GA on discrete sizing variable problems [30]. A common conclusion in the literature with respect to GA and SA is that they both require considerable user insight and adjustment to the parameters to get reasonable results [10].

1.2.3 Particle Swarm Optimization

Particle swarm optimization (PSO) is a new heuristic based method that has generated much recent interest. It is based on the self organizing behavior of a group with no leaders such as a flock of birds or a school of fish [31 and 32].

These groups of individuals have no knowledge of the behavior of the entire group (global behavior). They only have knowledge about their local environment, but they can converge and move as a group based on local individual information. They are capable of complex behavior such as flocking, homing, exploration, and herding [33, 34, and 35]. Bird flocking [35] and fish schooling [36] behavior are two of the most studied areas. When applying these methods to real world optimization problems an effective particle initialization scheme must be used. Several methods of initiation are presented in the literature [37, 38, 39, 40, and 41]. These methods are used mainly to ensure that the search space is uniformly covered. PSO and evolutionary algorithms (EA) such as GA and SA have many similarities, however, some literature suggests they should be treated separately [32]. Both methods use a stochastic search process. PSO does not use the concept of survival of the fittest. Unfit individuals in the PSO do not die. Also, unlike GA and SA, PSO is not easy to implement for discrete optimization problems.

The concept of PSO was first introduced by Kennedy and Eberhart [42]. Using a PSO based on swarms or flocks, they optimized non-linear functions. Kennedy and Eberhart also compared PSO to GA for non-linear function optimization, neural network learning, and robot task learning [43]. They showed that PSO is a very simple concept and it can be implemented with just a few lines of code. Their implementation only used primitive math operations and was also computationally inexpensive. Song and Gu studied the ability of PSO to find

global solutions [44]. Even though PSO is effective, they found there is no mathematical theory to support that it is a global optimizer. Langdon and Poli compared and contrasted PSO with a non-standard Newton-raphson based gradient method [45]. They found that a theoretical analysis of PSO is very difficult and that we do not have a good mathematical understanding of why PSO performs better or worse on a problem of a given type. Several researchers found PSO to perform better in early iterations but that it is not competitive with other methods when the number of iterations is increased [44, 45, and 47].

In recent years the concept of PSO has been applied to various engineering problems. Specifically, it has been applied to structural design optimization problems. Ant colony optimization (ACO), a type of PSO, was tested on steel frame optimization problems with discrete variables by Camp et al. [48]. In this research they compared ACO to GA and they found it more effective and less affected by poor initial solutions. Perez and Behdinan tested PSO on several well-known structural test problems [49]. The PSO method found better results on these test problems than any of the other optimization algorithms used in previous research.

1.2.4 Surrogate Modeling

Structural optimization, especially discrete structural optimization of practical problems, requires low computational cost and accuracy for all of the processes. By far the most computationally costly process is the FEA. The FEA

for large-scale three-dimensional problems and eigenfrequency problems becomes difficult to optimize practically.

The current literature suggests approximation methods for such large scale optimization models. Several different methods are reported in this literature. These include Response Surface Modeling (RSM), Radial Bias, Neural Network (NN), and Kriging [50-54, and 80].

The kriging model is one of the most popular methods. This method was originally developed for the mining industry to help model the location of minerals and gems. Sakata et al. reported good results using kriging methods on large-scale eigenfrequency problems [51]. The results were comparable with those from a NN method. One of the most attractive aspects of kriging is that it has the ability to estimate outputs in areas of the design space that have not been tested with the FEA [52]. In other words, it is effective at extrapolation as well as interpolation. The one draw back to kriging is that fitting the data and developing the model is complex and costly, because it requires an optimization routine. [50 and 52].

Low order polynomial approximations, also known as RSM, are often used because they are easy to implement and software is readily available [50]. RMS is often used when experimental data sets are available or when a combination of experimental and numerical data sets is employed [53]. In [50] it was concluded that radial bias and kriging methods performed better and were more accurate on large problems compared to some of the other methods.

In this research radial bias and NN were considered to be similar. This is because they are both modeled after biological systems and because they are in the same Matlab toolbox and use the same Matlab functions. Most of the literature found NN to have some of the best performance and most accurate results [50]. The NN method was even used as a benchmark for other methods [51]. The only drawbacks are the computational cost to train the network [50, 51, 54, and 55] and the necessity of a skilled operator to setup the network [55]. These drawbacks are easily overcome by using the latest Matlab NN toolbox. The toolbox makes it easy to setup and train complex NN's and the speed and accuracy greatly outweigh the cost of training the network.

1.2.5 Structural Optimization

Over the years three broad approaches to structural topology optimization have evolved based on grounded structures [11]. One is based on material homogenization [56] and one on material density [57]. The homogenization and material density approaches have been the subject of research in recent years and have few areas left to investigate when applied to DSO [56, 58, and 59]. These two techniques rely on the design space containing a fine mesh of elements. Voids are created or elements removed through the optimization process. A discrete structure will emerge from the optimization process. However, it may be difficult to create a structure of standard set of structural members using this process. Also, the structure created may not be optimal [11].

These two methods are very well suited to cast, molded, or formed parts that may take on any size or shape.

These methods generally use structural compliance as a constraint. Cheng and Jiang showed compliance is generally continuous over the feasible design domain in truss or frame topology problems and it should be considered as a global constraint. They also showed that stress and buckling constraints are discontinuous and are local (element) constraints for the same problems [82]. Using the idea of global and local constraints Cheng showed that stress or buckling constraint truss or frame topology problems are discrete and the solutions are generally different than compliance constraint problems [83].

The third approach to structural optimization is the grounded structure method. In this method a structure is made that includes all possible structural components (Figure 2). It should be noted that for some discrete optimization problems Figure 2 would not be considered fully grounded. This is because all possible nodes are not connected with members. In this example only connecting members of two discrete lengths are considered. Using these two lengths all possible combinations are shown in the figure. In this entire study a library of standard length members were considered.

The literature on discrete structural optimization generally refers to this as an incomplete grounded structure as opposed to a complete grounded structure where every possible node is connected [82 and 83].

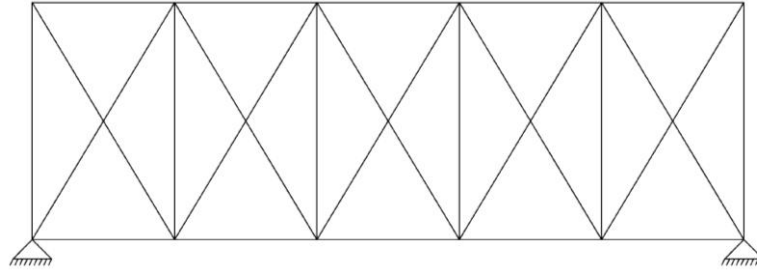


Figure 2. Typical grounded structure

Members are removed or added through the optimization process [9 and 11]. One problem is as the size of the structure increases the number of possible combinations increases exponentially. Many discrete optimization approaches have been proposed to solve these types of problems such as branch and bound, penalty function, Lagrange relaxation, sequential linearization, integer programming, SA, and GA [10] and [56]. Many of these techniques require the objective function to be monotonic. The design variables need to be continuous. When using standard steel cross sections that is rarely the case. For example, Table 1 and Figure 3 show standard S and C steel shapes:

Table 1. Standard steel cross sections

Area (sq. in.)	Moment of Inertia	Shape
1.67	2.52	S3x5.7
2.21	2.93	S3x7.5
1.47	1.85	C3x5
1.76	2.07	C3x6
1.59	3.85	C4x5.4

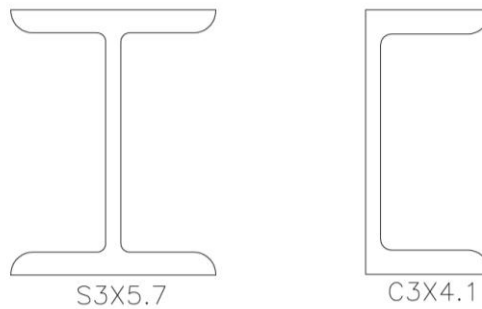


Figure 3. Standard steel S and C profiles

There is no consistent relationship between cross sectional area and moment of inertia, as one increases the other may decrease or increase. Some of the techniques applicable to discrete design variables, such as GA and SA, may produce a feasible solution, but the search on the discrete subspace mixed with continuous design variable (e.g., the length of each structural member) will make the search for a global solution slow and tedious.

1.3 Objective

In this research DSO methodologies were applied to MMT systems. Sizing and topology discrete numerical optimization is combined with FEA and high-speed FEA approximations to extend the size and type of MMT design problems that can be solved.

For this study optimal topology of a discrete structure, such as a truss or frame, is the optimal connection of elements between a set of given fixed nodes, including loading and support nodes. Also, in this study optimal structural sizing

is the optimization of the cross-sectional area and shape of the individual connection members. The structure's material, mode position, loads, and load positions were assumed to be given.

The specific objectives of this research were:

1. Develop an effective method of high-speed FEA approximation
2. Develop a discrete algorithm that will simultaneously optimize size, shape, and topology of MMT components
3. Compare the results, in terms of computing speed and accuracy, with current design optimization methods

CHAPTER 2

THEORETICAL BACKGROUND

2.1 Finite Element Analysis

FEA is currently one of the most accepted methods for finding the displacement, stress, strain, or natural frequency of complex structures. There are many commercially available FEA software packages. However, there are several advantages to developing a simple FEA routine. First, most commercial packages are general purpose and have unnecessary overhead. This includes graphical interfaces and many types of general elements. This overhead has an effect on the computational speed, especially when applied to optimization problems that require repeated FEA calls. The second advantage is the cost. Many commercial FEA packages are expensive. Not only is the initial cost high but the developed code cannot be distributed. For example, the code could be included in a group of online tools for educational or industrial users [60, 61 and 62]. Finally, other properties that could be useful in the optimization process can be calculated inside the FEA routine such as gradient, Jacobian, or Hessian [57, 63 and 81].

In this research all of the MMT components are assumed to have rigid connections, such as welded or tightly bolted joints. Therefore, only beam type elements are needed in the FEA. The generalized beam is shown in Figure 4.

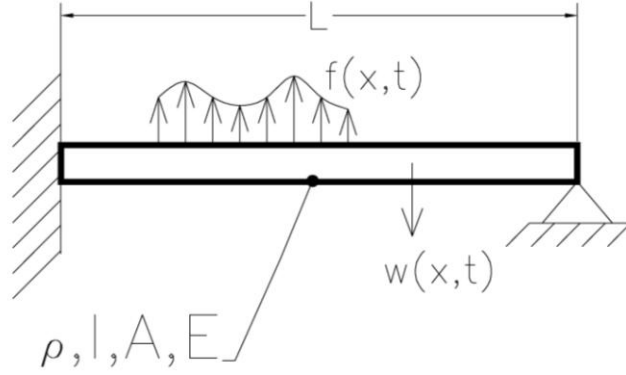


Figure 4. General Beam

The following uses an energy approach to set up the beam FEA element. The extended Hamilton's principle is:

$$\int_{t_1}^{t_2} (\delta T - \delta V + \delta W_{nc}) dt = 0 \quad (1)$$

where T is kinetic energy, V is strain energy and W_{nc} is the non-conservative work. Then the following are the variation of the kinetic energy, elastic energy, and non-conservative work for a beam element [64 and 81]:

The kinetic energy:

$$\begin{aligned} \int_{t_1}^{t_2} \delta T dt &= \int_{t_1}^{t_2} \delta \int_0^L \frac{1}{2} \rho A \dot{w}^2 dx dt = \int_{t_1}^{t_2} \int_0^L \rho A \dot{w} \delta \dot{w} dx dt \\ &= - \int_{t_1}^{t_2} \int_0^L \rho A \ddot{w} \delta w dx dt + \int_0^L \rho A \dot{w} \delta w \Big|_{t_1}^{t_2} dx \end{aligned} \quad (2)$$

Where t is the time, L is the beam length, ρ is the mass density, w is the transverse displacement, and A is the cross sectional area.

The elastic energy:

$$\begin{aligned}\int_{t_1}^{t_2} \delta V dt &= \delta \int_{t_1}^{t_2} \int_A \int_0^L \frac{1}{2} \sigma \epsilon dA dx dt = \delta \int_{t_1}^{t_2} \int_A \int_0^L \frac{1}{2} E \epsilon^2 dA dx dt \\ &= \delta \int_{t_1}^{t_2} \int_0^L \frac{1}{2} EI w''^2 dx dt = \int_{t_1}^{t_2} \int_0^L EI w'' \delta w'' dx dt\end{aligned}\quad (3)$$

Where E is Young's Modulus and I is the area moment of inertia.

The non-conservative work:

$$\int_{t_1}^{t_2} \delta W_{nc} dt = \int_{t_1}^{t_2} \int_0^L f \delta w dx dt \quad (4)$$

Where f is the transversely distributed external force.

Substituting equations 2, 3, and 4 into the Hamilton's extended equation (1) and integrating by parts gives the result:

$$\begin{aligned}\int_{t_1}^{t_2} \int_0^L \rho A \ddot{w} \delta w dx dt + \int_{t_1}^{t_2} \int_0^L EI w^{iv} \delta w dx dt \\ - \int_{t_1}^{t_2} EI w''' \delta w \Big|_0^L dt + \int_{t_1}^{t_2} EI w'' \delta w' \Big|_0^L dt = \int_{t_1}^{t_2} \int_0^L f \delta w dx dt\end{aligned}\quad (5)$$

Setting the coefficient of δw to zero yields the equation of motion:

$$\rho A \ddot{w} + EI w^{iv} = f \quad (6)$$

The boundary conditions have to specify: w or $EI w'''$; w' or $EI w''$ at $x = 0$ or L .

Figure 5(a) shows the free-body diagram of a cantilevered beam modeled using three two-node beam elements, where w_i and θ_i are the nodal

displacements and slopes of each node, l_i is the elemental length of the i th element, and $Q_1^{(1)}$ and $Q_2^{(1)}$ are the reaction force and moment acting on the first node. As shown in Figure 5(b), each element has four unknown nodal displacements. The displacement $w(x, t)$ within each element can be assumed to be:

$$w(x, t) = C_0 + C_1x + C_2x^2 + C_3x^3 \quad (7)$$

where x is a local coordinate with $0 \leq x \leq l_i$ for the i th element.

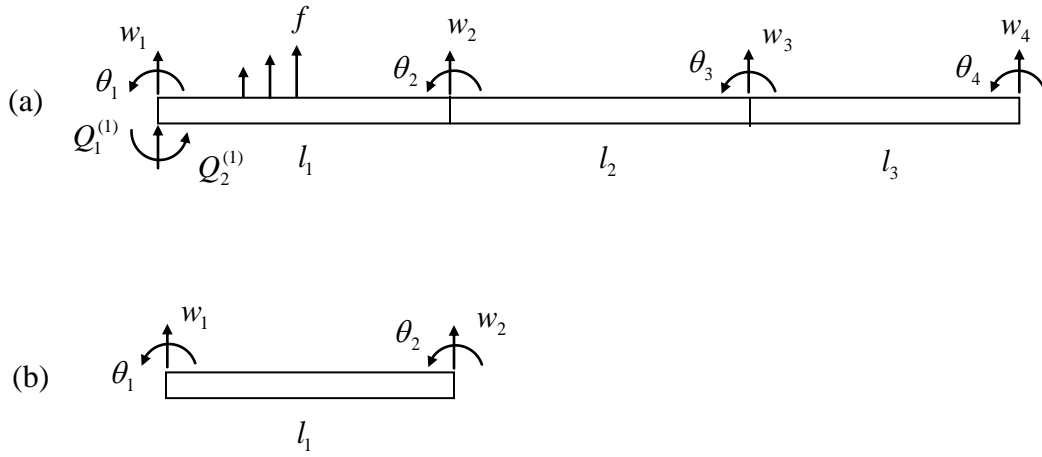


Figure 5. (a) The free-body diagram; (b) the first element.

For the first element:

$$w(0,t) = w_1 = C_0$$

$$w_x(0,t) = \theta_1 = C_1 \quad (8)$$

$$w(l,t) = w_2 = C_0 + C_1 l + C_2 l^2 + C_3 l^3$$

$$w_x(l,t) = \theta_2 = C_1 + 2C_2 l + 3C_3 l^2$$

Solving for C_i in terms of w_i and θ_i , and then substituting the results into equation (7) yields:

$$\begin{aligned} w(x,t) = & (1 - 3\frac{x^2}{l^2} + 2\frac{x^3}{l^3})w_1 + l(\frac{x}{l} - 2\frac{x^2}{l^2} + \frac{x^3}{l^3})\theta_1 \\ & + (3\frac{x^2}{l^2} - 2\frac{x^3}{l^3})w_2 + l(-\frac{x^2}{l^2} + \frac{x^3}{l^3})\theta_2 \end{aligned} \quad (9)$$

Equation (9) can be rewritten as:

$$\begin{aligned} w(x,t) = & N_1(x)w_1 + N_2(x)\theta_1 + N_3(x)w_2 + N_4(x)\theta_2 \\ = & \{w^{(1)}\}^T \{N\} = \{N\}^T \{w^{(1)}\}, \{w^{(1)}\} \equiv \{w_1 \quad \theta_1 \quad w_2 \quad \theta_2\}^T \end{aligned} \quad (10)$$

Where $N_i (i=1,2,3,4)$ are known as the shape functions (Hermite cubic or spline interpolation functions) given by:

$$\begin{aligned} N_1 = & 1 - 3\frac{x^2}{l^2} + 2\frac{x^3}{l^3}, \quad N_2 = l(\frac{x}{l} - 2\frac{x^2}{l^2} + \frac{x^3}{l^3}) \\ N_3 = & 3\frac{x^2}{l^2} - 2\frac{x^3}{l^3}, \quad N_4 = l(-\frac{x^2}{l^2} + \frac{x^3}{l^3}) \end{aligned} \quad (11)$$

It follows from equations (10) and (2) that:

$$\begin{aligned}
\int_{t_1}^{t_2} \delta T dt &= - \int_{t_1}^{t_2} \int_0^L \rho A \ddot{w} \delta w dx dt = - \int_{t_1}^{t_2} \left[\int_0^{l_1} \delta w \rho A \ddot{w} dx + \int_0^{l_2} \delta w \rho A \ddot{w} dx + \int_0^{l_3} \delta w \rho A \ddot{w} dx \right] dt \\
&= - \int_{t_1}^{t_2} \left[\int_0^{l_1} \{\delta w^{(1)}\}^T \{N\} \rho A \{N\}^T \{\ddot{w}^{(1)}\} dx \right] dt \\
&\quad - \int_{t_1}^{t_2} \left[\int_0^{l_2} \{\delta w^{(2)}\}^T \{N\} \rho A \{N\}^T \{\ddot{w}^{(2)}\} dx + \int_0^{l_3} \{\delta w^{(3)}\}^T \{N\} \rho A \{N\}^T \{\ddot{w}^{(3)}\} dx \right] dt \\
&= - \int_{t_1}^{t_2} \left[\{\delta w^{(1)}\}^T [m^{(1)}] \{\ddot{w}^{(1)}\} + \{\delta w^{(2)}\}^T [m^{(2)}] \{\ddot{w}^{(2)}\} + \{\delta w^{(3)}\}^T [m^{(3)}] \{\ddot{w}^{(3)}\} \right] dt
\end{aligned} \tag{12}$$

Where the elemental mass matrix is:

$$[m^{(i)}] \equiv \int_0^{l_i} \{N\} \rho A \{N\}^T dx, \quad i = 1, 2, 3 \tag{13}$$

If ρ and A are constants then:

$$[m^{(i)}] = \frac{\rho A l_i}{420} \begin{bmatrix} 156 & 22l_i & 54 & -13l_i \\ 22l_i & 4l_i^2 & 13l_i & -3l_i^2 \\ 54 & 13l_i & 156 & -22l_i \\ -13l_i & -3l_i^2 & -22l_i & 4l_i^2 \end{bmatrix} \tag{14}$$

The global (structural) mass matrix $[M]$ can be obtained by assembling the elemental mass matrices using the continuity of displacement and slope at each node as:

$$[M] = \begin{bmatrix} m_{11}^{(1)} & m_{12}^{(1)} & m_{13}^{(1)} & m_{14}^{(1)} & 0 & 0 & 0 & 0 \\ m_{21}^{(1)} & m_{22}^{(1)} & m_{23}^{(1)} & m_{24}^{(1)} & 0 & 0 & 0 & 0 \\ m_{31}^{(1)} & m_{32}^{(1)} & m_{33}^{(1)} + m_{11}^{(2)} & m_{34}^{(1)} + m_{12}^{(2)} & m_{13}^{(2)} & m_{14}^{(2)} & 0 & 0 \\ m_{41}^{(1)} & m_{42}^{(1)} & m_{43}^{(1)} + m_{21}^{(2)} & m_{44}^{(1)} + m_{22}^{(2)} & m_{23}^{(2)} & m_{24}^{(2)} & 0 & 0 \\ 0 & 0 & m_{31}^{(2)} & m_{32}^{(2)} & m_{33}^{(2)} + m_{11}^{(3)} & m_{34}^{(2)} + m_{12}^{(3)} & m_{13}^{(3)} & m_{14}^{(3)} \\ 0 & 0 & m_{41}^{(2)} & m_{42}^{(2)} & m_{43}^{(2)} + m_{21}^{(3)} & m_{44}^{(2)} + m_{22}^{(3)} & m_{23}^{(3)} & m_{24}^{(3)} \\ 0 & 0 & 0 & 0 & m_{31}^{(3)} & m_{32}^{(3)} & m_{33}^{(3)} & m_{34}^{(3)} \\ 0 & 0 & 0 & 0 & m_{41}^{(3)} & m_{42}^{(3)} & m_{43}^{(3)} & m_{44}^{(3)} \end{bmatrix} \quad (15)$$

Similarly, it follows from equations (10) and (3) that:

$$\begin{aligned} \int_{t_1}^{t_2} \delta V dt &= \int_{t_1}^{t_2} \int_0^L EI w'' \delta w'' dx dt \\ &= \int_{t_1}^{t_2} \left[\int_0^{l_1} \delta w'' EI w'' dx + \int_0^{l_2} \delta w'' EI w'' dx + \int_0^{l_3} \delta w'' EI w'' dx \right] dt \\ &= \int_{t_1}^{t_2} \left[\int_0^{l_1} \{\delta w^{(1)}\}^T \{N_{xx}\} EI \{N_{xx}\}^T \{w^{(1)}\} dx \right] dt \\ &+ \int_{t_1}^{t_2} \left[\int_0^{l_2} \{\delta w^{(2)}\}^T \{N_{xx}\} EI \{N_{xx}\}^T \{w^{(2)}\} dx + \int_0^{l_3} \{\delta w^{(3)}\}^T \{N_{xx}\} EI \{N_{xx}\}^T \{w^{(3)}\} dx \right] dt \\ &= \int_{t_1}^{t_2} [\{\delta w^{(1)}\}^T [k^{(1)}] \{w^{(1)}\} + \{\delta w^{(2)}\}^T [k^{(2)}] \{w^{(2)}\} + \{\delta w^{(3)}\}^T [k^{(3)}] \{w^{(3)}\}] dt \end{aligned} \quad (16)$$

Where the elemental stiffness matrix $[k^{(i)}] \equiv \int_0^{l_i} \{N_{xx}\} EI \{N_{xx}\}^T dx$ ($i = 1, 2, 3$). If E

and I are constant, one can obtain:

$$[k^{(i)}] = \frac{EI}{l_i^3} \begin{bmatrix} 12 & 6l_i & -12 & 6l_i \\ 6l_i & 4l_i^2 & -6l_i & 2l_i^2 \\ -12 & -6l_i & 12 & -6l_i \\ 6l_i & 2l_i^2 & -6l_i & 4l_i^2 \end{bmatrix} \quad (17)$$

The global stiffness matrix $[K]$ is obtained by assembling the elemental stiffness matrices as:

$$[K] = \begin{bmatrix} k_{11}^{(1)} & k_{12}^{(1)} & k_{13}^{(1)} & k_{14}^{(1)} & 0 & 0 & 0 & 0 \\ k_{21}^{(1)} & k_{22}^{(1)} & k_{23}^{(1)} & k_{24}^{(1)} & 0 & 0 & 0 & 0 \\ k_{31}^{(1)} & k_{32}^{(1)} & k_{33}^{(1)} + k_{11}^{(2)} & k_{34}^{(1)} + k_{12}^{(2)} & k_{13}^{(2)} & k_{14}^{(2)} & 0 & 0 \\ k_{41}^{(1)} & k_{42}^{(1)} & k_{43}^{(1)} + k_{21}^{(2)} & k_{44}^{(1)} + k_{22}^{(2)} & k_{23}^{(2)} & k_{24}^{(2)} & 0 & 0 \\ 0 & 0 & k_{31}^{(2)} & k_{32}^{(2)} & k_{33}^{(2)} + k_{11}^{(3)} & k_{34}^{(2)} + k_{12}^{(3)} & k_{13}^{(3)} & k_{14}^{(3)} \\ 0 & 0 & k_{41}^{(2)} & k_{42}^{(2)} & k_{43}^{(2)} + k_{21}^{(3)} & k_{44}^{(2)} + k_{22}^{(3)} & k_{23}^{(3)} & k_{24}^{(3)} \\ 0 & 0 & 0 & 0 & k_{31}^{(3)} & k_{32}^{(3)} & k_{33}^{(3)} & k_{34}^{(3)} \\ 0 & 0 & 0 & 0 & k_{41}^{(3)} & k_{42}^{(3)} & k_{43}^{(3)} & k_{44}^{(3)} \end{bmatrix} \quad (18)$$

The variation of non-conservative work, δW_{nc} , due to a distributed external force f is given by:

$$\begin{aligned} \int_{t_1}^{t_2} \delta W_{nc} dt &= \int_{t_1}^{t_2} \int_0^L f \delta w dx dt = \int_{t_1}^{t_2} \left[\int_0^{l_1} f \delta w dx + \int_0^{l_2} f \delta w dx + \int_0^{l_3} f \delta w dx \right] dt \\ &= \int_{t_1}^{t_2} \left[\{\delta w^{(1)}\}^T \{F^{(1)}\} + \{\delta w^{(2)}\}^T \{F^{(2)}\} + \{\delta w^{(3)}\}^T \{F^{(3)}\} \right] dt \end{aligned} \quad (19)$$

where the elemental force vector due to the distributed load is $\{F^{(i)}\} \equiv \int_0^{l_i} f \{N\} dx$. If

f is constant, $\{F^{(i)}\}$ for the i th element is given by:

$$\{F^{(i)}\} = \left\{ \frac{fl_i}{2} \quad \frac{fl_i^2}{12} \quad \frac{fl_i}{2} \quad -\frac{fl_i^2}{12} \right\}^T \quad (20)$$

Then the global force vector due to the distributed load of this three-element beam model is given by:

$$\{F\} = \left\{ \frac{fl_1}{2} \quad \frac{fl_1^2}{12} \quad \frac{fl_1}{2} + \frac{fl_2}{2} \quad -\frac{fl_1^2}{12} + \frac{fl_2^2}{12} \quad \frac{fl_2}{2} + \frac{fl_3}{2} \quad -\frac{fl_2^2}{12} + \frac{fl_3^2}{12} \quad \frac{fl_3}{2} \quad -\frac{fl_3^2}{12} \right\}^T \quad (21)$$

The equation of motion for this finite element model is given

$$[M]\{\ddot{w}\} + [C]\{\dot{w}\} + [K]\{w\} = \{F\} + \{Q\} \quad (22)$$

where $\{Q\}$ represents the global force vector due to concentrated loads on the beam. For this three-element beam model:

$$\{Q\} = \{Q_1^{(1)} \quad Q_2^{(1)} \quad 0 \quad 0 \quad 0 \quad 0 \quad 0 \quad 0\}^T \quad (23)$$

and $[C]$ is the damping matrix.

Assuming the system has no loads, external forces or damping the equation (22) can be reduced to:

$$[M]\{\ddot{w}\} + [K]\{w\} = 0 \quad (24)$$

Assuming the displacement vector can be represented in the form:

$$\{w\} = \{\Phi\}e^{\omega t} \quad (25)$$

Then

$$\{\ddot{w}\} = -\omega^2 \{\Phi\}e^{\omega t} \quad (26)$$

where $\{\Phi\}$ is the modal shape and ω is one of the natural frequencies.

Substituting (25) and (26) into equation (24) leads to:

$$([K] - \omega^2[M])\{\Phi\} = \{0\} \quad (27)$$

or in the generalized eigen-problem form:

$$[K]\{\Phi\} = \lambda[M]\{\Phi\} \quad (28)$$

where the eigenvalues λ are the square of the resonate frequencies of the structure and the eigenvectors $\{\Phi\}$ are the modal displacements. Directly

following the references [57] and [65] the complete system of force displacement equations can be written, in matrix form, as:

$$[K]\{w\} - \{F\} - \{Q\} = 0 \quad (29)$$

This example was limited to 2 degrees of freedom per node to save space. It is very easy to extend this example to more degrees of freedom. The FEA developed for this research used 2 node beam elements with 6 degrees of freedom per node. Also, the developed FEA code included the coordinate transformations so that three dimensional structures could be analyzed. For a complete treatment of the coordinate transformation see references [57, 65, 66, and 67].

2.2 High-Speed FEA Approximation

Currently, the most common practice for finding the deflection, stress, and/or natural frequency of a complex structure is to use FEA. When applied to DSO problems some major problems arise. As a structure's complexity increases, the size of the global matrices in the FEA increases. As the numbers of discrete members are added to the structure, the matrices become less sparse. Also, since the design variable space is now discontinuous, derivative based search algorithms have to search each and every discrete subspace. The large non-sparse matrices increase the computation effort of the problem. One solution is to approximate the FEA with some faster algorithm. The FEA has multiple inputs such as node locations, material, and geometric properties of the

elements. The outputs are the nodal displacements and/or modal frequencies (Eigenvalues). The relationship between the input and output is non-linear. Currently, one of the most researched and effective methods of approximating a non-linear system of multiple inputs and outputs, such as the structural analysis problems with load as input and displacement or stress as output, is through the use of an artificial neural network (ANN or NN) [68 and 69]. It is an obvious idea to apply NN to FEA, however, very little research has been done [11 and 70]. The previous works suggested very different NN architectures. One suggested a radial bias network [11], while the other had better results with a multi-layer feed forward architecture [70]. This work [68 and 70] has shown a major decrease in computational effort.

2.3 Basic NN Structure

The NN is simply a very large network of simple elements that are modeled roughly after a living creature's nervous system. One of the most attractive aspects of a NN is the fact that the elements are arranged in a parallel fashion. This leads to a parallel implementation in computer systems that in turn lead to very fast computations. As in biological systems, the simplest elements are called neurons.

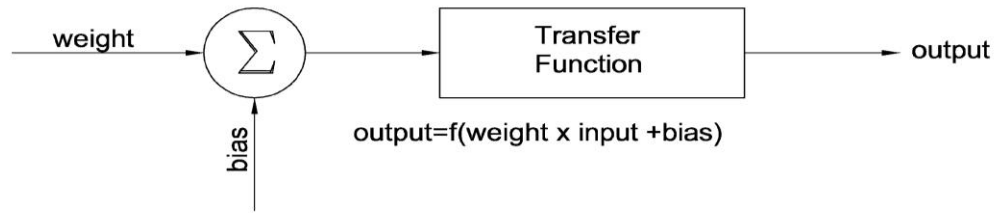


Figure 6. A typical neuron

Figure 6 shows a typical neuron where the sum of the weighted input and bias are transferred through the function f . The weight and bias become the design variables that are adjusted so that the neuron can be trained.

Many transfer functions are available with the Matlab NN toolbox [69].

Three of the most commonly used functions are the sigmoid, hyperbolic tangent, and linear functions. The following is a brief description of these functions.

Sigmoid function (LOGSIG):

$$f(n) = \frac{1}{1 + e^{-n}} \quad (30)$$

Hyperbolic tangent function (TANSIG):

$$f(n) = \frac{2}{1 + e^{-2n}} - 1 \quad (31)$$

Linear function (PURELIN):

$$f(n) = n \quad (32)$$

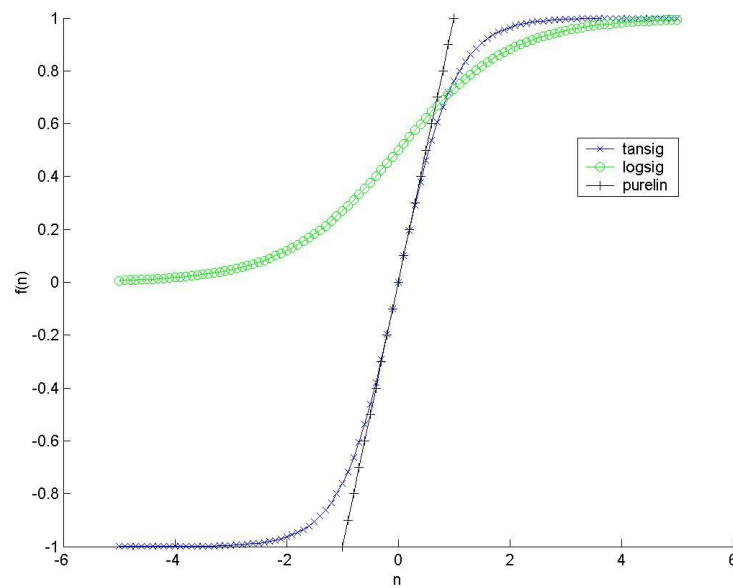


Figure 7. Transfer functions

Figure 7 shows the transfer functions. The TANSIG and LOGSIG are the so called “squashing” functions because they force the outputs to 0 to 1 or -1 to 1 respectively.

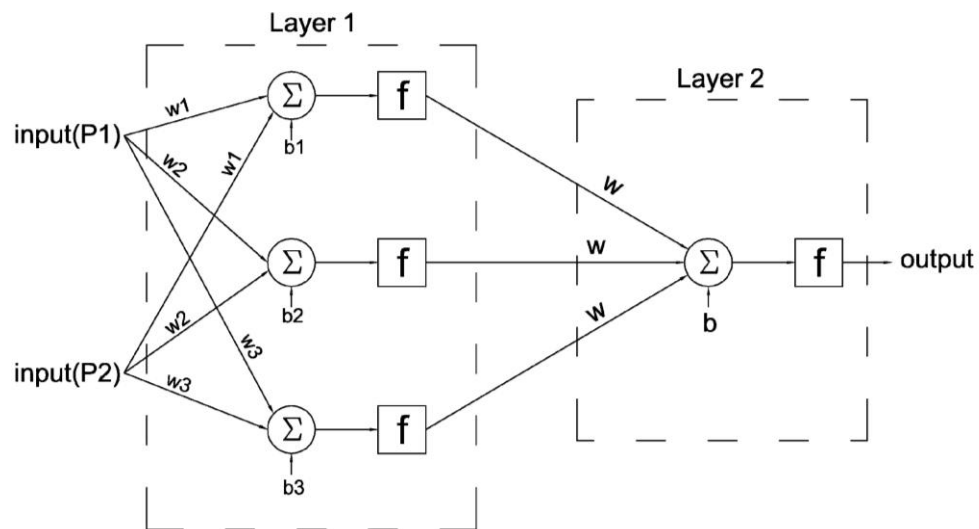


Figure 8. A typical 2 layer feed forward neural network

Figure 8 shows a typical network of neurons. Note how the structure is inherently parallel in nature. Even though the neurons and structure are very simple, if the numbers of neurons in the internal layers are large enough, the network can be trained to represent complex non-linear systems. These large NN's are good at approximating practically any non-linear function [69]. The number of inputs and outputs a NN can have is only limited by the computer

memory available. Therefore, a standard feed-forward NN of sufficient size should be able to approximate most FEA models.

Normally the NN is trained to approximate a function so that a set of inputs leads to a set of target outputs. In the case of approximating an FEA structural model, the inputs would be the material and geometric properties (shape), node locations, number and location of discrete components (topology), applied loads, and boundary conditions. The outputs would be nodal displacements and/or natural frequencies.

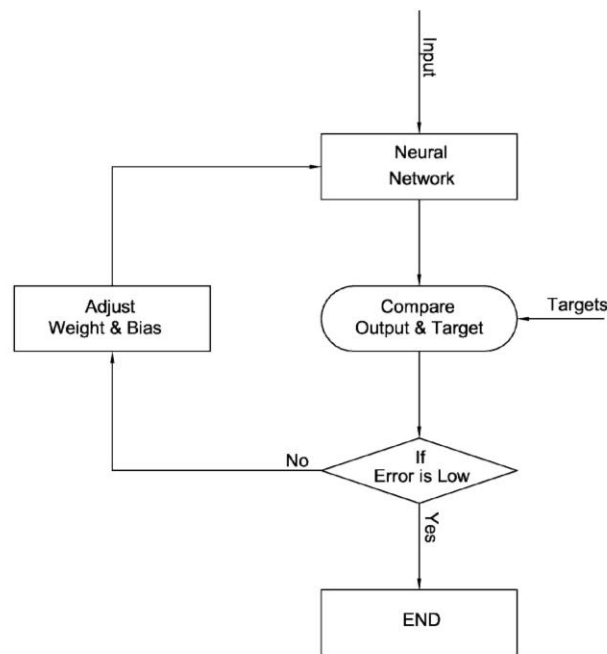


Figure 9. Neural network training flowchart

The training of a NN, as shown in Figure 9, is simply a large optimization problem that uses the weight and bias as the design variables. Most practical NN problems require many sets of inputs and targets to train. The literature suggests an alternative to a feed-forward network [11 and 70]. A radial bias network is the type that is very effective at non-linear approximations. They generally require more neurons than a feed-forward network but train in much less time [14].

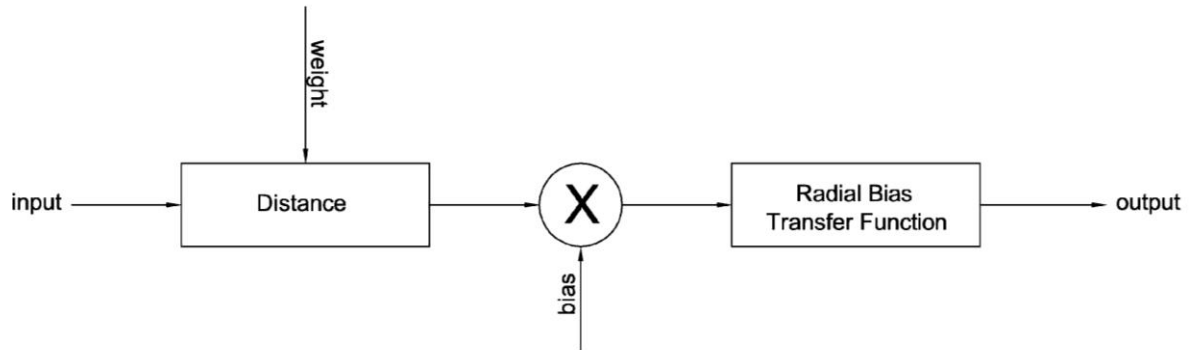


Figure 10. Typical radial bias neuron

The typical radial bias neuron is shown in Figure 10. The distance between the weight and input is multiplied by the bias and then sent to the radial bias function. In practice the system will have multiple inputs so the distance between the inputs and weights is their vector dot product. To train the radial bias network the training routine will create as many neurons as there are inputs. The weights

and bias are then optimized. If the error goal is not met, more neurons are added. Generally the number of neurons is much larger than the equivalent feed forward network.

2.4 NN Test

The effectiveness of the use of NN's as a FEA approximator was tested using a simple cantilever beam. A prismatic beam 36" long with a height of 1" and a width of 0.5" was selected. The beam was fixed on one end and a set of forces were applied to the other (Figure 11).

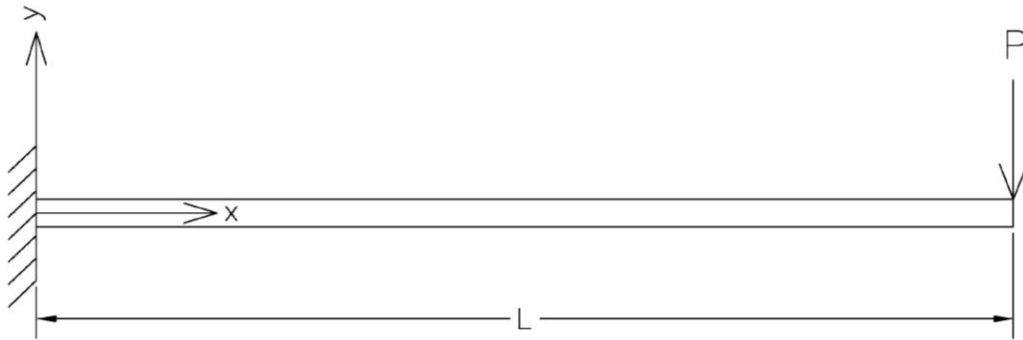


Figure 11. Test cantilever beam

The set of forces were randomly selected in the range of 10lbs. to 250lbs. The beam was discretized into 10 equal elements with two nodes apiece for a total of 11 nodes. The displacements at each node were calculated using the elastic equation:

$$EIy'' = -Px \quad (33)$$

Integrating equation (27) twice and applying the boundary conditions:

$$y = \frac{P}{6EI}(-x^3 + 3L^2x - 2L^3) \quad (34)$$

The displacements were also obtained using the FEA routine developed in the previous section. The applied loads (inputs) and FEA results (outputs) were used to train a standard feed-forward NN. The NN was then tested with an input of 90lbs. Table 2 and Figure 11 show the results compared to the analytical and FEA solutions. It also shows the average CPU times.

Table 2. Simple cantilever beam example displacements and CPU times

1"x0.5"x36" Simple Cantilever Beam with 90lbs load											
Node Number	1	2	3	4	5	6	7	8	9	10	CPU Time
Exact	-0.0041	-0.0157	-0.0340	-0.0582	-0.0875	-0.1209	-0.1577	-0.1971	-0.2381	-0.2799	0.0001
NN	-0.0041	-0.0157	-0.0340	-0.0582	-0.0875	-0.1209	-0.1578	-0.1971	-0.2381	-0.2799	0.0042
FEA	-0.0041	-0.0157	-0.0340	-0.0582	-0.0875	-0.1209	-0.1577	-0.1971	-0.2381	-0.2799	0.0470

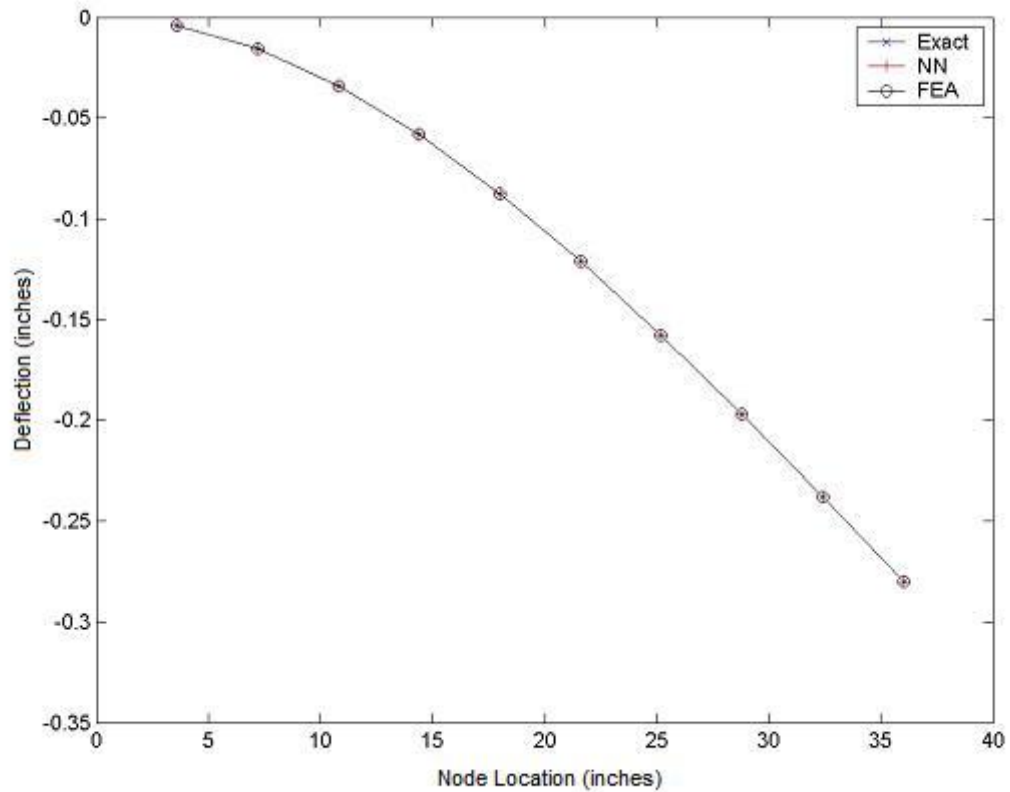


Figure 12. Simple beam nodal deflection.

The test was then repeated. This time the beam was changed to 1.75" high by 0.25" wide. The previously "learned" weights and biases were used as a starting point. The results are shown in Figure 13 and Table 3. Again, the FEA, NN, and the analytical solutions are the same. However, there is a large reduction in CPU time for the NN compared to the FEA. This reduction in CPU time would justify the use of the NN but not on a simple FEA problem like this. The NN training outweighs any gains. However, retraining the already learned network to a new but similar problem is very fast. Figure 14 shows the training

progress from the first problem and Figure 15 shows the retraining of the second.

The number of cycles for optimizing the weights and biases was reduced by a factor of over 300. The reduction in CPU time and the fast training of similar problems makes this NN approach suited for DSO of the MMT components.

Table 3. Modified simple cantilever beam example displacements and CPU times

1.75"x0.25"x36" Simple Cantilever Beam with 90lbs load										
Node Number	1	2	3	4	5	6	7	8	9	10
Exact	-0.0015	-0.0059	-0.0127	-0.0217	-0.0326	-0.0451	-0.0589	-0.0735	-0.0888	-0.1045
NN	-0.0015	-0.0059	-0.0127	-0.0217	-0.0326	-0.0451	-0.0589	-0.0735	-0.0889	-0.1045
FEA	-0.0015	-0.0059	-0.0127	-0.0217	-0.0326	-0.0451	-0.0589	-0.0735	-0.0888	-0.1045
										CPU Time
										0.0001
										0.0042
										0.0470

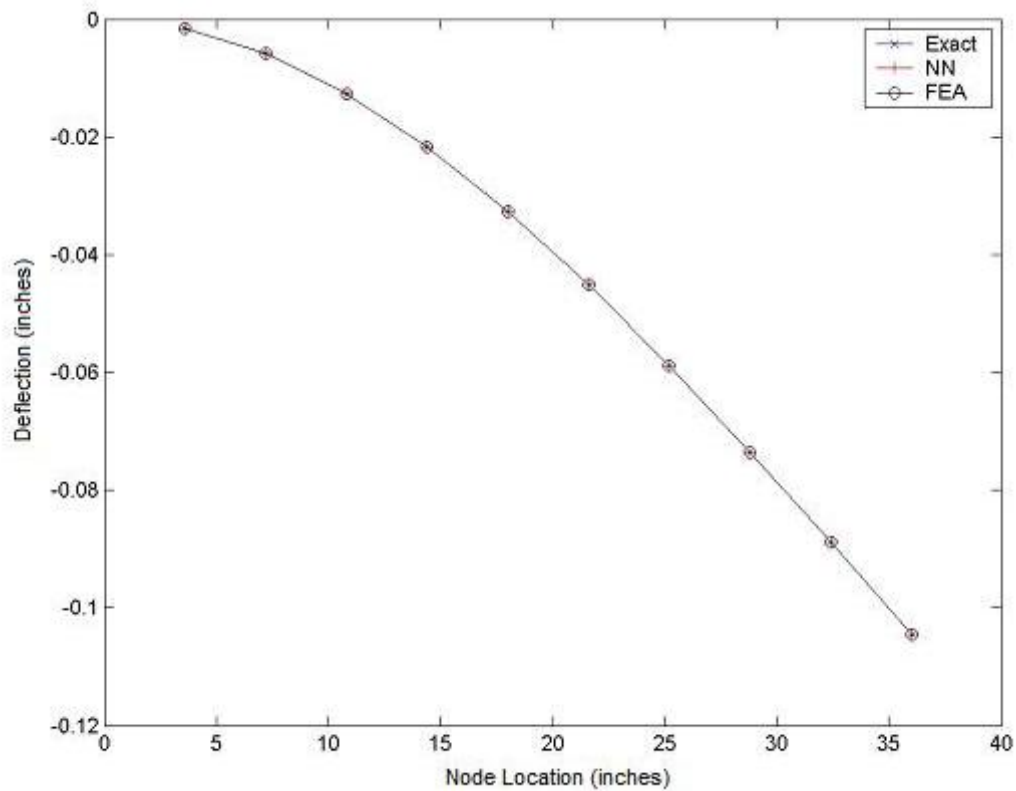


Figure 13. Modified simple beam nodal deflection.

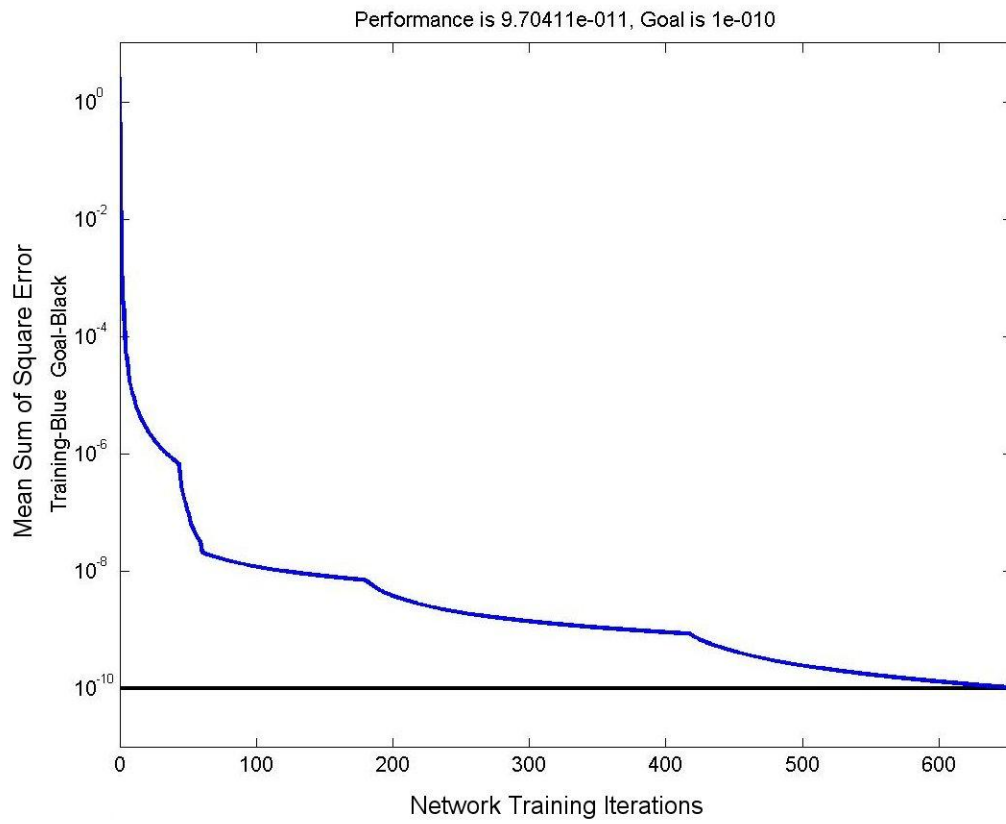


Figure 14. NN training with no previous weights and biases.

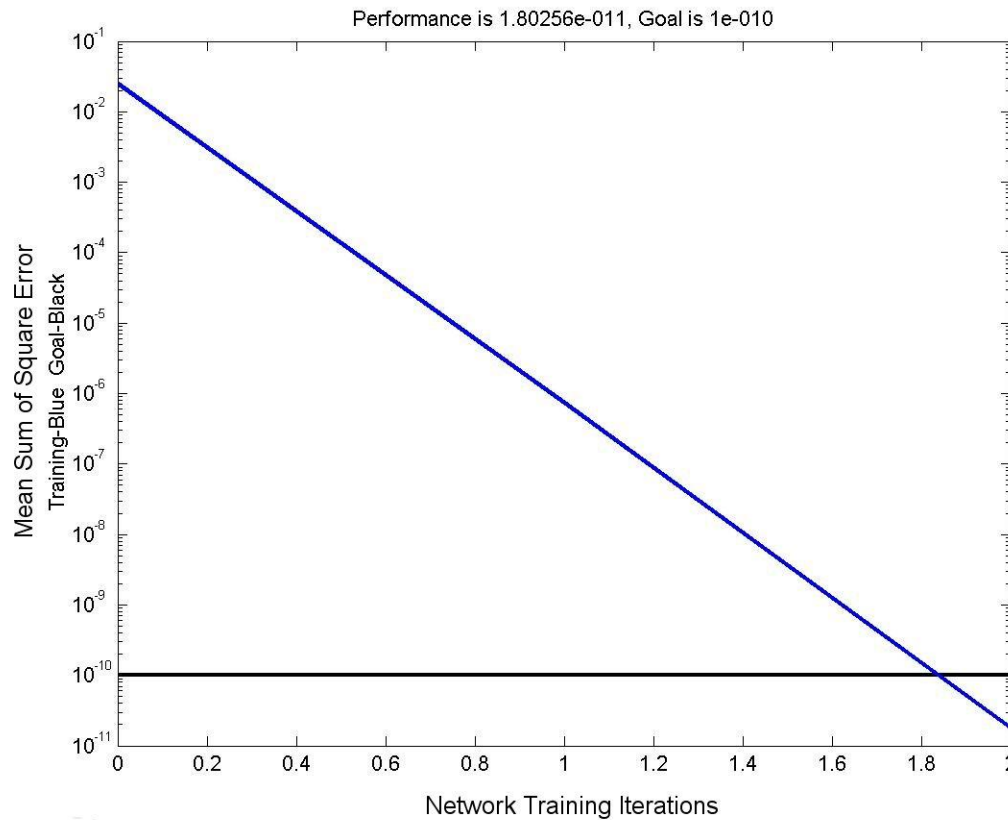


Figure 15. Training using previous weights and biases.

To test the effectiveness of a feed forward NN an FEA model of the side of a typical MMT base, shown in Figure 16, was created. The model was selected as 12" high by 36" long and nonsymmetrical coupled loads of -100lbs and 700lbs were applied. A training input set of 250 was created by randomly selecting the L shaped cross sections (angle beam), in the range of 0.5 in^2 to 2.0 in^2 , of the six members. The target set of nodal deflections was then created by running FEA on the 250 inputs. A feed forward NN was created and trained using the set of

random cross sections as inputs and the FEA nodal displacements as targets. To validate the effectiveness of the NN, a set of four cross sections properties were randomly selected from the available standard steel shapes. This set was used to test the NN ability to approximate the FEA and to compare the CPU time required for the calculations. These results are shown in Tables 4. Table 5 shows the standard steel element cross sections used for validating the NN.

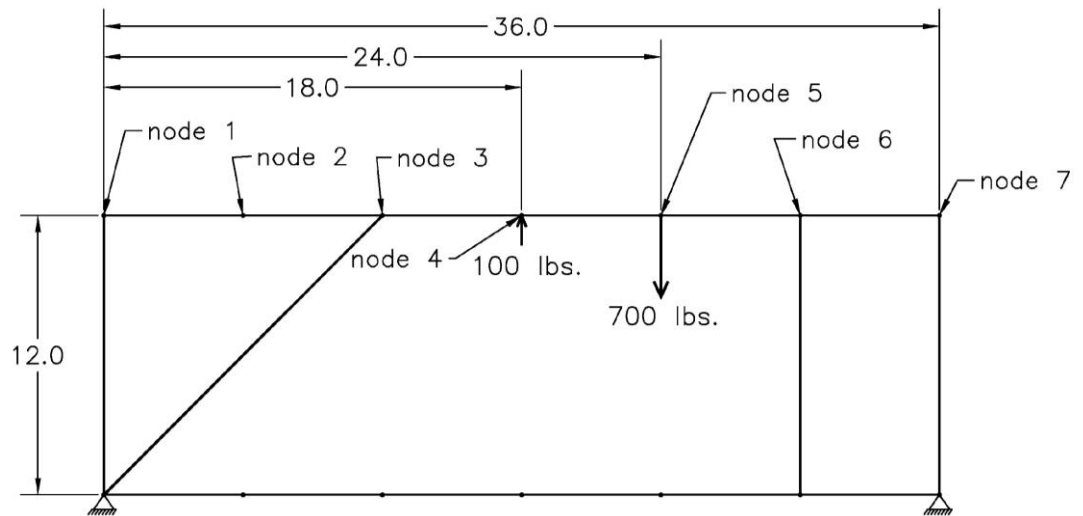


Figure 16. Side view of a typical MMT base component

Table 4. Nodal displacement and CPU time

Test Number 1								
node	1	2	3	4	5	6	7	CPU time
NN Displacements	0.0000	-0.0027	-0.0040	-0.0345	-0.0538	-0.0001	-0.0001	0.0075
FEA Displacements	0.0000	-0.0031	-0.0050	-0.0376	-0.0570	-0.0014	0.0000	0.0700
Difference	0.0000	0.0005	0.0010	0.0031	0.0032	0.0013	0.0001	0.0625
Test Number 2								
node	1	2	3	4	5	6	7	CPU time
NN Displacements	0.0000	-0.0010	-0.0024	-0.0035	-0.0034	-0.0013	0.0000	0.0050
FEA Displacements	0.0000	-0.0014	-0.0028	-0.0040	-0.0039	-0.0016	0.0000	0.0603
Difference	0.0000	0.0003	0.0005	0.0005	0.0004	0.0003	0.0000	0.0553
Test Number 3								
node	1	2	3	4	5	6	7	CPU time
NN Displacements	0.0000	-0.0012	-0.0031	-0.0059	-0.0065	-0.0015	0.0000	0.0050
FEA Displacements	0.0000	-0.0014	-0.0034	-0.0063	-0.0068	-0.0017	0.0001	0.0625
Difference	0.0000	0.0002	0.0003	0.0004	0.0004	0.0002	0.0000	0.0575
Test Number 4								
node	1	2	3	4	5	6	7	CPU time
NN Displacements	-0.0001	-0.0059	-0.0096	-0.0117	-0.0109	-0.0042	0.0000	0.0050
FEA Displacements	-0.0002	-0.0059	-0.0095	-0.0118	-0.0110	-0.0040	0.0002	0.0600
Difference	0.0001	0.0000	0.0001	0.0001	0.0001	0.0002	0.0001	0.0550

Table 5. Standard steel shapes

Test Number	Element 1	Element 2	Element 3	Element 4	Element 5	Element 6
1	L3/4x3/4x1/8	L2x2x1/2	L3/4x3/4x1/8	L1x1x1/4	L2x2x1/2	L2x2x1/2
2	L2x2x1/2	L2x2x1/2	L1x1x1/4	L1x1x1/4	L1x1x1/4	L1x1x1/4
3	L1x1x1/4	L2x2x1/2	L1x1x1/4	L1x1x1/4	L1x1x1/4	L1x1x1/4
4	L1x1x1/4	L1x1x1/4	L3/4x3/4x1/8	L3/4x3/4x1/8	L1x1x1/4	L1x1x1/4

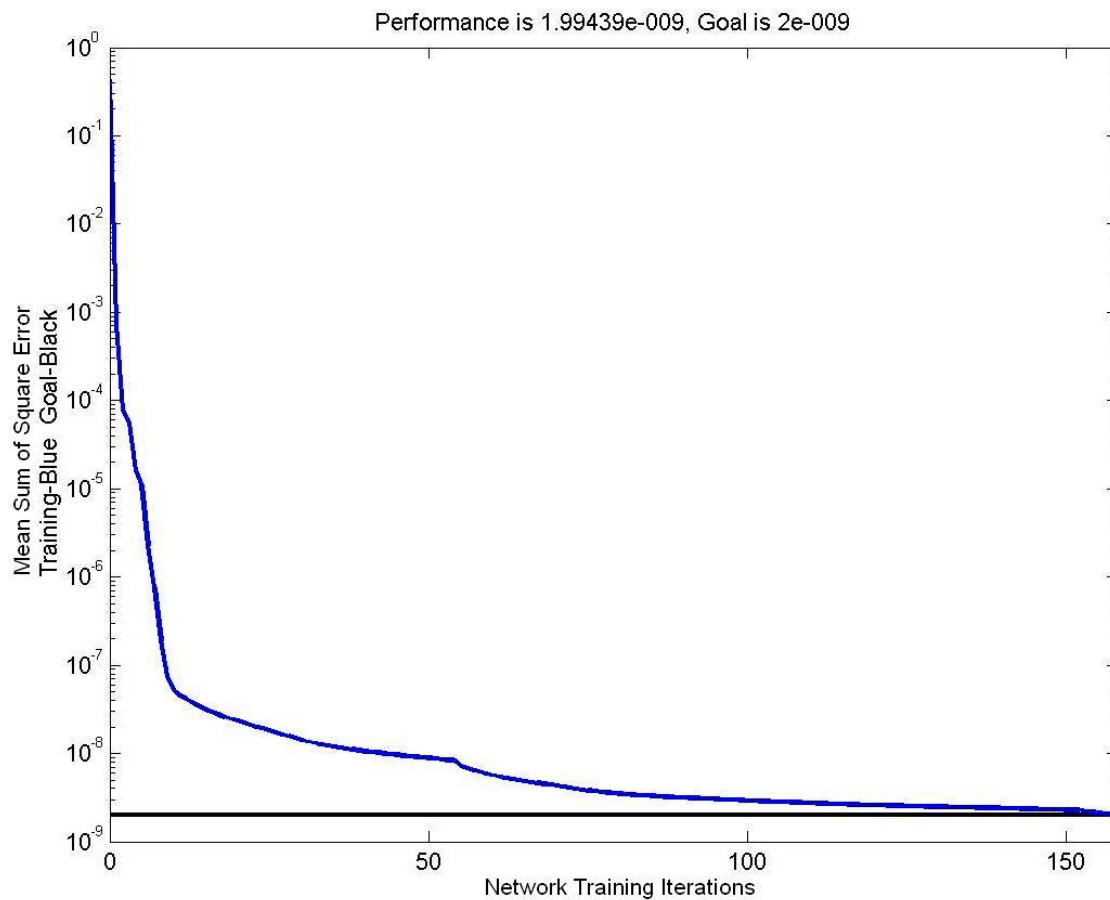


Figure 17. Training time with no previous weights and biases

One interesting aspect of the NN is the ability to quickly learn new functions that are close to the original. The topology in the previous model was slightly modified as shown in Figure 18.

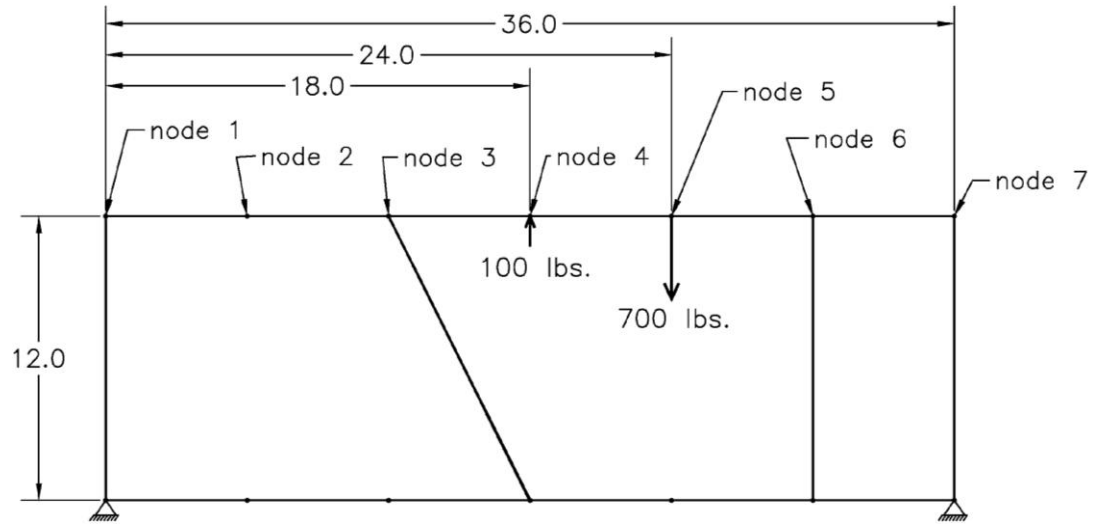


Figure 18. Modified structure topology

The same loads were applied and a new set of random training input data was generated. New NN's were created using the previous learned weights and biases. These new NN's were trained using the new topology and the maximum deflections; the calculation times are shown in Table 6. The randomly selected standard steel element cross sectional shapes are shown in Table 7.

Table 6. Displacements and CPU times for structure with new topology

Test Number 1								
node	1	2	3	4	5	6	7	CPU time
NN Displacements	0.0000	0.0003	-0.0006	-0.0047	-0.0071	-0.0026	0.0000	0.0075
FEA Displacements	0.0000	0.0003	-0.0005	-0.0044	-0.0065	-0.0022	0.0000	0.0678
Difference	0.0000	0.0000	0.0001	0.0004	0.0006	0.0004	0.0000	0.0603
Test Number 2								
node	1	2	3	4	5	6	7	CPU time
NN Displacements	0.0000	-0.0002	-0.0009	-0.0024	-0.0029	-0.0011	0.0000	0.0050
FEA Displacements	0.0001	-0.0004	-0.0013	-0.0026	-0.0029	-0.0011	0.0000	0.0600
Difference	0.0000	0.0003	0.0004	0.0002	0.0000	0.0000	0.0000	0.0550
Test Number 3								
node	1	2	3	4	5	6	7	CPU time
NN Displacements	0.0000	0.0001	-0.0012	-0.0069	-0.0111	-0.0063	-0.0001	0.0050
FEA Displacements	0.0000	0.0001	-0.0014	-0.0070	-0.0108	-0.0060	-0.0002	0.0625
Difference	0.0000	0.0000	0.0002	0.0001	0.0004	0.0003	0.0000	0.0575
Test Number 4								
node	1	2	3	4	5	6	7	CPU time
NN Displacements	0.0000	0.0001	-0.0010	-0.0049	-0.0069	-0.0025	0.0000	0.0050
FEA Displacements	0.0000	0.0001	-0.0009	-0.0047	-0.0067	-0.0024	0.0000	0.0603
Difference	0.0000	0.0000	0.0001	0.0002	0.0002	0.0001	0.0000	0.0553

Table 7. Standard steel shapes

Test Number	Element 1	Element 2	Element 3	Element 4	Element 5	Element 6
1	L1x1x1/4	L1x1x1/4	L2x2x1/2	L2x2x1/2	L1x1x1/4	L1x1x1/4
2	L2x2x1/2	L2x2x1/2	L3/4x3/4x1/8	L1x1x1/4	L1x1x1/4	L3/4x3/4x1/8
3	L1x1x1/4	L3/4x3/4x1/8	L1x1x1/4	L1x1x1/4	L1x1x1/4	L2x2x1/2
4	L1x1x1/4	L1x1x1/4	L1x1x1/4	L1x1x1/4	L1x1x1/4	L3/4x3/4x1/8

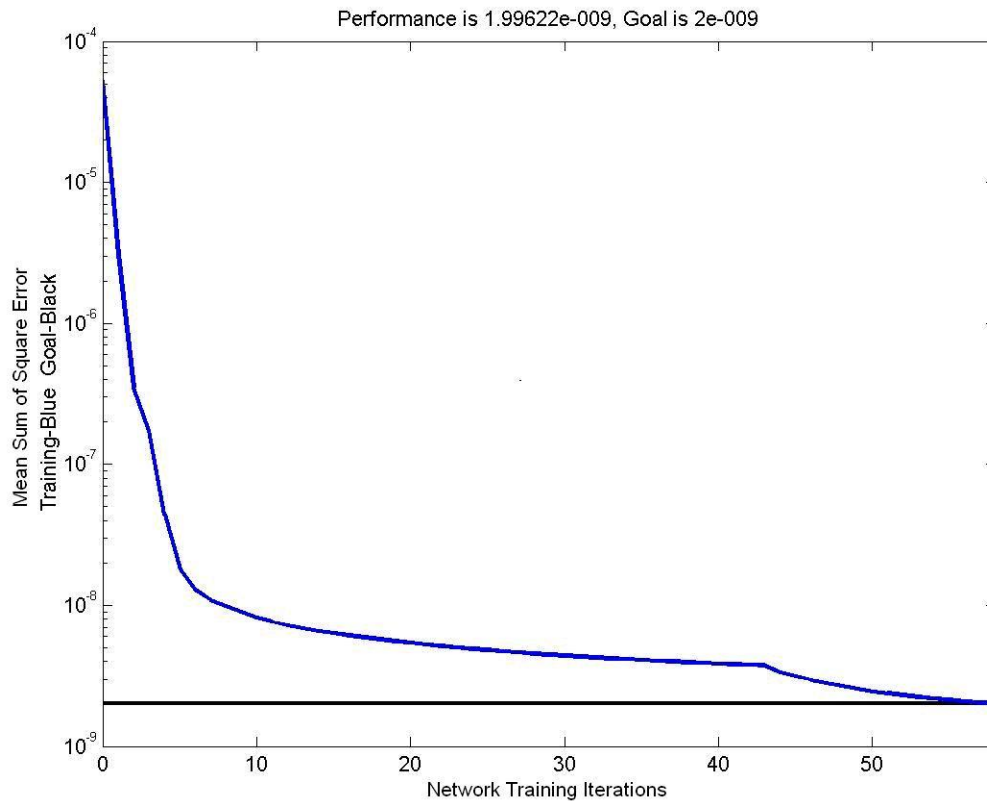


Figure 19. Time to retrain NN

A couple of interesting observations can be made from these results. First, the feed-forward NN was effective at approximating the FEA. The largest displacement error in this test was 0.001 inches and most of the errors were less than 0.0005 inches. This is much less than the displacement constraint used when the optimization of the MMT components. Second, the NN had order of magnitude reductions in computation times. The radial bias method failed to converge with this problem. The feed forward NN had better results and faster training times. Also, with the feed forward NN major reductions in training times can be realized by using information from previous networks.

2.5 NN training

Many methods to train NN's are included in the Matlab NN toolbox. Some of these algorithms are not useful for practical problems and the best method for fastest training is dependent on the problem [69]. The best training algorithm for a given problem depends on many factors, such as the size of the training set, the complexity of the problem, the size of the network, and the type of the problem (pattern recognition or function approximation) [69]. The easiest and fastest way to determine the best and fastest converging algorithm is by trial-and-error. Four of the most common high-performance algorithms were tested.

The four algorithms tested were the Matlab functions `traingda`, `trainrp`, `trainscg`, and `trainlm`. The first method was the steepest gradient descent with a variable step size (TRAINGDA). The second was the resilient back-propagation (TRAINRP) method. All of the networks in this research were used to approximate non-linear systems. This requires the use of “squashing” functions. Squashing functions take an infinite input and output with a range of -1 to 1. As the input gets very large or very small, their derivative goes to zero. This has a major impact on the steepest descent gradient based methods. The gradient may be very small while the network is training. This in turn causes very small changes in the weights and biases even though they are far from converging. The `trainrp` uses only the sign of the gradient, not the magnitude. It uses a separate variable for the step magnitude. This variable increases if the sign of

the gradient stays the same from step to step or decreases if the sign changes. This leads to faster learning and tends to reduce oscillations around the solution. The third algorithm tested performs a search along the conjugate gradient instead of the steepest descent direction (TRAINSCG). This usually produces faster convergence. The last algorithm tested used a modified Newton method (TRAINLM) that has a variable step size and direction. The TRAINLM function generally has the ability to train to a lower error level.

Figures 20, 21, 22, and 23 show the progress of training the networks derived from the structure shown in Figure 16 using the different algorithms. For the networks in this research the TRAINRP seemed to have the best performance when the error was higher. The TRAINLM had the best performance when training to a lower error. In all the proceeding tests and programs the TRAINRP was used for initial training then TRAINLM was used to reach a lower error.

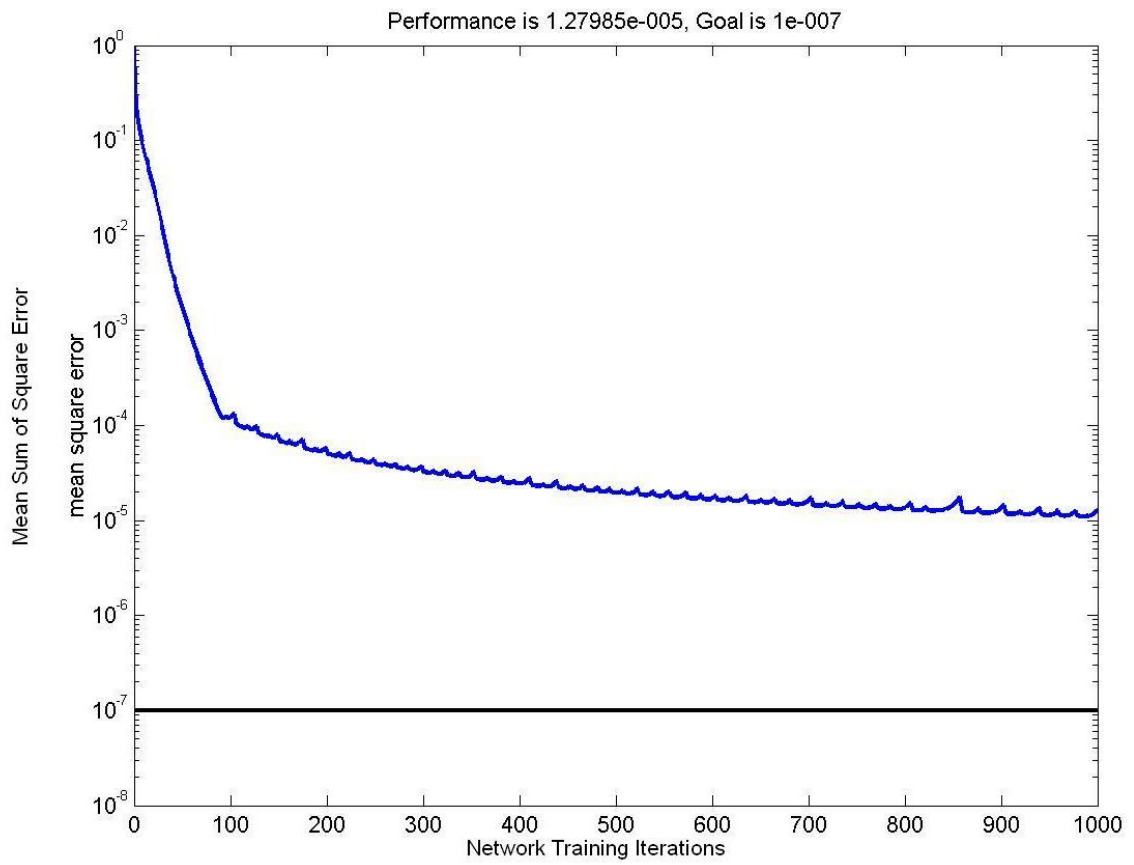


Figure 20. Training history for traingda

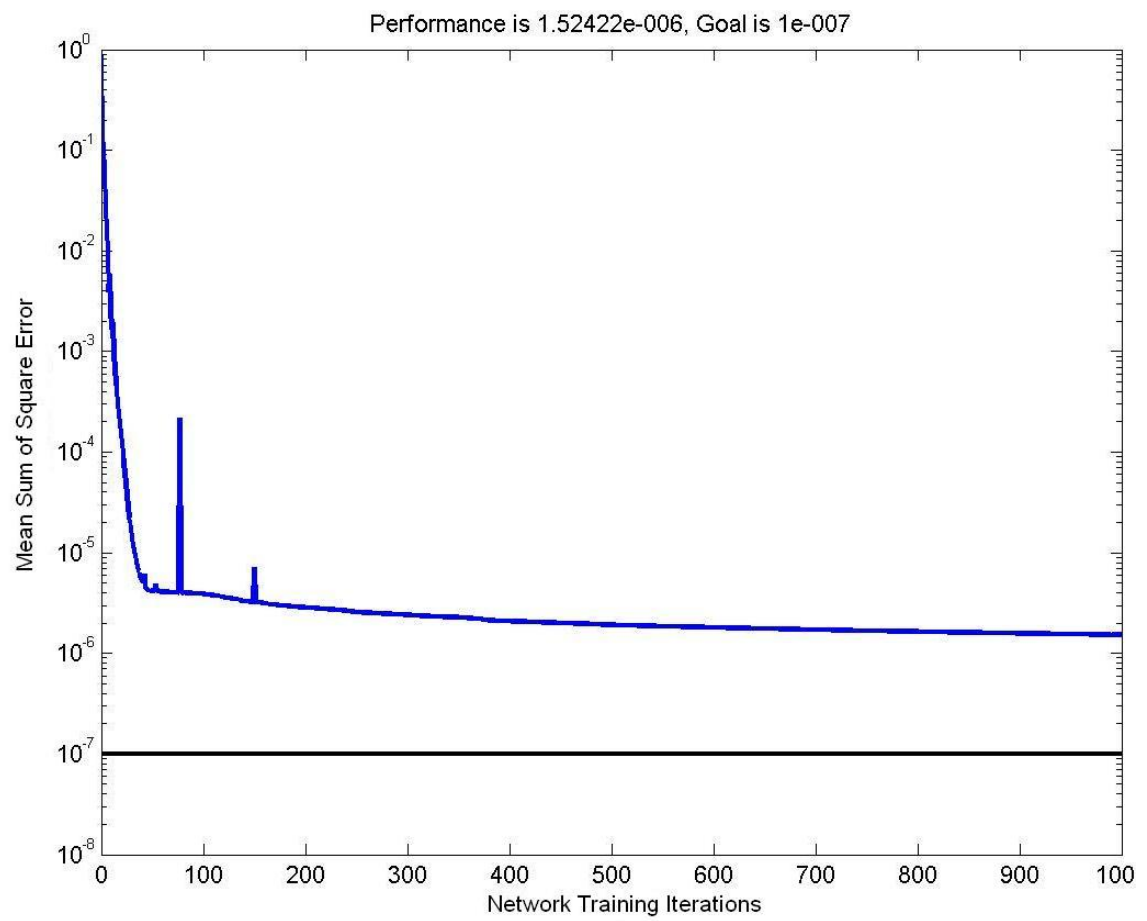


Figure 21. Training history for trainrp

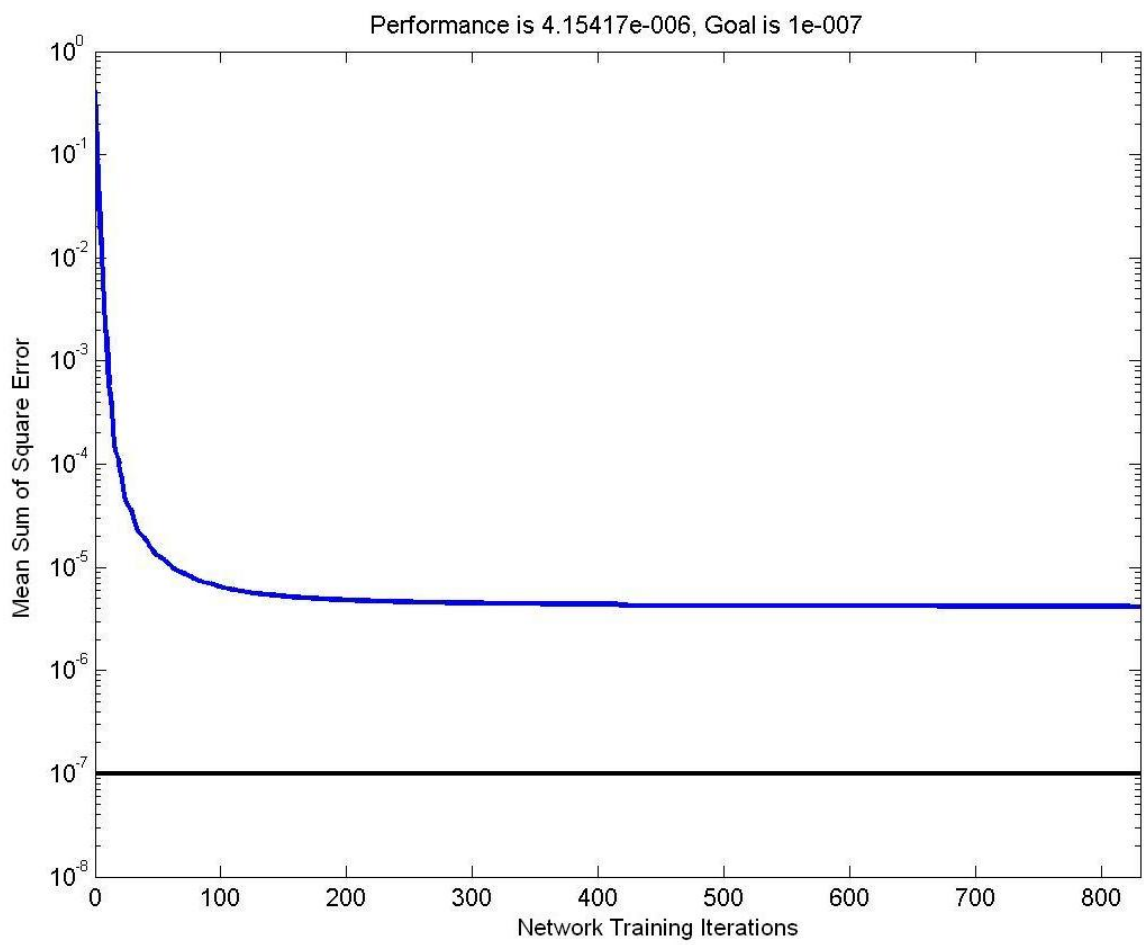


Figure 22. Training history for trainscg

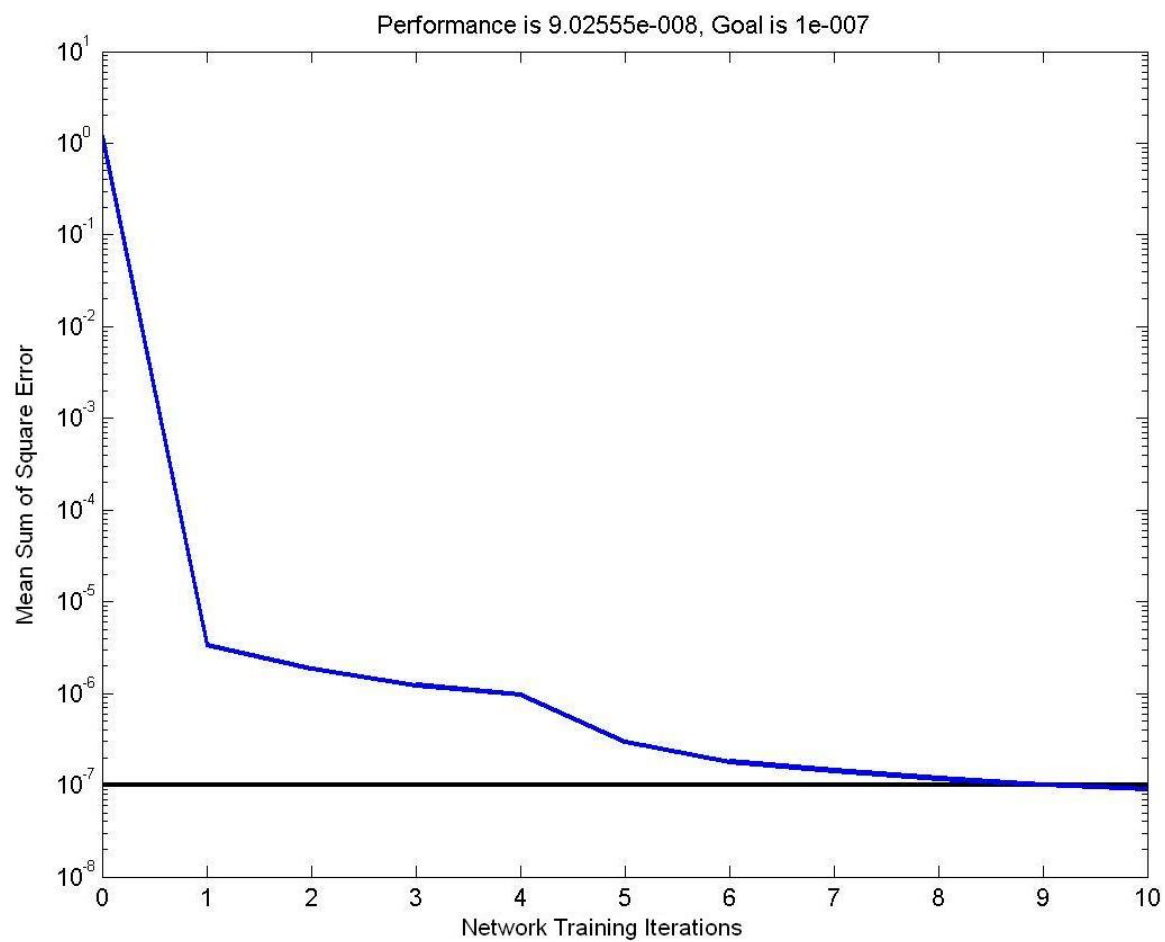


Figure 23. Training history for trainlm

2.6 General comments and results from NN test

The NN is not a cure all for computationally inefficient problems. It is, however, proven very useful in optimal MMT design. The following are some brief comments on NN.

- The steps to create and use a NN:
 1. Develop the network structure. This must be large enough and have enough hidden layers to represent the problem. There is no theoretical method to determine the correct structure. It is generally done through trial and error.
 2. Train the network. This is a large scale optimization problem. Accepted optimization techniques can be applied.
 3. Simulate the network. New inputs are given to the network. What was learned in the training is recalled and new outputs are produced.
- NN structures are inherently parallel. This leads to easy implementation to parallel computers and processors which leads to fast computations. However, this research was developed on a single computer and processor.
- Training is just a large scale optimization process. The weights and biases of the NN are adjusted (design variables) thereby minimizing the error between a known target and the output of the NN.

- The NN method can be a very effective universal approximation for FEA. However, the structure and the transfer functions must be carefully chosen. The number of nodes must be sufficiently large and the use of some non-linear transfer functions is required.
- For this research feed-forward NN gave better results than the radial bias networks.
- NN based FEA approximations are better at interpolation than extrapolation.
- NN calculations are much faster than FEA calculations. Generally, they are at least an order of magnitude faster. As the size of the problem increases, the NN calculations increase linearly while the FEA calculations increase exponentially.

Even though the use of NN approximation of FEA leads to faster calculations, FEA calculations should not simply be replaced with NN. The real advantage is to use the inherent “memory” properties of the NN along with the computational efficiencies to utilize previous designs. In other words, as new components are developed the optimal designs are captured in the NN and will influence future designs.

2.7 Optimization Algorithms

In this study the stated problem of optimizing MMT structures is completely discrete in nature. According to the literature review, most of the

previous work focused on GA, SA, or branch and bound methods for completely discrete problems. Also, guaranteeing that the GA or SA produced a global optimum is difficult. No clear mathematical proof exists to prove a global optimum is achieved. Branch and bound, on the other hand, is a global optimization algorithm. It may not be the most efficient, but at least it operates in polynomial time on general problems.

For this research a branch and bound method was used as the primary optimization algorithm. The branch and bound method has some other added properties that help meet the objectives of this project. It was shown previously that for practical real-world problems the FEA models would get large and an approximation is needed. The problem is when to use the FEA and when to switch to the approximation method? The branch and bound method has a clear point to make the switch. When the variables are relaxed the FEA is used and a neural network training set is generated. When the branches are fathomed with discrete variables the approximation is used. This has the advantage that most of the design space will be covered when the FEA is used and the training set is developed. A very robust NN approximator is developed using this method because the NN is generally better at interpolation than at extrapolation.

Applying the branch and bound method to the MMT optimization problem is not without challenges. Typically, the branch and bound method is used with a linear programming or gradient descent for the relaxation method [13]. However, these methods are not effective on non-convex or discontinuous problems [13].

The discrete MMT problem is both non-convex and discontinuous. For this study a robust continuous optimization algorithm is required for the relaxation.

Generally, the literature suggests a GA or SA based algorithm to overcome these problems [4 and 13]. However the literature also suggest these algorithms may be difficult to tune and implement. In recent years many researchers have successfully applied PSO to these types of discontinuous problems. The PSO has the advantages of being simple and easy to implement. It has also been shown to converge rapidly but it is difficult to specify the stopping criteria. For this reason a hybrid approach was chosen by using a PSO to quickly converge toward the best solution then switch to a fast gradient based method to converge on the solution. This PSO method had the added benefit of finding solutions distributed over the entire design space. This generally improved the training performance of the neural network.

2.8 Branch and Bound Discrete Optimization

A review of the current literature revealed that exhaustive enumeration is only possible for trivial problems [4 and 13]. Partial enumeration or heuristic methods are required for practical problems. One problem with heuristic methods is that it is very difficult to prove they will produce a global optimum on practical problems. The partial enumeration methods, specifically the branch and bound, method over-comes these problems [71]. It will produce a global optimum and in most cases it will operate in polynomial time.

The branch and bound method is based on the fact that the relaxed continuous solution is always better than the discrete solution. Using this fact, bounds can be created and large groups of potential discrete solution can be eliminated. The algorithm creates a tree structure with branches by systematically fixing and relaxing discrete variables. This creates a structure with nodes connected by links. Following the best path through the links and nodes is called fathoming. The use of the branch and bound method is best described with an example.

Consider the structural bracket shown in Figure 24. Assume the goal is to minimize the total amount of material in the structure and elements 1 and 2 can only be made of standard steel round bar stock. Also, assume the end of element 2 can assume only the two locations shown in the figure. The questions are: What is the optimal layout of element 2? What are the optimal cross sections of both elements? The bracket must not deflect more than 0.010" when it is supporting 30lbs.

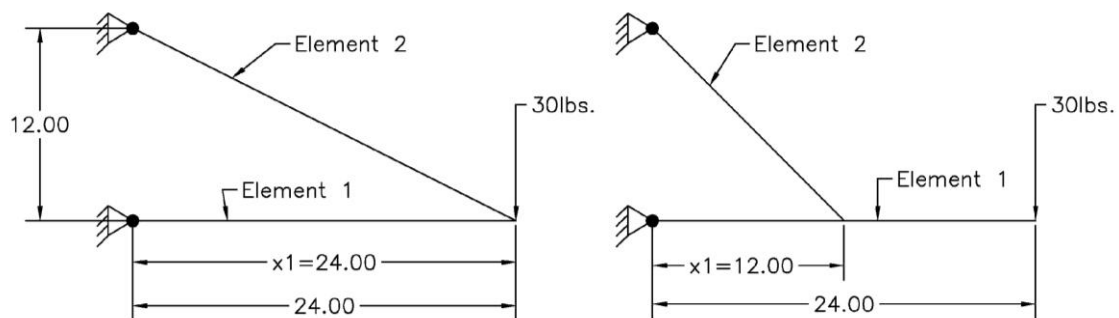


Figure 24. Structural Bracket Example

The formal optimization problem can then be stated as:

Minimize: $f(x_1, x_2, x_3) = 24\pi\left(\frac{x_2}{2}\right)^2 + \pi(\sqrt{144 + (x_1)^2})\left(\frac{x_3}{2}\right)^2$

$$x_1 \in [12, 24]$$

$$x_2 \in [0.5, 1.0, 1.25]$$

$$x_3 \in [0.125, 0.75, 1.25]$$

Subject to: $\delta \leq 0.010$

Where: δ is the maximum nodal deflection

X_2 is the diameter of element 1 cross section

X_3 is the diameter of element 2 cross section

The first variable x_1 is fixed and partial solutions are found. In this case x_1 only has two discrete possibilities. So, x_1 is fixed to these two values and the other variables are relaxed. In this example, a sequential quadratic programming method was used to find the optimal solutions. As shown in Figure 25, this produces two branches or partial solutions from node 0.

This method of fixing and relaxing variables is continued by following the path of the best solution until the tree is completely fathomed. Then, the partial solutions that are worse than the best fathomed solution are pruned or cut. This will leave only active or pruned partial solutions. An active partial solution is one that is not pruned but has not been fathomed. This is continued until all branches have been fathomed or pruned.

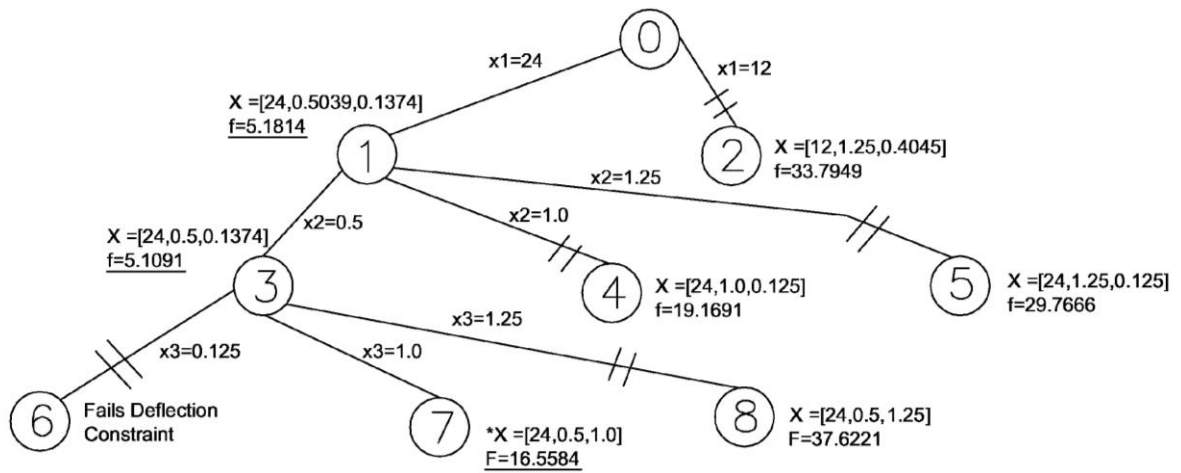


Figure 25. Branch and Bound Tree for the Structural Bracket Example

Structural Bracket Example

Start Node 0:

Root node where all variables are relaxed.

Node 1 & 2:

Discrete variable x_1 is assigned to each permissible discrete value. This creates two paths or branches. The optimal solution is found for each node by relaxing the other variables. Node 1 has the best solution so it will be fathomed.

Completion of Node 1:

Node 1 is expanded by setting the discrete variable x_2 to its permissible discrete values. This creates branches to nodes 3, 4, and 5. Node 3 has the best solution so it will be fathomed.

Completion of Node 3:

Node 3 is expanded by setting the discrete variable x_3 to its permissible discrete values. This creates branches to nodes 6, 7, and 8. Node 6 fails to produce a solution because it does not meet the displacement constraint. Node 7 produces the best solution. Since all the discrete variables at node 7 are assigned discrete values the solution at node 7 is considered the current best discrete solution. All of the nodes with solutions greater than node 7 are pruned.

All of the nodes have been pruned or fathomed. Therefore, node 7 is the global discrete optimal solution.

This example shows that the branch and bound method is effective in finding the global optimum of a typical discrete structural optimization problem. In this example a non-linear relaxation method was applied. Also, the algorithm used the non-equality constraint as an effective pruning mechanism.

The MMT optimization problems of this study were solved using the branch and bound method by fixing one variable at a time then relaxing the other variables. Fixing one variable at a time broke the problem into branches. These branches were then solved as continuous optimization problems. The continuous branches were then compared to discrete solutions and were

normally cut after a few iterations. This method was based on the fact that the continuous solution of each branch was always more optimal than the discrete solution. Also, the use of gradient-based methods provided continuous solutions with very little computational load.

For the MMT DSO problems branches were the topology of the structure. Another discrete design variable is the different shape of cross-sections of each structural members. The member's geometric properties were then relaxed and the continuous problem was solved. Figure 26 of the 2D problem of a typical side of a MMT base shows the typical branches. Figure 27 shows the overall flow of the branch and bound program as applied to the MMT DSO.

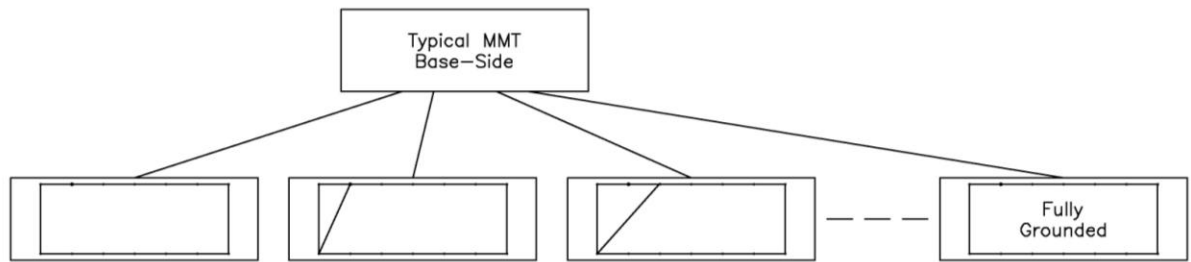


Figure 26. Tree for typical MMT base side

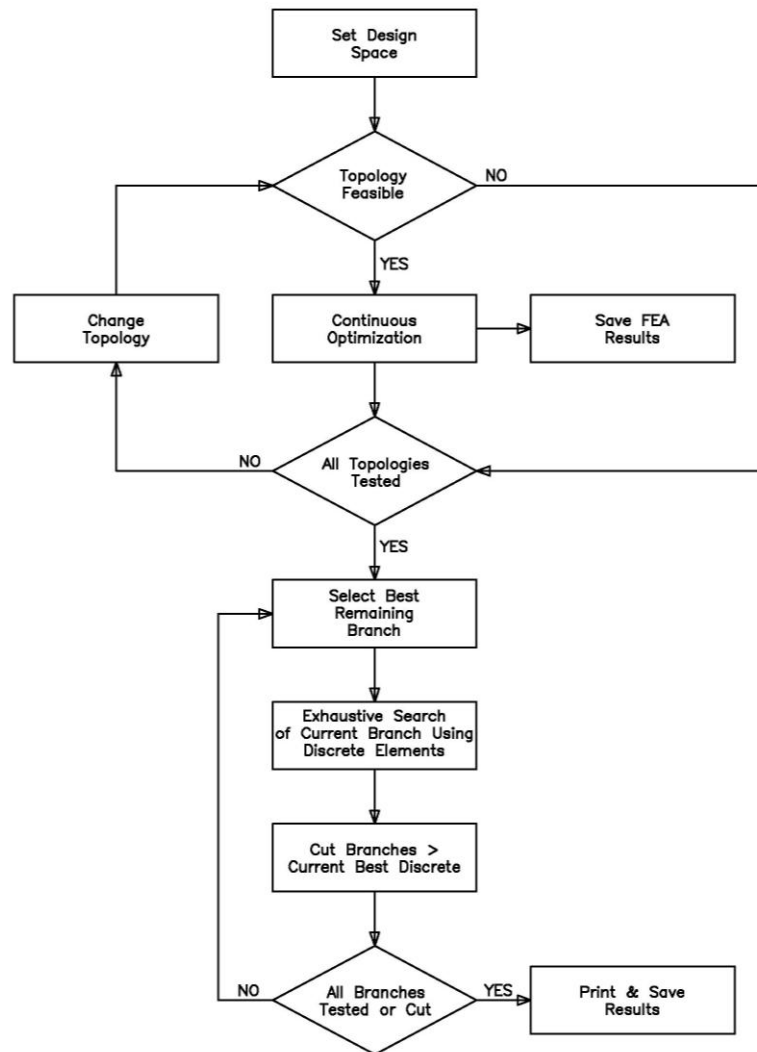


Figure 27. Branch and bound flowchart for MMT base side

For this research all of the members were assumed to have stock equal or unequal leg L cross-sections. This assumption leads to three design variables for each member (L_1 , L_2 , and t in Figure 28). Figure 28 also shows a typical branch topology; in this example there are 6 elements with 3 design variables or 18 continuous variables for this branch.

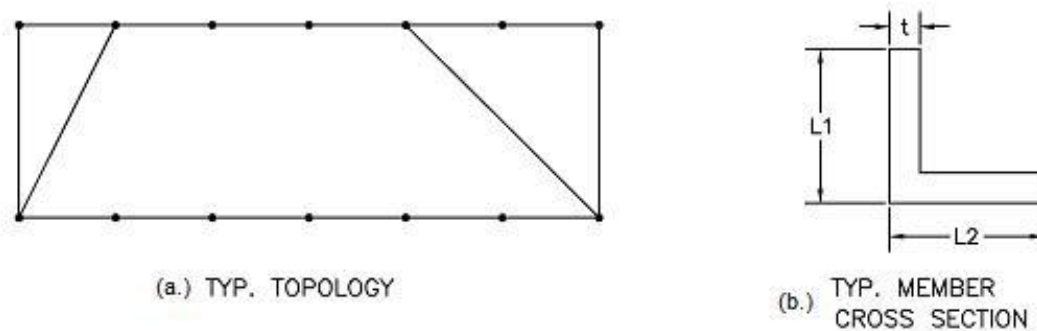


Figure 28. Typical topology and cross section

It was determined from testing examples that many of relaxed continuous optimization problems in this branch and bound structure were non-convex, discontinuous, or had many local minimums. Many of these branches had long convergent times when the variables were relaxed. It was obvious that some non-gradient methods were needed.

2.9 Hybrid continuous optimization

Conventional gradient-based optimization methods are very fast in solving smooth convex problems. However, for piecewise continuous, non-differentiable, or problems with many local minimums, they may become inefficient. In these

problems it was easy to see that each element was continuous but when assembled, it became piecewise continuous with many local minimums.

The most effective way to solve this type of non-smooth problem was to use a non-gradient based method. The most accepted non-gradient based methods include SA, GA, and pattern search algorithms [4 and 72]. These methods all have the problem that though they are assumed to be global algorithms, they may be slow to reach the required accuracy and global optimal.

One method reported to overcome this problem was to employ a hybrid approach that used both gradient and non-gradient based methods [72]. For problems like this with many smooth areas or local minimums, a SA, GA, or pattern search method was used to quickly get to the best smooth area then a fast gradient based method was used to find the accurate solution.

SA, GA, and pattern search methods can be difficult to implement and tune for a given problem [72]. Particle swarm optimization (PSO) is one of the methods to overcome parameter tuning difficulty. It is loosely based on animal swarming behavior by bees, birds, or fish. Compared to the other methods, it is easy to implement and has few parameters to tune [73].

PSO simulates the behaviors of feeding schools of fish or flocks of birds. The idea is simple. The swarm randomly heads out into a search area. The swarm then moves in the general direction toward the individual with the most food (best solution). The swarm moves together in general but individuals still

have some small random area to explore. After a very short time the swarm will converge in the area with the most food (best solution).

The algorithm for a PSO is not difficult to develop, implement, and tune [34]. First, the PSO is initialized with a group particle. The size of the swarm is the first parameter. Normally this is set to 25 to 50 particles [73]. This is arbitrary and dependent on the size of the search space. Second, the particles are randomly distributed across the design space and the solution (fitness) for each particle is found. The two best fitness values are stored. One is the value of the best particle called “pbest”; the other is what will become the overall or global best called “gbest”. After “pbest” and “gbest” are found, a velocity is found that will move all the particles in the general direction of the best solution.

$$V[] = V[] + c1 * rand() * (pbest[] - location[]) + c2 * rand() * (gbest[] - location[]) \quad (35)$$

where:

rand() is a vector of random numbers from 0 to 1

c1 and c2 are learning factors normally set to 2

location[] is the location of the particles in the design space

Location is a commonly used term in the PSO literature. It refers to the current values of the design variables in the design domain [31]. Then, for every iteration the location of the particles are updated:

$$location[] = location[] + V[] \quad (36)$$

The new velocity and locations are computed for each iteration. The algorithm is continued until the maximum number of iterations is reached or the change in “pbest” reaches a set minimum.

Compared to other optimization methods, the PSO tends to converge quickly on the solution but may take many iterations to reach a desired minimum error [73]. For this research a PSO with 50 particles was used and after 4 iterations it was assumed to be close to the global solution. The results of the PSO were then used as the initial values for the standard Matlab gradient based constrained nonlinear optimization function. The Matlab function quickly converged on a feasible solution. In this research the Matlab fmincon function using the sequential quadratic programming algorithm option was used exclusively. Figure 28 shows the flow diagram for the algorithm used to optimize each branch of the problem. The current literature suggest there is no mathematical proof to show the swarm has found a global solution. However, it suggests that a large swarm (greater than 20 particles) will find the area of the global solution, for most problems, in very few iterations [31].

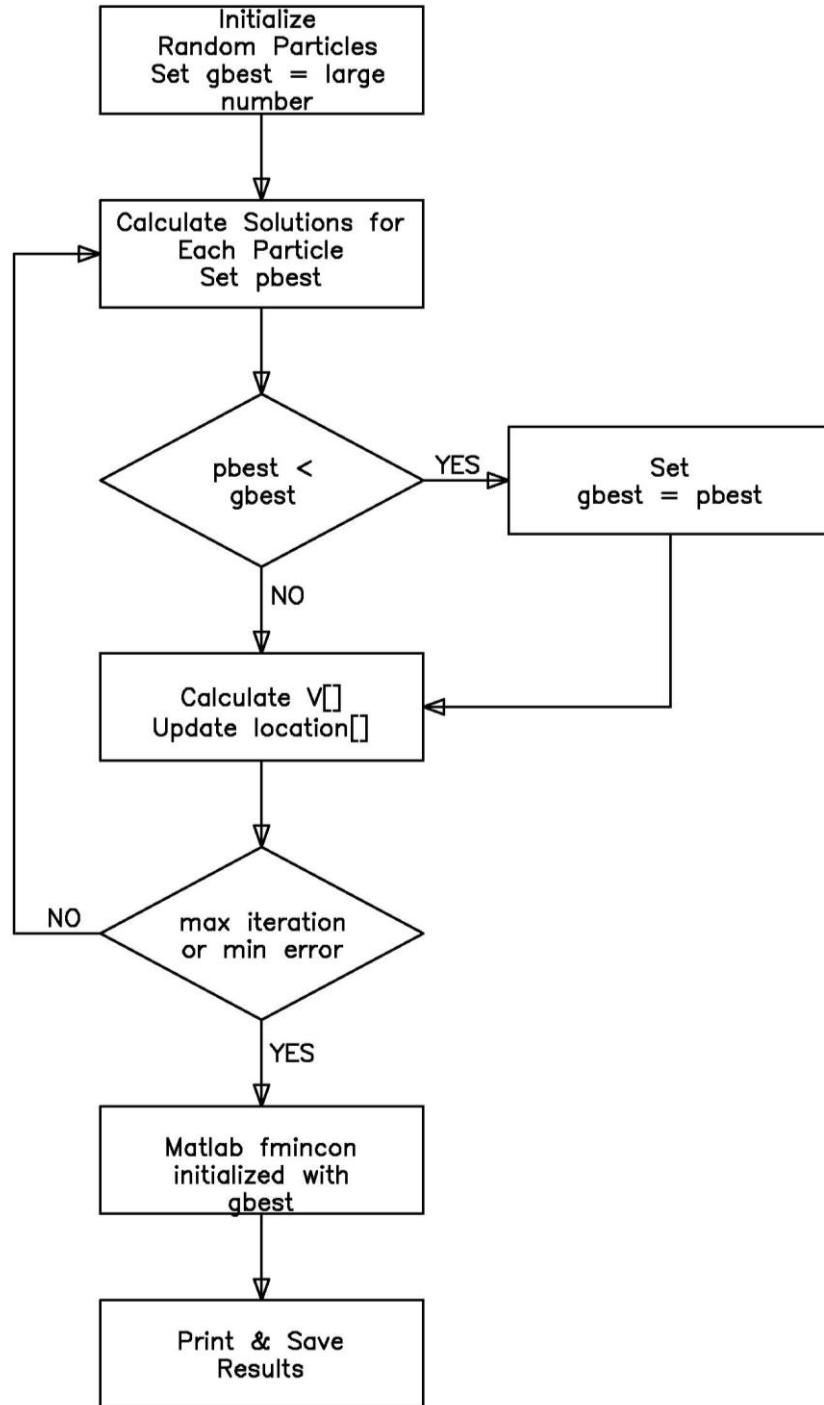


Figure 29. Particle swarm optimizer flowchart

CHAPTER 3

DISCREET OPTIMIZATION OF MMT STRUCTURES

3.1 Application of DSO, FEA, and NN

The side of a typical MMT base component was selected to test the combination of DSO using a branch and bound algorithm while using a parallel training NN method. A structure like the one in Figure 16 was developed. A fully grounded structure was considered. Throughout the design process elements were added and removed and the cross section of the elements were changed. This created a discrete topology and size problem. It was a discrete topology problem because the elements could be located at any of the discrete node locations. Also, removing or adding the elements was considered. The discrete sizing was used because the material properties and cross sections of all the elements were selected from the standard steel cross sections in Table 1. The formal optimization problem can be stated as:

$$\text{Minimize: } W = \sum_{i=1}^{N_e} \rho_i A_i L_i \quad (37)$$

Subject to:

Displacement

$$\frac{\delta_{ik}}{\delta_{\max}} - 1 \leq 0 \quad i = 1, NN; k = 1, 2, 3 \quad (38)$$

Frequency (Eigenvalues)

$$1 - \frac{\lambda}{\lambda_{dist}} \leq 0 \quad (39)$$

Von Mises Stress

$$\frac{\sigma_i}{\sigma_{yield}} - 1 \leq 0 \quad i = 1, NE \quad (40)$$

Euler Buckling

$$\frac{\sigma_i}{\sigma_{bi}} - 1 \leq 0 \quad i = 1, NE \quad (41)$$

Where: NE = total number of elements

NN = total number of nodes(joints)

Subscript k refers to the three coordinate directions

δ_{ik} is the nodal displacement

δ_{max} is the maximum allowable nodal displacement

λ is the first natural frequency of the structure

λ_{dist} is the disturbance frequency caused by the machining

σ_i is the Von Mises stress

σ_{yield} is the yield stress of the material

$$\sigma_{bi} = -(CA)/L^2$$

Where C is a constant. For example, a tubular member with a ratio of diameter to wall thickness of 10 is $C=3.966$ [85]

For typical machine tool design the displacement (rigidity) constraint is very small and therefore critical. The stress and buckling are far from critical so they can be removed from the optimization problem. For this MMT model, only the displacement and eigenvalues were considered for constraints.

Using only two internal elements and limiting the elements to four standard cross sections produces over 450 thousand discrete combinations. Using full enumeration and testing, each combination with FEA would require approximately five days of computational time. These computing time calculations are based on CPU times from a computer with a 2.33GHz Intel Core 2 Duo processor and 1Gbyte of RAM. Although this is not completely impractical, if just a few more members or cross sections are considered the problem becomes impractical and the idea of optimizing a complete MMT component is unobtainable. However, if NN approximation and branch and bound techniques are applied even complete MMT components can become practical. Figure 30 shows the general flow chart for the program. This research used only an interpretive computer language (Matlab). Considerably faster computing times could be realized using a compiler language such as FORTRAN or C thus leading to larger scale problems. It is assumed that similar reductions in CPU times would be realized using the methods developed in this research when implemented with compiled code.

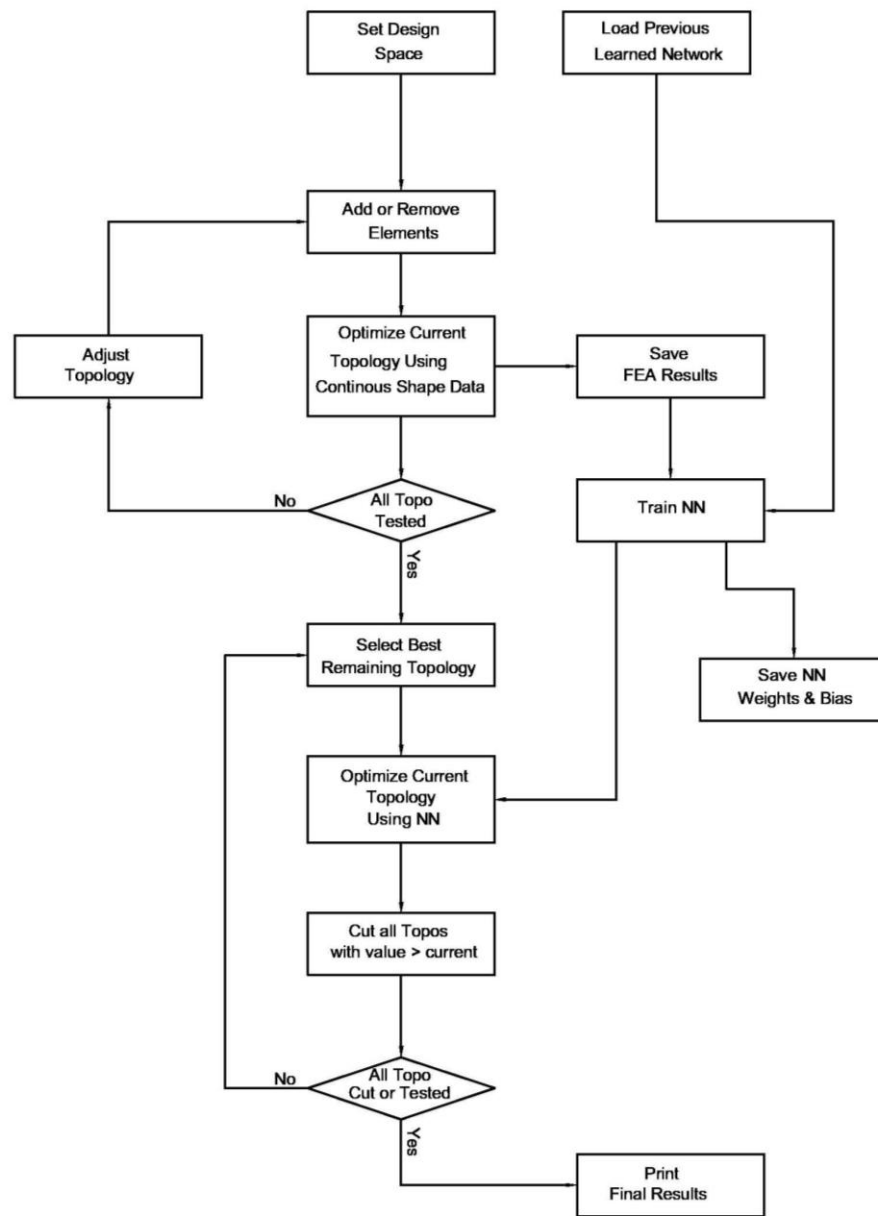


Figure 30. Parallel NN training and branch and bound

A program was developed to test this method on a side of a simple MMT base component like the one shown in Figure 16. Subprograms for the FEA and

NN were developed using Matlab. Even though only one computer was used in these tests the subprograms were used in a parallel method as shown in the flow diagram. These could easily be implemented on separate processors for large scale problems. The method was compared to the standard branch and bound method using only FEA.

Table 8. Optimization results for first load condition

						Total CPU	Volume
Member	1	2	3	4	5	Time (s)	in^3
FEA	L3/4x3/4x1/8	L2x2x1/2	L3/4x3/4x1/8	L3/4x3/4x1/8	L1x1x1/4	14.415	45.5156
NN	L3/4x3/4x1/8	L2x2x1/2	L3/4x3/4x1/8	L3/4x3/4x1/8	L1x1x1/4	1.162	45.5156

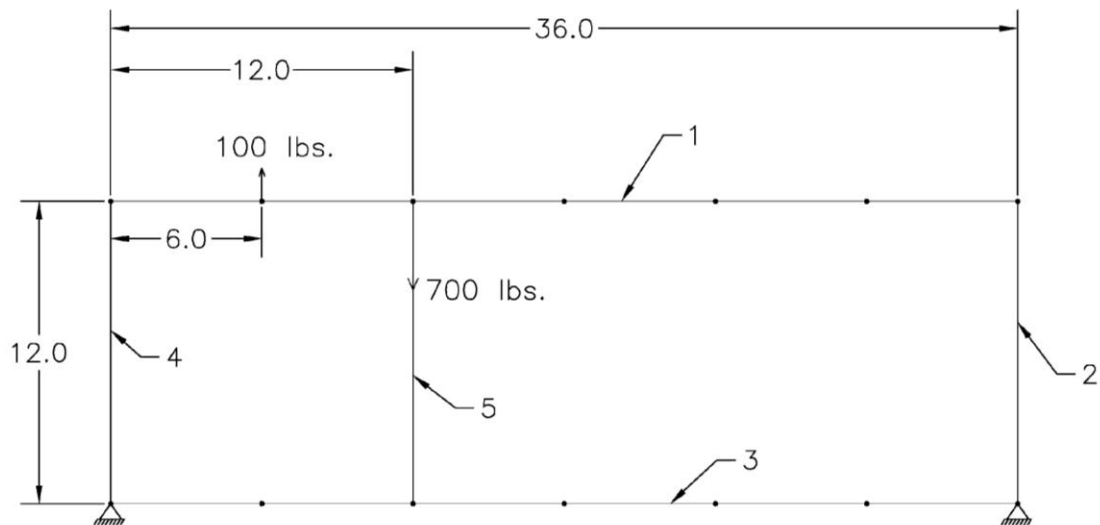


Figure 31. Optimal topology with element numbers for first load condition

Table 8 and Figure 31 show the results of both methods. Both methods have the same topography and material cross sections. However, the NN approach used

much less CPU time. This is a significant reduction in time and this reduction should get larger as the problem gets larger. The reduction in time will increase for two reasons. First, the FEA computations will be longer. Second, since the NN is trained for all the topologies, the time to remesh the FEA will be eliminated. The test was then repeated with the loads applied in different locations to simulate the MMT doing some common type of machining operation. Figure 32, 33, and 34 show the resulting optimal configurations. Table 9, 10, and 11 list the results.

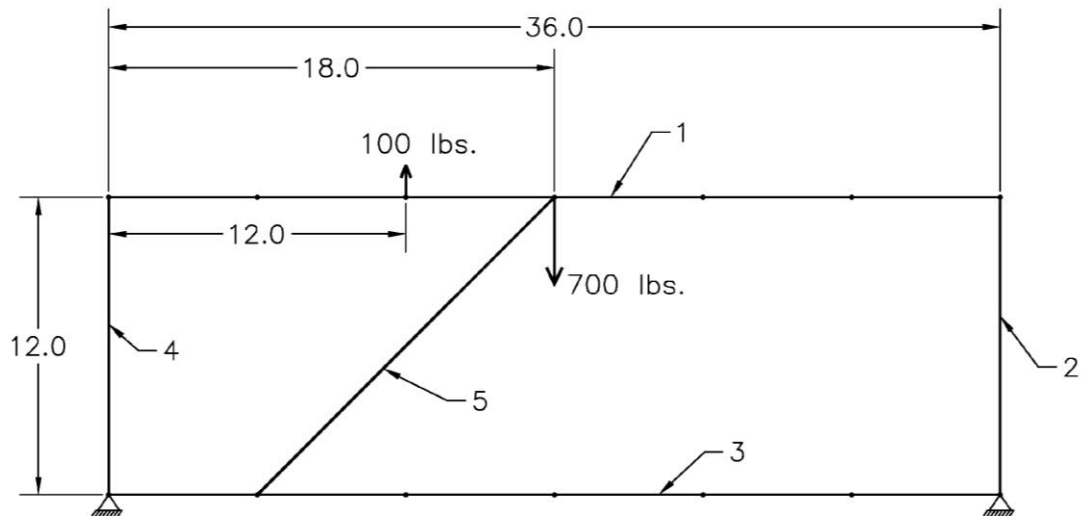


Figure 32. Optimal design for second load location

Table 9. Optimization results for second load condition

Member	1	2	3	4	5	Total CPU Time (s)	Volume in ³
FEA	L1x1x1/4	L2x2x1/2	L3/4x3/4x1/8	L2x2x1/2	L1x1x1/4	58.773	92.6745
NN	L1x1x1/4	L3/4x3/4x1/8	L1x1x1/4	L1x1x1/4	L3/4x3/4x1/8	4.618	75.5262

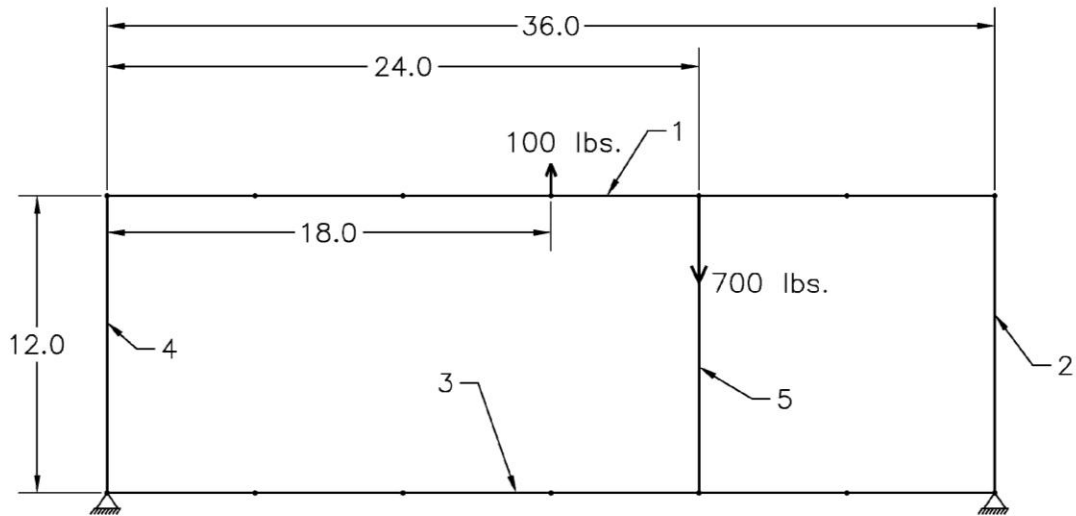


Figure 33. Optimal design for third load location

Table 10. Optimization results for third load condition

Member	1	2	3	4	5	Total CPU Time (s)	Volume in ³
FEA	L1x1x1/4	L2x2x1/2	L3/4x3/4x1/8	L3/4x3/4x1/8	L3/4x3/4x1/8	30.04	61.5469
NN	L1x1x1/4	L2x2x1/2	L3/4x3/4x1/8	L3/4x3/4x1/8	L3/4x3/4x1/8	2.444	61.5469

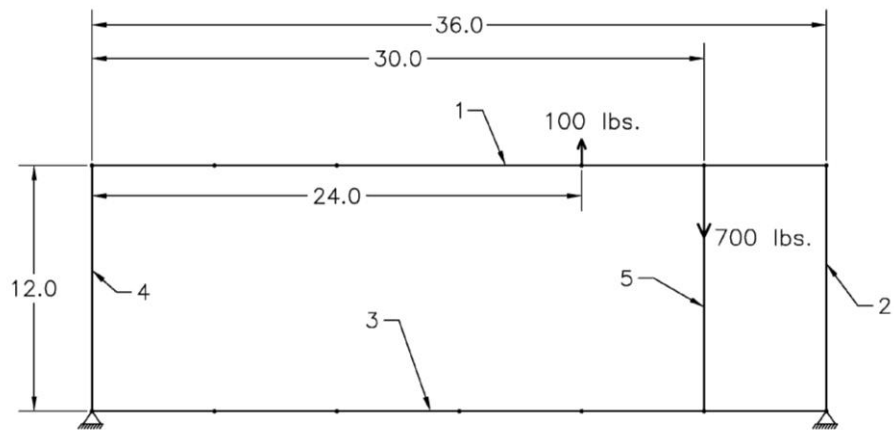


Figure 34. Optimal design for fourth load location

Table 11. Optimization results for forth load condition

Member	1	2	3	4	5	Total CPU Time (s)	Volume in ³
FEA	L1x1x1/4	L1x1x1/4	L3/4x3/4x1/8	L3/4x3/4x1/8	L3/4x3/4x1/8	14.23	50.625
NN	L1x1x1/4	L1x1x1/4	L3/4x3/4x1/8	L3/4x3/4x1/8	L3/4x3/4x1/8	1.202	50.625

3.2 Traditional Topology Optimization

The more traditional methods of topology optimization are well researched and many examples of programming code can be found in the literature [75]. Examples of running code can even be found on the internet [74]. Designs can be submitted and the topology takes shape real-time. Using this online code the typical MMT base-side developed previously was tested.

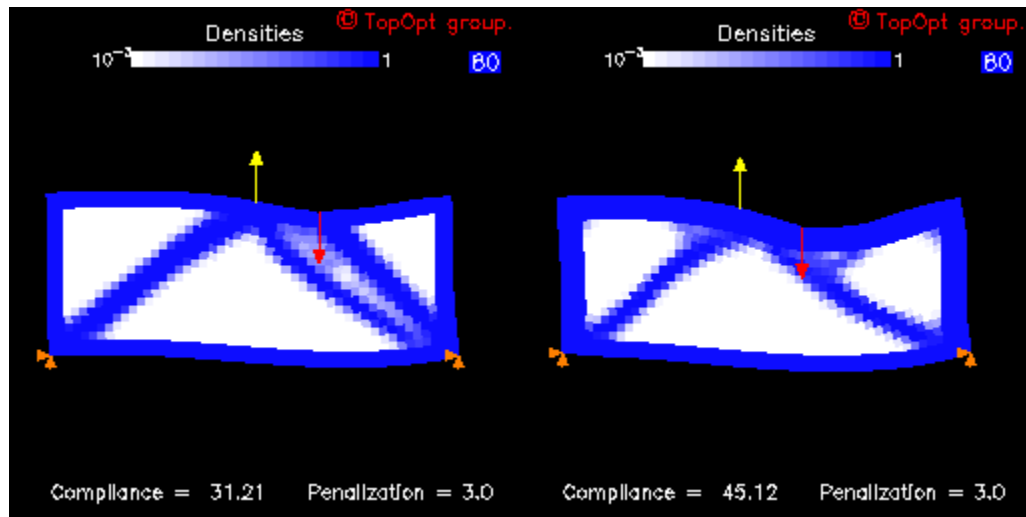


Figure 35. Optimal topology using material density method

Figure 35 shows some typical results from these tests. When compared to the branch and bound method used previously very different results were obtained. This is because the online program is very limited in the number and types of forces and boundary conditions that could be applied.

Several commercial software packages exist for solving topology optimization problems. These programs are closely tied to commercial FEA packages and have the same drawbacks as the commercial FEA packages. For

this research a very robust simple topology optimization routine was utilized. This was done by adding to and modifying Matlab code that was developed by others for public research and education projects [75]. The developers of this code included a simple but effective FEA routine that is built into the topology optimization code. The code was modified to accept the initial and boundary conditions and the applied loads for the two-dimensional MMT base side.

This code was based on the solid isotropic material with penalization (SIMP) approach [76]. In this approach the objective is to minimize the compliance of the system. The formal optimization problem can be stated as:

Minimize:

$$c(x) = U^T K U \quad (42)$$

or in terms of the elements:

$$c(x) = \sum_{e=1}^N (x_e)^p u_e^T k_e u_e \quad (43)$$

Subject to:

$$\frac{V(x)}{V_o} = f$$

$$K U = F$$

$$0 < x \leq 1 \quad \text{To avoid singularity } x \text{ is greater than and not equal to } 0.$$

Where:

U and u_e are the global and elemental displacements

F is the global force vector

K and k_e are the global and elemental stiffness matrices

x is the design variable (relative density)

N is the design domain

p is the penalization constant

$V(x)$ is the material volume

V_o is the design domain volume

f is the prescribed volume fraction

The FEA for this problem was discretized into square elements with nodes at each corner. The nodes had 2 degrees of freedom. The elemental stiffness matrix was derived using the method previously described.

The optimization part of the code used a heuristic updating method that directly follows the literature [56, 75 and 77]. The design variables were formulated as:

$$x_e^{new} = \begin{cases} \max(x_{\min}, x_e - m) \\ \text{if } x_e B_e^n \leq \max(x_{\min}, x_e - m), \\ x_e B_e^n \\ \text{if } \max(x_{\min}, x_e^{-m}) < x_e B_e^n < \min(1, x_e + m), \\ \min(1, x_e + m) \\ \text{if } \min(1, x_e + m) \leq x_e B_e^n \end{cases} \quad (44)$$

Where:

m is the move limit

n is the damping coefficient and is set to 0.5

B_e is the optimality condition

$$B_e = \frac{-\frac{\partial c}{\partial x_e}}{\lambda \frac{\partial V}{\partial x_e}} \quad (45)$$

Where:

λ is the Lagrangian multiplier

$\frac{\partial c}{\partial x_e}$ is the sensitivity of the objective function, and

$$\frac{\partial c}{\partial x_e} = -p(x_e)^{p-1} u_e^T k_e u_e \quad (46)$$

One major problem existed with implementing this approach. The existence of a solution was not ensured and the results were sensitive to how refined the domain was discretized. Spatial zones of oscillation occurred frequently. This is commonly called the checker-boarding phenomenon [56, 77, 78, and 79]. A filter method that was adapted from digital image processing was shown to reduce or eliminate these problems [75]. Directly following the literature the mesh-independent filter is [74 and 75]:

$$\frac{\partial c}{\partial x_e} = \frac{\frac{1}{N}}{x_e \sum_{f=1}^N \hat{H}_f} \sum_{f=1}^N \hat{H}_f x_f \frac{\partial c}{\partial x_f} \quad (47)$$

Where:

$$H_f = r_{\min} - \text{dist}(e, f), \{f \in N \mid \text{dist}(e, f) \leq r_{\min}\}, e = 1, \dots, N$$

The new mesh-independent filtered sensitivities (47) are used in place of the original sensitivities (46).

This code was tested on the typical MMT base-side. Figure 36 shows the results with the same loads and boundary conditions from the previous test applied.

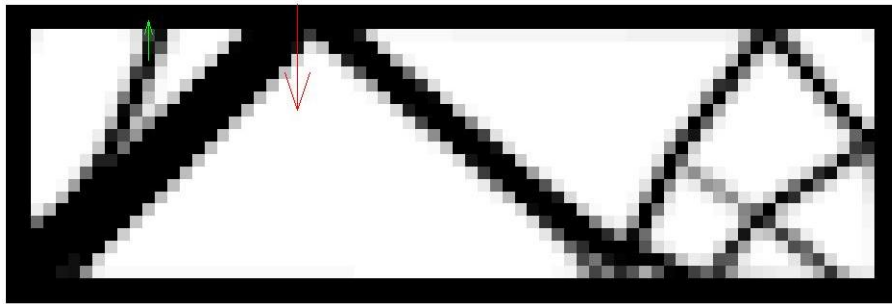


Figure 36.(a) Load Case 1

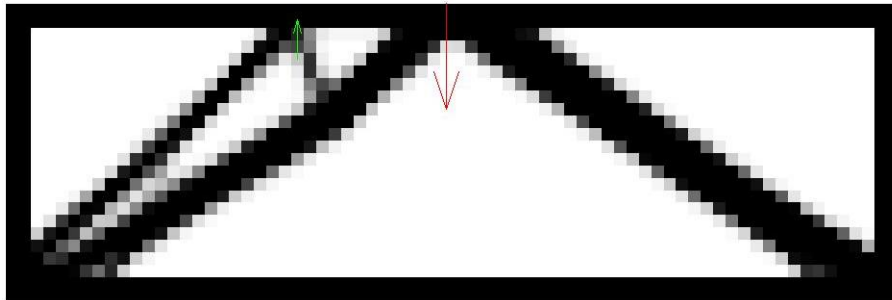


Figure 36.(b) Load Case 2

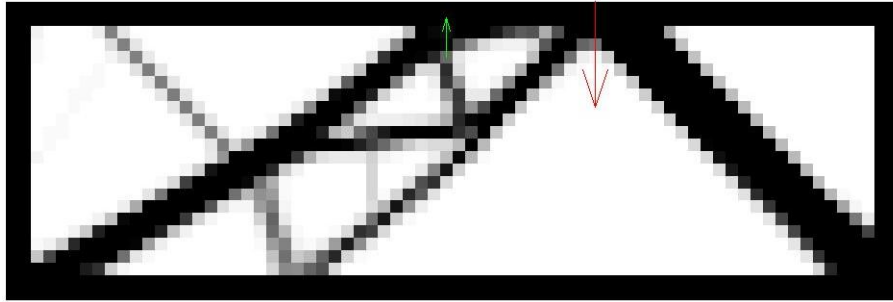


Figure 36.(c) Load Case 3

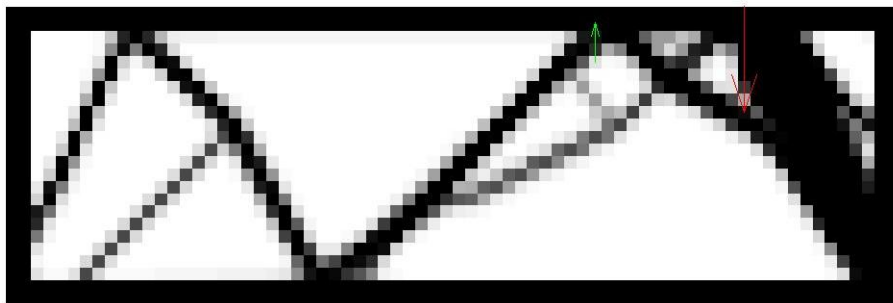


Figure 36.(d) Load Case 4

Figure 36. Optimal topology using material distribution method

These results show very different topologies than the ones from the branch and bound method. There are several reasons for the differences. First, the branch and bound method used a constrained optimization method with very small constraints on the displacement (x , y and rotation around z for the nodes along the top edge of the structure) and natural frequency and the material volume was minimized. The material distribution method minimized the compliance of the structure and the material volume was an equality constraint.

Sankaranarayanan et al. compared topology optimization of trusses for minimum weight using a method with stress and displacement constraints to a method using a minimum compliance constraint. They showed for some truss problems the stress and displacement constraint method produced different and generally better results [84]. Second, the branch and bound includes the inherent constraints that the members must be terminated at discrete nodes. Finally, the literature suggests the material distribution method may not be the most effective for layout problems like this if the prescribed fraction of material volume is too low compared to the design domain volume [75 and 76]. For this code and this problem, it was found that it failed to converge with prescribed volumes less than approximately 25 percent. It was also found through experimentation that the online code failed to converge with prescribed volumes less than approximately 25 percent. However, feasible optimal designs were found that had less than 10 percent of the actual design domain using the branch and bound method. Some topologies were found to have less than 4 percent. Actually, for most structural steel designs, using standard shapes and minimizing the amount of steel used, this material distribution method may not be effective because the space frame or truss would generally include less than 25 percent of the total volume. This method would be better suited for plastic molded, cast metal, or formed sheet metal designs where the material volume is a greater percent of the total design space and rib or reinforcing member location would be total a continuous variable.

The test was repeated. This time a lateral force was add along with the vertical force to simulate a typical milling operation. The results from the branch and bound method using NN is shown in figure 37. Figure 38 through 41 show the results from the material density method with varying amounts of percent material. As expected with lower amounts of material (25% to 30%) the method tends to converge slowly on a solution. With larger amounts of material the results are close to the branch and bound method and the topologies are similar.

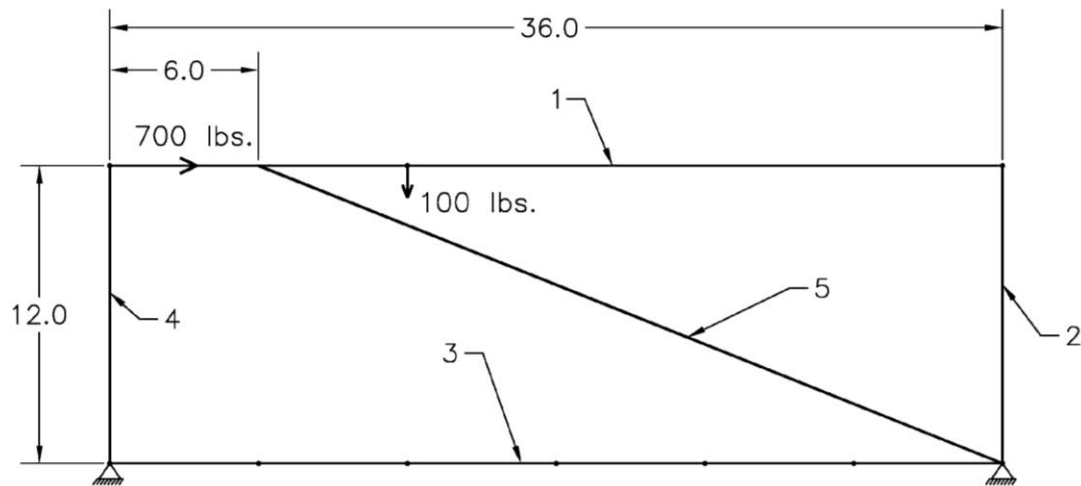


Figure 37. Discrete optimization using NN with lateral load

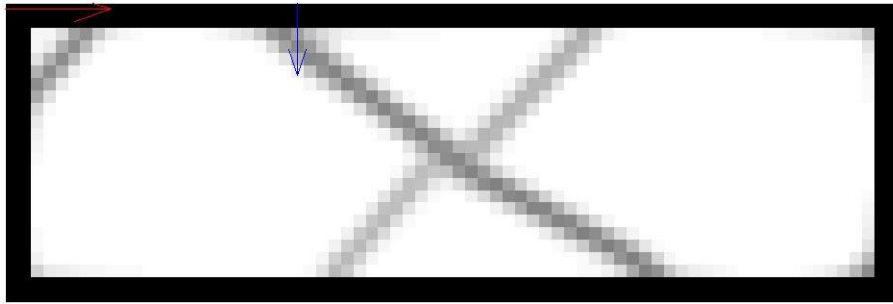


Figure 38. Discrete optimization using the material density method and 25% volume

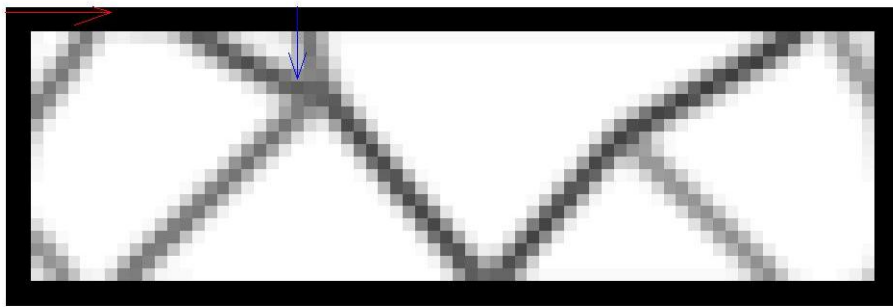


Figure 39. Discrete optimization using the material density method and 30% volume

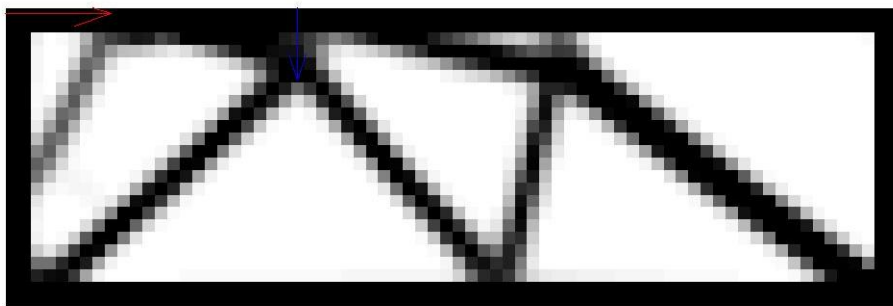


Figure 40. Discrete optimization using the material density method and 40% volume

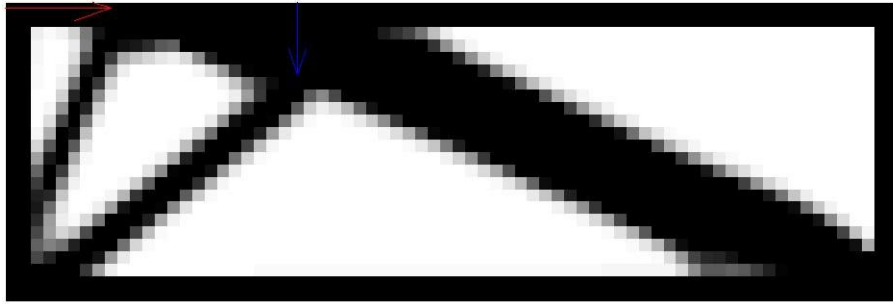


Figure 41. Discrete optimization using the material density method and 50% volume

3.3 Large Scale MMT Base Optimization

The use of the branch and bound DSO routine was tested on a typical MMT base. This included using a hybrid continuous optimization approach for each branch. This combined a traditional gradient based method with the PSO method. The inputs and results from each branch or topology were saved and later used for the NN training. After the initial NN was trained for the first topology the weights and biases were saved for future training. Nonsymmetrical multiple loads were applied to simulate a typical machining operation. A common MMT base size of 36"x12"x12" was selected. A set of 3 standard L channel steel shapes that ranged in flange size from $\frac{3}{4}$ " to 2" and in flange thickness from $\frac{1}{8}$ " to $\frac{1}{2}$ " were selected as the discrete set. Table 12 shows the DSO results along with the CPU times.

Table 12. Element sections and CPU times for 3D MMT base

Element Number	Standard Steel L Shape
1	L3/4x3/4x1/8
2	L2x2x1/2
3	L3/4x3/4x1/8
4	L2x2x1/2
5	L2x2x1/2
6	L3/4x3/4x1/8
7	L2x2x1/2
8	L3/4x3/4x1/8
9	L2x2x1/2
10	L1x1x1/4
11	L1x1x1/4
12	L2x2x1/2
13	L1x1x1/4
14	L2x2x1/2
CPU Time	6h 19min.

One result that should be noted from this test is that the NN training for this large scale problem was approximately 5 minutes. This is insignificant compared to the over 6 hours it took to solve this 3 dimensional large-scale problem. Given the number of function calls required to solve this problem using the NN approach and the average time for the FEA of this structure, the problem would take approximately 150 hours to solve just using FEA. This is not impossible, but it is impractical and was not completed for this case. The code for this project was developed entirely on an interpretative based computer language. If it was developed or converted to a compiled language such as FORTRAN much lower CPU times could be realized. However, the relative reduction in times is a good indication of how effective this approach is on practical industrial problems. The final optimal topology with the applied loads is shown in Figure 42. To help visualize the results and topology a Matlab function was developed that

created an AutoLISP program. This AutoLISP program was then run in AutoCAD to produce a detail 3D drawing of the final design (Figure 43). This is useful in not only seeing the topology but the orientation of the cross sections of the steel shapes.

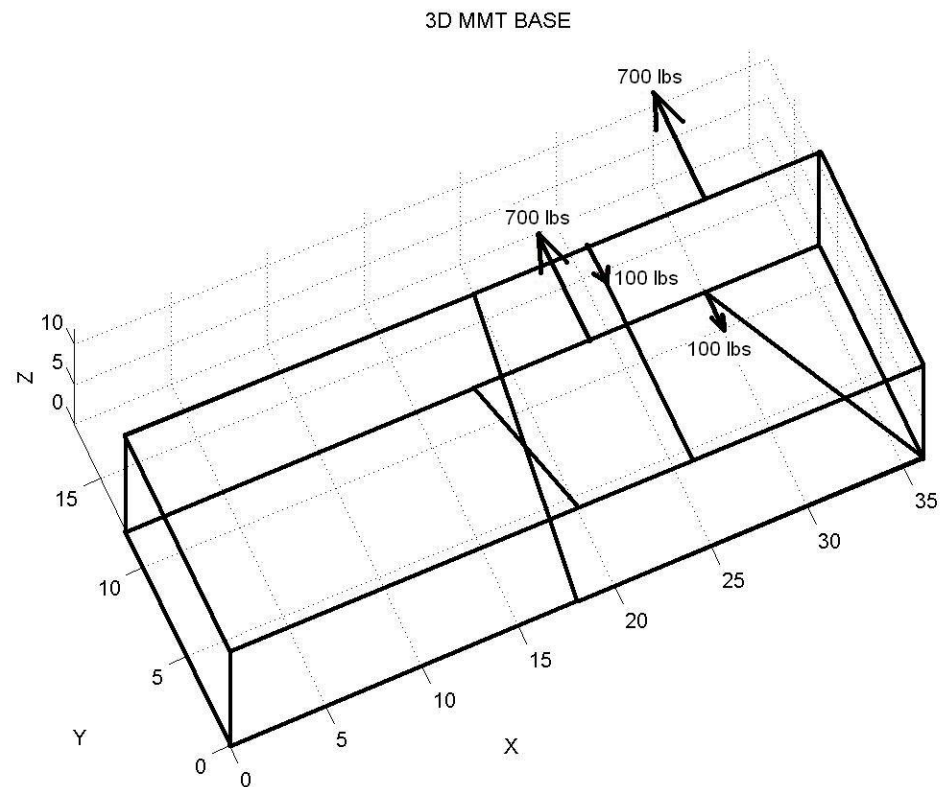


Figure 42. The optimal topology with applied loads

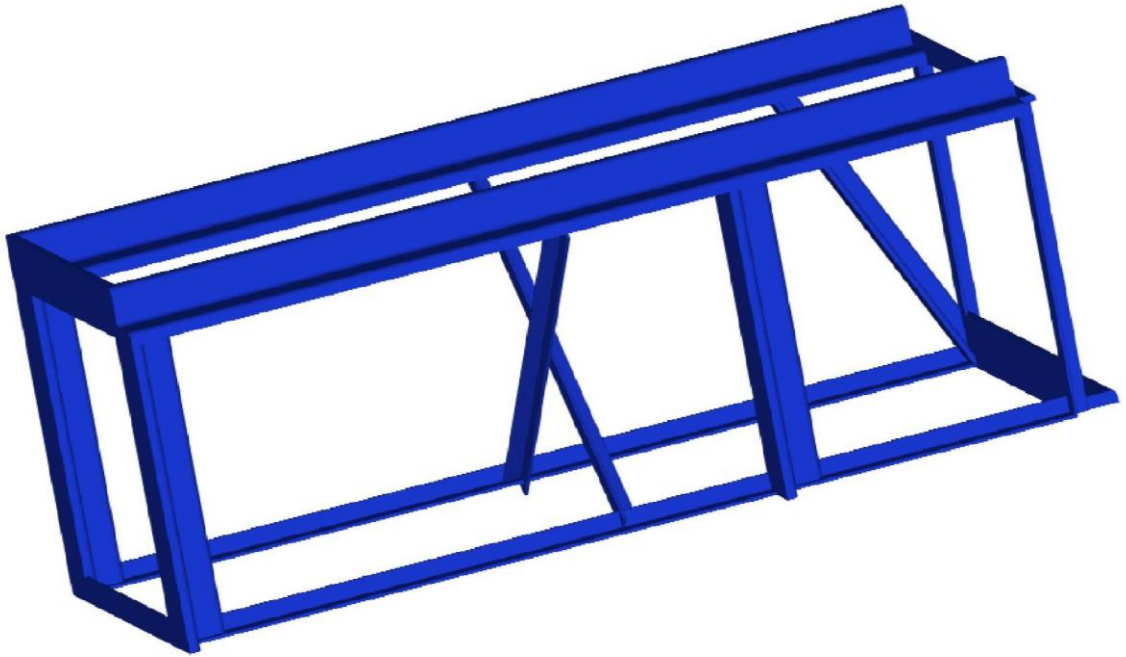


Figure 43. Program generated 3D model

CHAPTER 4

CONCLUSTION AND FUTURE WORK

4.1 Conclusion

A unique and novel method of discrete optimization has been developed for the design of MMT components. A branch and bound method was used that included a method that was parallel in nature to generate the data needed to train a feed-forward NN. The continuous optimization of the individual branches used a hybrid method that combined particle swarm and traditional gradient base optimization. This hybrid method proved effective in optimizing the piecewise continuous branches while at the same time generating data that became useful for training the NN. The feed-forward NN was then shown to be effective at not only approximating the FEA but also the inherent memory of the network became useful for approximating similar disigns. The method was tested on a large scale 3D problem and it was shown that using only the FEA the problem becomes impractical but implementing the NN along with the FEA makes it feasible. The overall results from this research can be summarized as follows:

- The use of a feed-forward NN was very effective as a FEA approximator.
- The NN was effective at approximating more than just the FEA, for example, multiple meshings of the FEA, multiple topologies, and eigenfrequencies.

- The hybrid approach was required for the continuous part of the branch and bound method because of all the local minimums. This also helped generate the training data for the NN.
- The traditional material distribution methods of topological optimization are not suited to this type of discrete structural optimization problem because the amount of material volume compared to the total design space volume is very small.
- The method was successful on a large-scale structure that would be impractical using other methods.

4.2 Future Research

In this problem the FEA was limited to linear elastic members. This method of using NN approximation should be very effective on non-linear elements. Fluid mechanics, heat transfer, and impact problems are just a few of the FEA problems that when applied to large-scale optimization problems are computationally expensive. The NN's in these cases could be taught whole families of similar problems with many of the pre and post processing operations included in the NN.

All of the joints in this research were considered to be fixed and solid. Referring to Figure 42 it can be seen that some of the joints would be impossible to connect. This is because the optimization routine considered the orientation of the cross sections. Also, a completely fixed solid joint is not practical. A

complete study of the joints should be considered. A method of quickly building and recycling of MMT components will require a complete and detail design of the joints.

The NN structure is very significant in the success of the structure optimization. In this study, large NN structures were used. This structure was large enough to handle any of the topologies and parameters. However, the structure was almost always larger than required. Further studies should include an adaptive type of NN structure.

The whole branch and bound process and the NN method is inherently parallel. It would take very little effort to convert the code used in this research to run over a network on multiple computers. Each continuous branch or topology could be optimized on a separate computer. Then, as each branch finished each computer could start training individual NN's. The NN's could then easily be implemented on multiple computers. Further research on very large scale nonlinear optimization could be realized using many computers over a network or the internet.

REFERENCES

1. The American Society of Mechanical Engineers, *Modular Machine Tool Standards*, ASME B5.43M – 1979.
2. J.K. Lenstra, A.H.G. Rinnooy Kan, and A. Schrijver, “History of Mathematical Programming”, *Stichting Mathematisch Centrum*, 1991.
3. L. Fortnow, S. Homer, *A Short History of Computation Complexity, The History of mathematical Logic*, North-Holland, Amsterdam, 2002/2003.
4. Venkataraman, P., *Applied Optimization with Matlab Programming*, John Wiley & Sons, Inc, New York, 2002
5. Vanderplaats, G. N., *Numerical Optimization Techniques for Engineering Design with Applications*, McGraw-Hill, 1984.
6. Chapman, C.D. and Jakiela, M.J., “Genetic Algorithm-Based Structural Topology Design with Compliance and Topology Simplification Considerations”, *J. of Mechanical Design*, v.118, pp.89-98, 1996.
7. Reddy, G.M. and Cagan,J., “An improved Shape Annealing Algorithm for Truss Topology Generation”, *J. of Mechanical Design*, V.117, pp.315-321,1995.
8. Shea, K., Cagan, J. and Fenves, S.J.,”A Shape Annealing Approach to Optimal Truss Design With Dynamic Grouping of Members”, *J. of Mechanical Design*, v.119, pp.388-394, 1997.
9. Lu, K. and Kota, S., “Topology and Dimensional Synthesis of Compliant Mechanisms Using Discrete Optimization”, *J. of Mechanical Design*, v.128, pp.1080-1091, 2006.
10. Thanedar, P.B. and Vanderplaats, G.N., “Survey of Discrete Variable Optimization for Structural Design”, *J. of Structural Engineering*, v.121, issue 2, pp. 3001-3006, 1995.
11. Gutkowski, W., *Discrete Structural Optimization*, International Center for Mechanical Sciences, Springer Wien, New York, 1997.
12. Parker, R. G., and R. L. Rardin, *Discrete Optimization*, Academic Press, Boston, 1988.

13. Foulds, L. R., *Optimization Techniques An Introduction*, Springer-Verlag, New York, 1981.
14. Land, A and A. Doig, "An Automatic Method of Solving Discrete Programming Problems", *Econometrica* 28:497-520, 1960.
15. Dakin, R. S., "A Tree Search Algorithm for Mixed Integer Programming Problems", *Computer J.* 8:250-255, 1965.
16. Little, J. D. C., K. G. Murty, D. W. Sweeney, and C. Karel, "An Algorithm for the Traveling Salesman Problem", *Operations Research*, 11:972-989, 1963.
17. Edmonds, J., "Optimum Branchings", *Journal of Research of the National Bureau of Standards*, B71:233-240, 1967.
18. Gupta, O. K. and A. Ravindran, "Nonlinear Integer Programming and Discrete Optimization", *Journal of Mechanical Design*, 105:106-164, 1983.
19. Roth R. H., "An Approach to Solving Linear Discrete Optimization Problems", *Journal of the Ass. for Computing Machinery*, Vol. 17, No. 2, pp. 303-313, 1970.
20. Goldstein, A. J. and A. B. Lesk, "Common Feature Techniques for Discrete Optimization", *Proceedings of the 13th Conference on Design Automation IEEE*, pp. 232-244, San Francisco, CA, 1976.
21. More, J. J., R. A. Tapia, and M. H. Wright, "Optimization", *Program Directions for Computational Mathematics - DOE*, 1979.
22. Sergienko, I. V., "Trends in the Development of Methods of Discrete Optimization and Their Software Base", *Cybernetics*, vol. 18 no. 6 pp. 754-764, 1982.
23. Shcherbina, O. A., "Tree Decomposition and Discrete Optimization Problems: A Survey", *Translated from Kibernetika I Sistemnyi Analiz*, No. 4 pp. 102-118, 2007.
24. Balling, R. J., "Optimal Steel Frame Design by Simulated Annealing", *Journal of Structural Engineering*, vol. 106 no. 6 pp. 1780-1795, 1991.

25. Kocer, F. Y. and J. S. Arora, "Standardization of Steel Pole Design Using Discrete Optimization", *Journal of Structural Engineering*, vol. 123 no. 3 pp. 345-349, 1997.
26. Rajeev, S. and C. S. Krishnamoorthy, "Discrete Optimization of Structures Using Genetic Algorithms", *Journal of Structural Engineering*, vol. 118 no. 5 pp. 1233-1250, 1992.
27. Koumoussis, V. K. and P. G. Georgiou, "Genetic Algorithms in Discrete Optimization of Steel Truss Roofs", *Journal of Computing in Civil Engineering*, vol. 8 no. 3 pp. 309-325. 1994.
28. Camp, C., S. Pezeshk, and G. Cao, "Optimized Design of Two-Dimensional Structures Using a Genetic Algorithm", *Journal of Structural Engineering*, vol. 124 no. 5 pp. 551-559. 1998.
29. Lu, K. and S. Kota, "Topology and Dimensional Synthesis of Compliant Mechanisms Using Discrete Optimization", *Journal of Mechanical Design*, 128:1080-1091, 2006.
30. Lee, K. S. and Z. W. Geem, "A new Structural Optimization Method for Structures with Discrete Sizing Variables", *Computers and Structures*, vol. 82 issue 9-10 pp. 781-798, 2004.
31. Clerc, M, *Particle Swarm Optimization*, ISTE Ltd., Newport Beach, CA, 2006.
32. Engelbrecht, A. P., *Fundamentals of Computational Swarm Intelligence*, John Wiley & Sons, West Sussex, England, 2005.
33. Bayazit, O. B., J-M. Lien, and N.M. Amato, "Roadmap-Based Flocking for Complex Environments", *Proceedings of the 10th Pacific Conference on Computer Science and Applications*, pp. 104-113, 2002.
34. Mataric, M. J., "Interaction and Intelligent Behavior", PhD Dissertation, Department of Electrical and Computer Engineering, MIT, 1994.
35. Reynolds, C. W., "Flocks, Herds, and Schools: A Distributed Behavioral Model", *Computer Graphics*, vol. 21 no. 4 pp. 25-34, 1987.
36. Partridge, B. L., "The Structure and Function of Fish Schools", *Scientific American*, 246:114-123, 1982.

37. Parsopoulos, K. E. and M. N. Vrahatis, "Particle Swarm Optimizer in Noisy and Continuously Changing Environments", *Proceedings of the IASTED International Conference on Artificial Intelligence and Soft Computing*, pp. 289-294, 2001.
38. Brits, R., "Niching Strategies for Particle Swarm Optimization", Master Thesis, Department of Computer Science, University of Pretoria South Africa, 2002.
39. Brits, R., A. P. Engelbrecht, and F. Van den Bergh. „A Niching Particle Swarm Optimizer“, *Proceedings of the 4th Asia-Pacific Conference on Simulated Evolution and Learning*, pp.692-696, 2002.
40. Brits, R., A. P. Engelbrecht, and F. Van den Bergh, "Solving Systems of Unconstrained Equations using Particle Swarm Optimization", *Proceedings of the IEEE Conference on Systems, Man, and Cybernetics*, 3:102-107, 2002.
41. Parsopoulos, K. E. and M. N. Vrahatis. "Initializing the Particle Swarm Optimizer using the Nonlinear Simplex Method", *Advances in Intelligent Systems, Fuzzy Systems, Evolutionary computation*, pp. 216-221, 2002.
42. Kennedy, J. and R. Eberhart, "Particle Swarm Optimization", *Proceedings of the IEEE International Joint Conference on Neural Networks*, pp. 1942-1948, 1995.
43. Kennedy, J. and R. Eberhart, "A New Optimizer Using Particle Swarm Theory", *6th International Symposium on Micro Machine and Human Science*, pp. 39-43, 1995.
44. Song, M-P. and G-C. Gu, "Research on Particle Swarm Optimization: A Review" *Proceedings of the 2004 Interenational Conference on Machine Learning and Cybernetics*, 4:2236-2241, 2004.
45. Langdon, W. B. and R. Poli, "Evolving Problems to Learn About Particle Swarm Optimizers and Other Search Algorithms", *IEEE Transactions on Evolutionary Computation*, vol. 11 no. 5 pp.561-578, 2007.
46. Angeline, P., "Evolutionary Optimization Versus Particle Swarm Optimization: Philosophy and performance difference", *Proceedings of the Evolutionary Programming Conference*, San Diego, 1998.

47. Li, L. J., Z. B. Huang, F. Liu, and Q. H. Wu, "A Heuristic Particle Swarm Optimizer for Optimization of Pin Connected Structures", *Computers and Structures*, 85:340-349, 2007.
48. Camp, C. V., B. J. Bichon, and S. P. Stovall, "Design of Steel Frames Using Ant Colony Optimization", *Journal of Structural Engineering*, vol. 131 no. 3 pp. 369-379, 2005.
49. Perez, R. E. and K. Behdinan, "Particle Swarm Approach for Structural Design Optimization", *Computers and Structures*, 85:1579-1588, 2007.
50. Jansson, N., W.D. Wakeman, J.-A.E. Manson, Optimization of Hybrid Thermoplastic Composite Structures Using Surrogate Models and Genetic Algorithms, *Composite Structures*, **80** 21-31, Elsevier 2007
51. Sakata, S., F. Ashida, M. Zako, Structural Optimization Using Kriging Approximation, *Comput. Methods Appl. Mech. Engrg.* **192**, 923-939, Elsevier 2003.
52. Shao, T., S. Krishnamurty, "Surrogate Model Updating Using Clustering in a Genetic Algorithm Setup", *ASME 2006 international Design Engineering Technical Conferences & Computers and Information in Engineering Conference*, DETC2006-99491, Philadelphia, PA, 2006.
53. Rikards, R., H. Abramovich, J. Auzins, A. Korjamins, O. Ozolinsh, K. Kalnins, T. Green, "Surrogate Models for Optimum Design of Stiffened Composite Shells", *Composite Structures*, **63**, 243-251, 2004.
54. Bisangi, C., L. Lanzi, "Post-buckling optimization of composite stiffened panels using Neural Networks", *Compos. Struct.*, **58**, 237-247, 2002.
55. Carpenter, W.C., J.F.M. Barthelemy, A Comparison of Polynomial Approximations and Artificial Neural Nets as Response Surfaces, A Collection of Technical Papers, *The 33rd AIAA/ASME/ASCE/AHS/ASC Structures, Structural Dynamics, and Materials Conference*, Dallas, TX, 1992.
56. Bendsoe, M.P., *Optimization of Structural Topology, Shape, and Material*, Springer-Verlag, Berlin, Germany, 1995.
57. Huebner, K., Dewhirst, D., Smith, D., and Byrom, T., *The Finite Element Methods for Engineers*, John Wiley & Sons, Inc., New York, 2001.

58. Liang, Q.Q., *Performance-based Optimization of Structures*, Spon Press, New York, 2005.
59. Rozvany, G.I.N., *Topology Optimization in Structural Mechanics*, Springer Wien, New York, 1997.
60. Lin, Y., Zhang, Y., and Harby, D., "Development of a Digital Case Library for Mechanical Design Education", *Proceedings of Capstone Design Forum*, Seoul, Korea, 2003.
61. Lin, Y., Harby, D., Jang, D., and Zheng, W., "Teaching Capstone Design in the Globalization Environment", *Proceedings ASEE Annual Conference and Exposition*, Salt Lake City, UT, 2004.
62. Lin, Y. and Harby, D., "Web-based Tools and Course Materials for Teaching Capstone Design internationally", *Proceedings ASEE Annual Conference and Exposition*, Chicago, IL, 2006.
63. Smith, D., Class Notes MAE401, University of Missouri-Columbia, 2005.
64. Pai, P. F., Class Notes MAE7208, University of Missouri-Columbia, 2004.
65. Reddy, J.N., *An Introduction to the Finite Element Method*, McGraw-Hill, 1993.
66. Zienkiewicz, O.C., and Taylor, R. L., *The Finite Element Method, vol. 1 Basic Formulation and Linear Problems*, McGraw-Hill, 1989.
67. Zienkiewicz, O.C., and Taylor, R. L., *The Finite Element Method, vol. 2 Solid and Fluid Mechanics, Dynamics and Non-linearity*, McGraw-Hill, 1989.
68. Harby, D., "Real-time Statistical Process Controller", M.S. Thesis, University of Missouri – Columbia, MO 2000.
69. Demuth, H., Beale, M., and Hagan, M., *Neural Network Toolbox User's Guide*, The MathWorks, Inc., Natick, MA, 2006.
70. Liu, Y., "Efficient Methods for Structural Analysis of Built-up Wings", PhD Dissertation, Virginia Polytechnic Institute and State University, 2000.

71. Nemhauser, G. L. and L. A. Wolsey, *Integer and Combinational Optimization*, John Wiley & Sons, New York, 1988.
72. Doherty, D., M. A. Freeman, and R. Kumar, "Optimization with MATLAB and the Genetic Algorithm and Direct Search Toolbox", *Matlab Digest*, <http://www.mathworks.com> , 2004.
73. Hu, X., "Particle Swarm Optimization: Tutorial", <http://www.swarmintelligence.org/tutorials.php>, 2006.
74. Sigmund, O, <http://www.topopt.dtu.dk>, 2007.
75. Sigmund, O., "A 99 line topology optimization code written in Matlab", *Struct Multidisc Optim* 21, 120-127, Springer-Verlag 2001.
76. Bendsoe, M.P., "Optimal shape design as a material distribution problem", *Struct. Optim.* 1, 193-202, 1989.
77. Bendsoe, M.P., "Generating Optimal Topologies in Structural Design Using a Homogenization Method", *Computer methods in applied mechanics and engineering*, 71, 197-224, 1988.
78. Sigmund, O., Petersson, J., "Numerical instabilities in topology optimization: a survey on procedures dealing with checkerboards, mesh-dependencies", *Struct Multidisc Optim*, 16, 68-75, Springer – Berlin, 1998.
79. Beckers, M., "Topology optimization using a dual method with discrete variables", *Structural Optimization*, 17, 14-24, Springer-Verlag 1999.
80. Sasena, M., P. Papalambros, and P. Goovaerts, "Global Optimization of Problems with Disconnected Feasible Regions Via Surrogate Modeling", *9th AIAA/ISSMO Symposium on Multidisciplinary Analysis and Optimization*, AIAA2002-5573, Atlanta, GA, 2002.
81. Pai, P. F., *Geometrically Exact Structural Analysis (GESA) User's Guide*, Mechanical and Aerospace Engineering Department, University of Missouri, Columbia, 2004.
82. Cheng, G. D., Z. Jiang, "Study on topology Optimization with Stress Constraints", *Eng. Opt.*, 20:129-148, 1992.
83. Cheng, G. D., "Some Aspects of Truss Topology Optimization", *Structural Optimization*, vol. 10, issue 3-4, pp. 173-179, 1995.

84. Sankaranarayanan, S., R. T. Haftka, and R. K. Kapania, "Truss Optimization with Simultaneous Analysis and Design", *AIAA Journal*, vol. 32, no. 2, pp. 420-424, 1994.
85. Beer, F. P, and Johnston, Jr., E. R., *Mechanics of Material*, McGraw-Hill, New York, 1981.

APPENDIX

Appendix A: MATLAB FEA Functions

```
function [x, ielem]=mymesh()
global X b h d enac num_ele
% this function generates the mesh for a typical
%MMT base structure
% %uncomment the following for testing
% b=36;
% h=12;
% d=12;

j=0;
for i=1:enac+1
    x(i,1)=j;
    x(i,2)=h;
    x(i,3)=0;
    x(i+enac+1,1)=j;
    x(i+enac+1,2)=0;
    x(i+enac+1,3)=0;
    x(i+(enac+1)*2,1)=j;
    x(i+(enac+1)*2,2)=h;
    x(i+(enac+1)*2,3)=d;
    x(i+(enac+1)*3,1)=j;
    x(i+(enac+1)*3,2)=0;
    x(i+(enac+1)*3,3)=d;
    j=j+(b/enac);
end
for i=1:enac
    ielem(i,1)=i;
    ielem(i,2)=i+1;
    ielem(i+enac,1)=i+enac+1;
    ielem(i+enac,2)=i+enac+2;
    ielem(i+enac*2,1)=i+enac*2+2;
    ielem(i+enac*2,2)=i+enac*2+3;
    ielem(i+enac*3,1)=i+enac*3+3;
    ielem(i+enac*3,2)=i+enac*3+4;
end
tot_ele=enac*4;
cn1=1; cn2=enac+1; cn3=enac+2; cn4=(enac+1)*2; cn5=2*enac+3;
cn6=(enac+1)*3; cn7=3*enac+4; cn8=(enac+1)*4;
ielem(tot_ele+1,:)= [cn1 cn3];
ielem(tot_ele+2,:)= [cn2 cn4];
ielem(tot_ele+3,:)= [cn5 cn7];
```

```

ielem(tot_ele+4,:)=cn6 cn8];
ielem(tot_ele+5,:)=cn1 cn5];
ielem(tot_ele+6,:)=cn3 cn7];
ielem(tot_ele+7,:)=cn2 cn6];
ielem(tot_ele+8,:)=cn4 cn8];

% add stiffners that are not part of the optimization
ielem(tot_ele+9,:)=4 25];
ielem(tot_ele+10,:)=11 18];

%extra elements
if num_ele==1
    ielem(tot_ele+11,:)=round(enac/b*X(1,1))+1 round(enac/b*X(2,1))+8];
end

if num_ele == 2
    ielem(tot_ele+11,:)=round(enac/b*X(1,1))+1 round(enac/b*X(2,1))+8];
    ielem(tot_ele+12,:)=round(enac/b*X(3,1))+15 round(enac/b*X(4,1))+22];
    %***** add two ielem for extra elements
End

function eleprop=myeleprop(L)
global enac num_ele

vl=size(L,1);
L2=L(1:vl/2)*1.25+0.75;
t=L(vl/2+1:vl)*.375+.125;

%set up the element properties
for i=1:enac
    eleprop(i,:)=Lsection(L2(1),t(1));
    eleprop(i+enac,:)=Lsection(L2(2),t(2));
    eleprop(i+enac*2,:)=Lsection(L2(3),t(3));
    eleprop(i+enac*3,:)=Lsection(L2(4),t(4));
end
tot_ele=enac*4;
eleprop(tot_ele+1,:)=Lsection(L2(5),t(5));
eleprop(tot_ele+2,:)=Lsection(L2(6),t(6));
eleprop(tot_ele+3,:)=Lsection(L2(7),t(7));
eleprop(tot_ele+4,:)=Lsection(L2(8),t(8));
eleprop(tot_ele+5,:)=Lsection(L2(9),t(9));
eleprop(tot_ele+6,:)=Lsection(L2(10),t(10));

```

```

eleprop(tot_ele+7,:)=Lsection(L2(11),t(11));
eleprop(tot_ele+8,:)=Lsection(L2(12),t(12));

% add stiffners that are not part of the optimization
eleprop(tot_ele+9,:)=Lsection(2.0,0.5);
eleprop(tot_ele+10,:)=Lsection(2.0,0.5);

%extra elements
if num_ele==1
    eleprop(tot_ele+11,:)=Lsection(L2(13),t(13));
end

if num_ele == 2
    eleprop(tot_ele+11,:)=Lsection(L2(13),t(13));
    eleprop(tot_ele+12,:)=Lsection(L2(14),t(14));
end
% end extra elements

function y = mymass(rho,A,x1,y1,z1,x2,y2,z2)
% This fuction creates the elemental mass matrix
% This uses the lumped masses
L = sqrt((x2-x1)*(x2-x1) + (y2-y1)*(y2-y1) + (z2-z1)*(z2-z1));
w1 = rho*A*L/2;
w2 = (rho*A*L^3)/24;
kprime = [w1 0 0 0 0 0 0 0 0 0 0 ;
    0 w1 0 0 0 0 0 0 0 0 0 ;
    0 0 w1 0 0 0 0 0 0 0 0 ;
    0 0 0 w2 0 0 0 0 0 0 0 ;
    0 0 0 0 w2 0 0 0 0 0 0 ;
    0 0 0 0 0 w2 0 0 0 0 0 ;
    0 0 0 0 0 0 w1 0 0 0 0 ;
    0 0 0 0 0 0 0 w1 0 0 0 0 ;
    0 0 0 0 0 0 0 0 w1 0 0 0 ;
    0 0 0 0 0 0 0 0 0 w2 0 0 ;
    0 0 0 0 0 0 0 0 0 0 w2 0 ;
    0 0 0 0 0 0 0 0 0 0 0 w2];
if x1 == x2 & y1 == y2
    if z2 > z1
        Lambda = [0 0 1 ; 0 1 0 ; -1 0 0];
    else
        Lambda = [0 0 -1 ; 0 1 0 ; 1 0 0];
    end
else

```

```

CXx = (x2-x1)/L;
CYx = (y2-y1)/L;
CZx = (z2-z1)/L;
D = sqrt(CXx*CXx + CYx*CYx);
CXy = -CYx/D;
CYy = CXx/D;
CZy = 0;
CXz = -CXx*CZx/D;
CYz = -CYx*CZx/D;
CZz = D;
Lambda = [CXx CYx CZx ; CXy CYy CZy ; CXz CYz CZz];
end
R = [Lambda zeros(3) zeros(3) zeros(3) ;
zeros(3) Lambda zeros(3) zeros(3) ;
zeros(3) zeros(3) Lambda zeros(3) ;
zeros(3) zeros(3) zeros(3) Lambda];
y = R'*kprime*R;

function y = mystiff(E,G,A,Iy,Iz,J,x1,y1,z1,x2,y2,z2)
%this function creates the elemental stiffness matrix
L = sqrt((x2-x1)*(x2-x1) + (y2-y1)*(y2-y1) + (z2-z1)*(z2-z1));
w1 = E*A/L;
w2 = 12*E*Iz/(L*L*L);
w3 = 6*E*Iz/(L*L);
w4 = 4*E*Iz/L;
w5 = 2*E*Iz/L;
w6 = 12*E*Iy/(L*L*L);
w7 = 6*E*Iy/(L*L);
w8 = 4*E*Iy/L;
w9 = 2*E*Iy/L;
w10 = G*J/L;
kprime = [w1 0 0 0 0 0 -w1 0 0 0 0 0 ;
0 w2 0 0 0 w3 0 -w2 0 0 0 w3 ;
0 0 w6 0 -w7 0 0 0 -w6 0 -w7 0 ;
0 0 0 w10 0 0 0 0 -w10 0 0 ;
0 0 -w7 0 w8 0 0 0 w7 0 w9 0 ;
0 w3 0 0 0 w4 0 -w3 0 0 0 w5 ;
-w1 0 0 0 0 0 w1 0 0 0 0 0 ;
0 -w2 0 0 0 -w3 0 w2 0 0 0 -w3 ;
0 0 -w6 0 w7 0 0 0 w6 0 w7 0 ;
0 0 0 -w10 0 0 0 0 w10 0 0 ;
0 0 -w7 0 w9 0 0 0 w7 0 w8 0 ;
0 w3 0 0 0 w5 0 -w3 0 0 0 w4];

```

```

if x1 == x2 & y1 == y2
    if z2 > z1
        Lambda = [0 0 1 ; 0 1 0 ; -1 0 0];
    else
        Lambda = [0 0 -1 ; 0 1 0 ; 1 0 0];
    end
else
    CXx = (x2-x1)/L;
    CYx = (y2-y1)/L;
    CZx = (z2-z1)/L;
    D = sqrt(CXx*CXx + CYx*CYx);
    CXy = -CYx/D;
    CYy = CXx/D;
    CZy = 0;
    CXz = -CXx*CZx/D;
    CYz = -CYx*CZx/D;
    CZz = D;
    Lambda = [CXx CYx CZx ; CXy CYy CZy ; CXz CYz CZz];
end
R = [Lambda zeros(3) zeros(3) zeros(3) ;
     zeros(3) Lambda zeros(3) zeros(3) ;
     zeros(3) zeros(3) Lambda zeros(3) ;
     zeros(3) zeros(3) zeros(3) Lambda];
y = R'*kprime*R;

function y = myassemble(K,k,i,j)
% this function assembles the M or K matrix into the global matrix
for i1=1:6
    for i2=1:6
        K(6*i-(6-i1),6*i-(6-i2))=K(6*i-(6-i1),6*i-(6-i2))+k(i1,i2);
        K(6*i-(6-i1),6*j-(6-i2))=K(6*i-(6-i1),6*j-(6-i2))+k(i1,i2+6);
        K(6*j-(6-i1),6*i-(6-i2))=K(6*j-(6-i1),6*i-(6-i2))+k(i1+6,i2);
        K(6*j-(6-i1),6*j-(6-i2))=K(6*j-(6-i1),6*j-(6-i2))+k(i1+6,i2+6);
    end
end
y = K;

```

Appendix B: MATLAB Program Used to Test FEA Approximation

```

clear all
close all

% Set up all the constants

```

```

p=10; %force in grams
l=36; %length in meters
b=.5; %width in meters
h=1; %height in meters
l=1/3*b*h^3; %elastic equation
E=30e6; % modulus in pascals

% Generate some data to train the NN
ii=0;
while p<=250
tx=0;
for j=1:10
    tx=tx+(l/10);
    x(j)=tx;
    y(j)=(p/(6*E*l))*(tx^3-3*l*tx^2);
end
ii=ii+1;
P(ii)=p;
p=p+20;
T(:,ii)=y';
end

% build and train the NN
minP=min(P');
maxP=max(P');
PR=[minP',maxP'];
layer1=round(4*size(P,1));
layer2=round(2*size(T,1));
outlayer=size(T,1);
% ***** build NN and train *****
net = newff(PR,[layer1 outlayer],{'tansig','purelin'},'trainlm');
net.trainParam.goal=1e-10;
net.trainParam.show=100;
net.trainParam.epochs=1000;
[net, tr]=train(net,P,T);

%test the NN by entering a new load
p=input('input any load between 20-250 \n');

% Get the deflections from the elastic equation
cpu0=cputime;

```



```

for i=1:10000
    tx=0;
    for j=1:10
        tx=tx+(l/10);
        x(j)=tx;
        y(j)=(p/(6*E*I))*(tx^3-3*I*tx^2);
    end
end
cpu_exact=(cputime-cpu0)/10000;

%Get the deflections from the NN
cpu0=cputime;
for i=1:100
    ny=sim(net,p);
end
cpu_NN=(cputime-cpu0)/100;

%Get the deflection from FEA
cpu0=cputime;
yFEA=myfea('beam1dtest',p,l);
cpu_FEA=cputime-cpu0;

%plot the results
plot(x,y,'bx-',x,ny,'r+-',x,yFEA(2:11),'ko-')
legend('Exact','NN','FEA')
ylabel('deflection')

disp([' Exact ' ' NN ' ' FEA']);
disp(['y' ny yFEA(2:11)']);
disp('CPU usage');
disp([cpu_exact cpu_NN cpu_FEA]);

clear all
close all

% Set up all the constants
p=10; %force in grams
l=36; %length in meters
b=.5; %width in meters
h=1; %height in meters
I=1/3*b*h^3; %elastic equation
E=30e6; % modulus in pascals

```

```

%pretrain NN
% Generate some data to train the NN
p=10;
ii=0;
while p<=250
tx=0;
for j=1:10
    tx=tx+(l/10);
    x(j)=tx;
    y(j)=(p/(6*E*l))*(tx^3-3*l*tx^2);
end
ii=ii+1;
P(ii)=p;
p=p+20;
T(:,ii)=y';
end

% build and train the NN
minP=min(P');
maxP=max(P');
PR=[minP',maxP'];
layer1=round(4*size(P,1));
layer2=round(2*size(T,1));
outlayer=size(T,1);
% ***** build NN and train *****
net = newff(PR,[layer1 outlayer],{'tansig','purelin'},'trainlm');
net.trainParam.goal=1e-10;
net.trainParam.show=100;
net.trainParam.epochs=1000;
disp(['  base ' ' height'])
disp([b h])
[net, tr]=train(net,P,T);
% save the weights and bias for later
w1=net.IW{1,1};
w2=net.LW{2,1};
b1=net.b{1,1};
b2=net.b{2,1};
save pw1.txt w1 -ascii;
save pw2.txt w2 -ascii;
save pb1.txt b1 -ascii;
save pb2.txt b2 -ascii;
pause

```

```

% Generate some data to train the NN
b=.5; %width in meters
h=1.2; %height in meters
l=1/3*b*h^3; %elastic equation
p=10;
ii=0;
while p<=250
tx=0;
for j=1:10
    tx=tx+(l/10);
    x(j)=tx;
    y(j)=(p/(6*E*I))*(tx^3-3*I*tx^2);
end
ii=ii+1;
P(ii)=p;
p=p+20;
T(:,ii)=y';
end

% build and train the NN
minP=min(P');
maxP=max(P');
PR=[minP',maxP'];
layer1=round(4*size(P,1));
layer2=round(2*size(T,1));
outlayer=size(T,1);
% ***** build NN and train *****
net = newff(PR,[layer1 outlayer],{'tansig','purelin'},'trainlm');
net.trainParam.goal=1e-10;
net.trainParam.show=100;
net.trainParam.epochs=1000;
% load previous NN weights and bias
load -ascii pw1.txt;net.IW{1,1}=pw1;
load -ascii pw2.txt;net.LW{2,1}=pw2;
load -ascii pb1.txt;net.b{1,1}=pb1;
load -ascii pb2.txt;net.b{2,1}=pb2;
disp(['   base ' '   height'])
disp([b h])
[net, tr]=train(net,P,T);

%test the NN by entering a new load
p=input('input any load between 20-250 \n');

```

```

% Get the deflections from the elastic equation
cpu0=cputime;

for i=1:10000
    tx=0;
    for j=1:10
        tx=tx+(l/10);
        x(j)=tx;
        y(j)=(p/(6*E*I))*(tx^3-3*I*tx^2);
    end
end
cpu_exact=(cputime-cpu0)/10000;

%Get the deflections from the NN
cpu0=cputime;
for i=1:100
    ny=sim(net,p);
end
cpu_NN=(cputime-cpu0)/100;

%Get the deflection from FEA
cpu0=cputime;
yFEA=myfea('beam1dtest',p,l);
cpu_FEA=cputime-cpu0;

%plot the results
%figure(2)
plot(x,y,'bx-',x,ny,'r+-',x,yFEA(2:11),'ko-')
legend('Exact','NN','FEA')
ylabel('deflection')

disp([' Exact ' ' NN ' ' FEA']);
disp(['y' ny yFEA(2:11)']);
disp('CPU usage');
disp([cpu_exact cpu_NN cpu_FEA]);

function fea_def = myfea(filename,pforce,newl)
% This code is from Dr. Smith's class
% This is the main program that controls the execution of the various
% finite element computations. Global arrays are defined and sizes of
% arrays are set, as required. The is executed by typing:
%
```

```

% >> myfea('filename')
%
% at the MATLAB prompt where 'filename' refers to the input file named
% filename.txt in the current directory. This program calls all of the
% functions needed to run a finite element simulation. It also contains
% the calculations that invert the global reduced stiffness matrix and
% performs the back substitution step that computes the unknown nodal
% degrees-of-freedom. Reaction loads are then computed.
%
% define global arrays
% yFEA is the solution
global ielem iprops eprops elname iforce force idisp disp
global kff kpf kpp uf up pf pp yFEA
global x utot estress efor etype shear moment xplot
%
% close all graphs
close all
%
% assign input filename
filename = [filename '.txt'];
%
% read input file
[nnode,nel,nforce,ndisp,etype,ndof,nenode]=fea_input(filename);
%
% print input values to screen
%[nnode nel nforce ndisp etype ndof nenode]

%
% initialize equation numbers for dofs
ieqn = initialize(nnode,ndisp,idisp,ndof);
%
% initialize global matrices;
utot=zeros(nnode*ndof,1);
ptot=zeros(nnode*ndof,1);
kff = zeros(nnode*ndof-ndisp);
kpf = zeros(ndisp,nnode*ndof-ndisp);
kpp = zeros(ndisp,ndisp);
uf = zeros(nnode*ndof-ndisp,1);
up = disp';
pf = zeros(nnode*ndof-ndisp,1);
pp = zeros(ndisp,1);
estress = zeros(nel,1);
efor = zeros(nel,1);

```

```

eprops(1,2)=newl;
%
% compute and assemble element stiffness matrix and draw geometry
% figure(1)
% title('Model')
% xlabel('X'), ylabel('Y'), zlabel('Z')
% hold('on')
% grid('on')
XYZ=zeros(nel,3);
for i = 1:nel;
    icode = 2;
    XYZ(1,:)=x(ielem(i,1),:);
    XYZ(2,:)=x(ielem(i,2),:);
    %plot3(XYZ(:,1),XYZ(:,2),XYZ(:,3),'k')
    [eldat,ieqn] = feval(elname,eprops(iprops(i,:),:),ielem(i,1:2),ieqn,icode,i);
    assemkp(eldat,ieqn,ndof,nenode,icode);
end
%
% compute and assemble element load vector
for i = 1:nel;
    icode = 1;
    [eldat,ieqn] = feval(elname,eprops(iprops(i,:),:),ielem(i,1:2),ieqn,icode,i);
    assemkp(eldat,ieqn,ndof,nenode,icode);
end
%
% apply nodal forces
force=-pforce;
for i = 1:nforce;
    num = iforce(i,1)*ndof + iforce(i,2) - ndof;
    pf(ieqn(num)) = pf(ieqn(num)) + force(i);
end
%
% solve system of equations
uf = kff\(pf - kpf'*up);
%
% compute nodal reactions
pp = kpp*up + kpf*uf;
%
% complete global displacement and force vector
%
for i = 1:nnode*ndof;
    if (ieqn(i) < 0);

```

```

        utot(i,1) = up(-ieqn(i));
        ptot(i,1) = pp(-ieqn(i));
    else
        utot(i,1) = uf(ieqn(i));
        ptot(i,1) = pf(ieqn(i));
    end
end
%
%postprocess
for i = 1:nel
    icode = 0;
    [eldat,ieqn] = feval(elname,eprops(iprops(i,:),:),ielem(i,1:2),ieqn,icode,i);
    shear(i)=(eldat(1)-eldat(3))/2;
    moment(i)=(-eldat(2)+eldat(4))/2;
    xplot(i)=(x(i)+x(i+1))/2;
end
fea_output(etype,utot,ptot,nnode);
fea_def=yFEA;

function ieqn = initialize(nnode,ndisp,idisp,ndof)
%
% This function is used to count the number of equations in the model and
% assign element equation numbers. Equation numbers increase from zero for
% free dofs and decrease from zero for prescribed dofs.
%
%set total degrees of freedom
ndoftot = nnode*ndof;
%
% initialize ieqn
ieqn = zeros(1,ndoftot);
%
% identify fixed degrees of freedom
ifixed = 0;
for i = 1:ndisp;
    ifixed = ifixed + 1;
    num = idisp(i,1)*ndof + idisp(i,2) - ndof;
    ieqn(num) = -ifixed;
end
%
% identify free degrees of freedom
ifree = 0;
for i = 1:ndoftot;
    if ieqn(i) == 0;

```

```

        ifree = ifree + 1;
        ieqn(i) = ifree;
    end
end

function [nnode,nel,nforce,ndisp,etype,ndof,nenode] = fea_input(filename)
%
% This function reads the input file filename.txt in the current directory.
% It starts by reading the number of nodes, elements, applied loads,
% prescribed displacements and element type. It then reads nodal data,
% element data, load data, prescribed displacement data and finally, the
% element properties. The number of nodal dofs, nodes per element, and
% number of element properties are also assigned for each element type.
%
%define global arrays
global ielem iprops eprops elname iforce force idisp disp
global x knl DV DVid
%
% open input file
fid = fopen(filename,'r');
%
% read number of nodes, elements, applied forces and prescribed displacements,
and element type
nnode = fscanf(fid,'%d',1);
nel = fscanf(fid,'%d',1);
nforce = fscanf(fid,'%d',1);
ndisp = fscanf(fid,'%d',1);
etype = fscanf(fid,'%d',1);
%[nnode nel nforce ndisp etype ndof nenode]
% set properties related to element properties
% set knl to non-linear default
knl = 0;
switch etype
case 1
    ndof = 1;
    nenode = 2;
    neprops = 1;
    elname = 'spring1d';
case 2
    ndof = 2;
    nenode = 2;
    neprops = 2;
    elname = 'truss2d';

```



```

case 3
    knl = 1;
    ndof = 1;
    nenode = 2;
    neprops = 3;
    elname = 'spring1d_n1';
case 4
    ndof = 2;
    nenode = 2;
    neprops = 3;
    elname = 'beam1d';
end
%
% read nodal data
x = zeros(nnode,3);
for j = 1:nnode;
    dummy = fscanf(fid,'%d',1);
    x(j,1:3) = fscanf(fid,'%g',3);
end
%
% read element data
ielem = zeros(nel,nenode);
iprops = zeros(1,nel);
for j = 1:nel;
    fscanf(fid,'%d',1);
    iprops(j) = fscanf(fid,'%d',1);
    ielem(j,1:nenode);
    ielem(j,1:nenode) = fscanf(fid,'%d',nenode)';
end
%
% read applied loads
iforce = zeros(nforce,2);
force = zeros(1,nforce);
for j = 1:nforce;
    iforce(j,1:2) = fscanf(fid,'%d',2)';
    force(j) = fscanf(fid,'%g',1);
end
%
% read applied displacements
idisp = zeros(ndisp,2);
disp = zeros(1,ndisp);
for j = 1:ndisp
    idisp(j,1:2) = fscanf(fid,'%d',2)';

```

```

    disp(j) = fscanf(fid,'%g',1);
end
%
% read element properties
nprops = max(iprops);
eprops = zeros(nprops,nprops);
for j = 1:nprops;
    fscanf(fid,'%d',1);
    eprops(j,1:nprops) = fscanf(fid,'%g',nprops)';
end
%
% design sensitivity analysis
DV=fscanf(fid,'%d',1);
for j=1:DV;
    DVid(j,1:2)=fscanf(fid,'%d',1);
end
%

function fea_output(etype,utot,ptot,nnode)
%
% This function is used to output finite element results to the
% MATLAB window or, perhaps, to a file (not included here).
%
% print the following to the screen
% calculates system compliance for springs
% prints element force and stress for rods
global efor estress shear moment xplot x yFEA
switch etype
case 1,3
    syscomp=dot(utot,ptot)
case 2
    efor
    estress
case 4
    X=zeros(nnode,1);
    %disp(sprintf('number of nodes: %i',nnode));
    for i=1:nnode;
        deflection(i)=utot(i*2-1);
        slope(i)=utot(i*2);
        X(i)=x(i,1);
        if i==(nnode+1)/2
            %disp(sprintf('theta 2=%0.4g ',slope(i)));
        end
    end
end

```

```

end

%disp(sprintf('max deflection=%0.4g',(max(abs(deflection)))));

yFEA=deflection;
% figure(2)
% title('Moment')
% hold('on')
% plot(xplot,moment,'b')
% figure(3)
% title('Shear')
% hold('on')
% plot(xplot,shear,'g')
% figure(4)
% title('deflection')
% hold('on')
% plot(X,deflection,'r')
End

function [elmat,ieleqn] = beam1d(eprop,lnodes,ieqn,icode,i)
%
% This function computes the element load vector (case 1) and
% element stiffness matrix (case 2) for a 1-D beam element. Note
% that the element load vector is zero. It starts by forming the
% element equation numbers that are required to assemble the global
% matrices.
global x utot estress efor
%
% determine length, sin, and cos
i1x=x(lnodes(1),:);
i2x=x(lnodes(2),:);
L=abs(i2x(1)-i1x(1));
k=[6 3*L -6 3*L;3*L 2*L^2 -3*L L^2;-6 -3*L 6 -3*L;3*L L^2 -3*L 2*L^2];
nenode = 2;
ndof = 2;
jj = 0;
for j1 = 1:nenode;
    for j2 = 1:ndof;
        jj = jj + 1;
        numj = lnodes(j1)*ndof + j2 - ndof;
        idof(jj,1)=numj;
        ieleqn(jj) = ieqn(numj);
        if icode==0

```

```

            euv(jj)=utot(numj);
        end
    end
end
%
% evaluate element matrices
uloc=utot(idof(:,1));
switch icode
case 0
    %postprocess: moment and shear
    eldat = ((eprop(1)*eprop(2)*2)/L^3)*k*uloc-(eprop(3)*L/2)*[1;L/6;1;-L/6];

case 1
    % compute element load vector
    eldat = (eprop(3)*L/2)*[1;L/6;1;-L/6];
case 2
    % compute element stiffness matrix
    eldat = ((eprop(1)*eprop(2)*2)/L^3)*k;
end

```

Appendix C: MATLAB Program For DSO of Typical MMT Base Side

```
%*****Continous Constrained Optimization
% for typical 2D MMT Base Side
% this program generates all of the branches
% and finds the continous optimal solution
% for each branch and save them to a file
%-----
clear all
close all
global X b h d enac num_ele nn_save nu_sol nu_fea P T LOAD
nn_save=0;
nu_sol=0;
nu_fea=1;
b=36;
h=12;
d=12;
X=zeros(4,3);
X(2,2)=h; X(4,2)=h;
X(3,3)=d; X(4,3)=d;

LOAD=[2 2 75; 3 2 -700];

enac=6; % number of elements across the top
% set the number of extra elements
num_ele=0;

%set optimazation options
% options =
optimset('LargeScale','off','DiffMaxChange',.5,'DiffMinChange',0.005,'Diagnostics'
,'off','Display','off','TolFun',0.1,'TolCon',0.01,'TolX',0.05);
options =
optimset('LargeScale','off','DiffMaxChange',1,'DiffMinChange',0.005,'Diagnostics',
'off','Display','off','TolFun',2.0,'TolCon',0.01,'TolX',0.1);

%% optimize with no extra elements
LB = zeros(8,1);
UB = ones(8,1);
%test worst case for feasible solution
if mynonlin_cons_2d(UB) <= 0
    clear P T;
    global P T
```

```

        P=zeros(100,13);
        T=zeros(100,7);
        nu_fea=1;
        nn_save=1;
        nu_sol=nu_sol+1
        mynonlin_cons_2d(UB);
        mynonlin_cons_2d(LB);
        x0=mypso2d(LB);
        x0=x0';
    %         options =
    optimset('LargeScale','off','DiffMaxChange',.5,'DiffMinChange',0.005,'Diagnostics'
    ,'off','Display','off','TolFun',0.1,'TolCon',0.01,'TolX',0.05);
        [fx, fval, exitflag, output, lambda] =
    fmincon('obj_2d',x0,[],[],[],LB,UB,'mynonlin_cons_2d',options);
        xtemp=[X(1,1) X(2,1) X(3,1) X(4,1)];
        save(strcat('X',num2str(nu_sol)),'X','-ascii');
        save(strcat('P',num2str(nu_sol)),'P','-ascii');
        save(strcat('T',num2str(nu_sol)),'T','-ascii');
        sol(nu_sol)=fval;

        nn_save=0;
    end
    %% end no extra elements

    %% optimize with one extra elements
    % set the number of extra elements
    num_ele=1;
    clear x0 UB LB;
    LB = zeros(10,1);
    UB = ones(10,1);
    X(1,1)=0;X(2,1)=0;X(3,1)=0;X(4,1)=0;
    for xi=1:(enac+1)
        X(1,1)=0;
        for xj=1:(enac+1)

            %test worst case for feasible solution

            if mynonlin_cons_2d(UB) <= 0
                clear P T;
                global P T
                P=zeros(100,13);
                T=zeros(100,7);
                nu_fea=1;

```

```

        nn_save=1;
        nu_sol=nu_sol+1
        mynonlin_cons_2d(UB);
        mynonlin_cons_2d(LB);
        x0=mypso2d(LB);
        x0=x0';

        %x0=LB+.5;
        %
        options =
        optimset('LargeScale','off','DiffMaxChange',.5,'DiffMinChange',0.005,'Diagnostics'
        ,'off','Display','off','TolFun',0.1,'TolCon',0.01,'TolX',0.05);
        [fx, fval, exitflag, output, lambda] =
        fmincon('obj_2d',x0,[],[],[],[],LB,UB,'mynonlin_cons_2d',options);

        xtemp=[X(1,1) X(2,1) X(3,1) X(4,1)];
        save(strcat('X',num2str(nu_sol)), 'X', '-ascii');
        save(strcat('P',num2str(nu_sol)), 'P', '-ascii');
        save(strcat('T',num2str(nu_sol)), 'T', '-ascii');
        sol(nu_sol)=fval;

        nn_save=0;
        end

        X(1,1)=X(1,1)+b/enac;
        end
        X(2,1)=X(2,1)+b/enac;
        end
        X(1,1)=0;X(2,1)=0;X(3,1)=0;X(4,1)=0;
        %save the solutions
        save sol.txt sol -ascii;

function pbest=mypso2d(L)
% this function uses particle swarm to optimize the
%continous branch of a typical MMT Base Side
% this is the 2D version
global X b h d enac num_ele nn_save nu_sol P T nu_fea LOAD
%pass the following to the function once it works
wmax=0.9;
wmin=0.4;
itmax=8;
errmax=.0001;
c1=2;
c2=2;

```

```

N=50;
D=size(L,1);

i=1:itmax;
W=wmax-((wmax-wmin)/itmax)*i;

% Initialization of positions
a=0;
b=1;
x=a+(b-a)*rand(N,D,1);

for i=1:N
    F(i,1)=myext_penalty2d(x(i,:));
end

[C,l]=min(abs(F(:,1)));
pB=C;
gB=pB;
XX(1,1)=l;
gbest(1,:)=x(l,:);
pbest=gbest;
for i=1:N
    V=c1*rand*(pbest-x(i,:))+c2*rand*(gbest-x(i,:));
    x(i,:)=x(i,:)+V;
end

jj=0;
while jj<itmax

    for i=1:N
        x(i,:)=myclamped(x(i,:),0,1);

        F(i,1)=myext_penalty2d(x(i,:));
    end
    [C,l]=min(abs(F(:,1)));
    gbest(1,:)=x(l,:);
    gB=C;

    for i=1:N
        V=W(jj+1)*c1*rand*(pbest-x(i,:))+c2*rand*(gbest-x(i,:));
        x(i,:)=x(i,:)+V;
    end
end

```



```

    if gB<pB
        pB=gB;
        pbest=gbest;

    end
    jj=jj+1;
    %sol(jj,1:(D+1))=[pB pbest'];
end

function [c, ceq] = mynonlin_cons_2d(L)
% this function take cross sectional data L2 and t
% and returns the deflection and 1st natural freq of the
% structure
%
global X b h d enac num_ele nn_save nu_sol P T nu_fea LOAD
%remove the following after testing
b=36;
h=12;
d=12;
enac=6;

nnode=2;% nnode = number of nodes/element
ndof=6;% ndof=number of degrees of freedom/node

%mesh the model
[x, ielem]=mymesh2d;
%get element properties
eleprop=myeleprop2d(L);

nnode=size(x,1);% nnode=total number of nodes
nel=size(ielem,1);% nel=total number of elements
%
%set BC and loads
BC=zeros(nnode,ndof); %zero=free 1=fixed
BC([enac+2 (enac+1)*2],1:6)=1;
%BC([enac+2 tot_ele+2],1:6)=1;
BC(1:nnode,3:5)=1;

F(1:nnode*ndof)=0;

XYZ=zeros(nel,3);

```

```

K=zeros(nnode*ndof,nnode*ndof);
M=zeros(nnode*ndof,nnode*ndof);

%element and cs data for book example delete for final
% use the Lsection program to replace
% Set up all the constants
E=30e6;
G=11.5e6;
rho=0.286;

%get element stiffness matrices then put in global stiffness matrix
% set the lumped mass matrix
for i = 1:nel;
    A=eleprop(i,1);
    ly=eleprop(i,2);
    lz=eleprop(i,3);
    J=eleprop(i,4);

    k=mystiff(E,G,A,ly,lz,J,x(ielem(i,1),1),x(ielem(i,1),2),x(ielem(i,1),3),x(ielem(i,2),1),
    x(ielem(i,2),2),x(ielem(i,2),3)));

    m=mymass(rho,A,x(ielem(i,1),1),x(ielem(i,1),2),x(ielem(i,1),3),x(ielem(i,2),1),x(iel
    em(i,2),2),x(ielem(i,2),3)));
    M=myassemble(M,m,ielem(i,1),ielem(i,2));
    K=myassemble(K,k,ielem(i,1),ielem(i,2));
end

% compute and assemble element load vector force vector
i2=1;i3=1;
for i = 1:nnode;%loop thru each node
    for i1=1:ndof;%loop thru each dof in the node
        if BC(i,i1) == 0;
            %set up book keeping for partition
            bk(i3)=i2;
            i3=i3+1;
        end
        i2=i2+1;
    end
end
% Insert forces into global force vector
for i=1:size(LOAD,1);
    F((LOAD(i,1)-1)*6+LOAD(i,2))=LOAD(i,3);
end

```

```

%partition the system of eq.
m=zeros(size(bk,2),size(bk,2));
k=zeros(size(bk,2),size(bk,2));
f(1:size(bk,2))=0;
for i=1:size(bk,2);
    for i1=1:size(bk,2);
        m(i,i1)=M(bk(i),bk(i1));
        k(i,i1)=K(bk(i),bk(i1));
    end
    f(i)=F(bk(i));
end
%

%solve for 1st natural frequency
w=eig(k,m);
w1=sqrt(abs(w(1)));

%solve for displacements
u=k\b';

%Setup Global Nodal Displacement Vector
U(1:nnode*ndof)=0;
for i=1:size(bk,2);
    U(bk(i))=u(i);
end

%calculate the global nodal force vector
F=K*U';

%set max deflection and natural freq.
md=0.005;mf=40;
% nonlinear inequality constraints returned as vector c

for i=1:(enac+1)
    ydisp(i)=U((i-1)*6+2);
    % ydisp(i+(enac+1))=U(((i+(2*enac+3))-2)*6+2);
end

if nn_save==1
    temp=zeros(13,1);
    temp(2:size(L,1)+1,1)=L;
    temp(1,1)=num_ele;
    P(nu_fea,:)=temp';

```

```

    T(nu_fea,:)=ydisp;
    nu_fea=nu_fea+1;
    clear temp;
end
c=max(abs(ydisp))-md;

% nonlinear equality constraints returned as vector ceq
ceq = []; % there are no nonlinear equality
           % constraints in this problem

function [c, ceq] = myext_penalty2d(L)
% this function take cross sectional data L2 and t
% and returns the deflection and natural freq of the
% structure
%***** This uses external penalty function
%***** used for the PSO because it is
%***** unconstrained
%
global X b h d enac num_ele nn_save nu_sol P T nu_fea LOAD
%remove the following after testing
b=36;
h=12;
d=12;
enac=6;

volume=obj_2d(L);

nenode=2;% nenode = number of nodes/element
ndof=6;% ndof=number of degrees of freedom/node

vl=size(L,1);
L2=L(1:vl/2)*1.25+0.75;
t=L(vl/2+1:vl)*.375+.125;

%mesh the model
[x, ielem]=mymesh2d;
%get element properties
eleprop=myeleprop2d(L);

nnode=size(x,1);% nnode=total number of nodes
nel=size(ielem,1);% nel=total number of elements
%
```

```

%set BC and loads
BC=zeros(nnode,ndof); %zero=free 1=fixed
BC([enac+2 (enac+1)*2],1:6)=1;
BC(1:nnode,3:5)=1;

F(1:nnode*ndof)=0;

XYZ=zeros(nel,3);
K=zeros(nnode*ndof,nnode*ndof);
M=zeros(nnode*ndof,nnode*ndof);

%element and cs data for book example delete for final
% use the Lsection program to replace
% Set up all the constants
E=30e6;
G=11.5e6;
rho=0.286;

%get element stiffness matrices then put in global stiffness matrix
% set the lumped mass matrix
for i = 1:nel;
    A=eleprop(i,1);
    ly=eleprop(i,2);
    lz=eleprop(i,3);
    J=eleprop(i,4);

    k=mystiff(E,G,A,ly,lz,J,x(ielem(i,1),1),x(ielem(i,1),2),x(ielem(i,1),3),x(ielem(i,2),1),
    x(ielem(i,2),2),x(ielem(i,2),3)));

    m=mymass(rho,A,x(ielem(i,1),1),x(ielem(i,1),2),x(ielem(i,1),3),x(ielem(i,2),1),x(iel
    em(i,2),2),x(ielem(i,2),3)));
    M=myassemble(M,m,ielem(i,1),ielem(i,2));
    K=myassemble(K,k,ielem(i,1),ielem(i,2));
end

% compute and assemble element load vector force vector
i2=1;i3=1;
for i = 1:nnode;%loop thru each node
    for i1=1:ndof;%loop thru each dof in the node
        if BC(i,i1) == 0;
            %set up book keeping for partition

```

```

        bk(i3)=i2;
        i3=i3+1;
    end
    i2=i2+1;
end
end
% Insert forces into global force vector
for i=1:size(LOAD,1);
    F((LOAD(i,1)-1)*6+LOAD(i,2))=LOAD(i,3);
end
%partition the system of eq.
m=zeros(size(bk,2),size(bk,2));
k=zeros(size(bk,2),size(bk,2));
f(1:size(bk,2))=0;
for i=1:size(bk,2);
    for i1=1:size(bk,2);
        m(i,i1)=M(bk(i),bk(i1));
        k(i,i1)=K(bk(i),bk(i1));
    end
    f(i)=F(bk(i));
end
%

%solve for 1st natural frequency
w=eig(k,m);
w1=sqrt(abs(w(1)));

%solve for displacements
u=k\l'f';

%Setup Global Nodal Displacement Vector
U(1:nnode*ndof)=0;
for i=1:size(bk,2);
    U(bk(i))=u(i);
end

%calculate the global nodal force vector
F=K*U';

%set max deflection and natural freq.
md=0.005;mf=40;
% nonlinear inequality constraints returned as vector c

```

```

%Get the y disp for the top surface
for i=1:(enac+1)
    ydisp(i)=U((i-1)*6+2);

end

if nn_save==1
    temp=zeros(13,1);
    temp(2:size(L,1)+1,1)=L;
    temp(1,1)=num_ele;
    P(nu_fea,:)=temp';
    T(nu_fea,:)=ydisp;
    nu_fea=nu_fea+1;
    clear temp;
end
% external penalty function
c=volume + 5000*(max(abs(ydisp))-md)^2;

% nonlinear equality constraints returned as vector ceq
ceq = []; % there are no nonlinear equality
          % constraints in this problem

function = discrete_2d()
% this function loads the branch data from the continuous optimization
% It test the best topos and cuts branches. Can either do NN or FEA
% If NN it can load previous weights and bias or generate new.
clear all
close all
global X b h d enac num_ele nn_save nu_sol nu_fea P T LOAD
nn_save=0;

%** set hidden layer size factor
hls=1.5;
%*** get input from user
pretrain=input('pretrain NN? 1=yes 0=no');
useNN=input('use NN? 1=yes 0=no');

LOAD=[2 2 75; 3 2 -700];

nu_sol=0;
nu_fea=1;
enac=6; % number of elements across the top
% set the number of extra elements

```

```

num_ele=1;

%load and sort the continuous sol. for each branch
load sol.txt -ascii;
[Y,l]=sort(sol);
sol_temp=10000;

j=1;
cpu_seconds=0;
while sol_temp>sol(j)
i=l(j);
p=load(strcat('P',num2str(i)),'-ascii');
t=load(strcat('T',num2str(i)),'-ascii');
topo=load(strcat('X',num2str(i)),'-ascii');
P=p';
T=t';
X=topo
clear t p topo;

if useNN == 1 %*** test if NN *****
% ***** build NN and train *****
minP=min(P');
maxP=max(P');
PR=[minP',maxP'];
layer1=round(1.5*size(P,1));
layer2=round(layer1/2);
outlayer=size(T,1);
%net = newff(PR,[layer1 outlayer],{'logsig','tansig','traincgf');
net = newff(PR,[layer1 layer2 outlayer],{'tansig', 'logsig','purelin'},'trainrp');
%net.trainParam.mem_reduc=4;
net.trainParam.goal=1e-6;
net.trainParam.show=100;
net.trainParam.epochs=2000;
if pretrain > 0
% load previous NN weights and bias
load -ascii pw1.txt;net.IW{1,1}=pw1;
load -ascii pw2.txt;net.LW{2,1}=pw2;
load -ascii pw3.txt;net.LW{3,2}=pw3;
load -ascii pb1.txt;net.b{1,1}=pb1;
load -ascii pb2.txt;net.b{2,1}=pb2;
load -ascii pb3.txt;net.b{3,1}=pb3;
net = newff(PR,[layer1 layer2 outlayer],{'tansig', 'logsig','purelin'},'trainlm');

```



```

    net.trainParam.goal=1e-10;
    net.trainParam.epochs=150;
end %***** end pretrain *****
%**** train network *****
net=train(net,P,T);
pretrain=2;%***** use pretrained data for future test ***
%***** finish build and train the NN *****

```

```

% save the weights and bias for later
w1=net.LW{1,1};
w2=net.LW{2,1};
w3=net.LW{3,2};
b1=net.b{1,1};
b2=net.b{2,1};
b3=net.b{3,1};
save pw1.txt w1 -ascii;
save pw2.txt w2 -ascii;
save pw3.txt w3 -ascii;
save pb1.txt b1 -ascii;
save pb2.txt b2 -ascii;
save pb3.txt b3 -ascii;
end %***** end NN test *****

```

```

%***** test each branch *****
k=0; cpu0=cputime;
for k1=1:3
    for k2=1:3
        for k3=1:3
            for k4=1:3
                for k5=1:3

```

```

L=[k1; k2; k3; k4; k5];
temp=zeros(13,1);
dL=dlsection(L);
temp(2:size(dL,1)+1,1)=dL;
temp(1,1)=num_ele;
if useNN == 1
    ydisp=sim(net,temp);

```

```

else

```

```

        ydisp = fea_2d_test(dL)';
    end
    k=k+1;

    if max(abs(ydisp))<=.009
        sol_temp1=obj_2d(dL);
        if sol_temp1<sol_temp
            sol_temp=sol_temp1;
            sol_dL=dL;
            dX=X;
            sol_disp=ydisp;
        end
    end
end

        end
    end
end
end
end
j=j+1;
cpu1=cputime;cpu_seconds=cpu_seconds+(cpu1-cpu0)
end %end the while
%plot final topo.
X=dX
[x, ielem]=mymesh2d;

nnode=size(x,1);% nnode=total number of nodes
nel=size(ielem,1);% nel=total number of elements
figure(1)
title('Model')
xlabel('X'), ylabel('Y'), zlabel('Z')
hold('on')
grid('on')
XYZ=zeros(nel,3);

for i = 1:nel;
    XYZ(1,1:3)=x(ielem(i,1),1:3);
    XYZ(2,1:3)=x(ielem(i,2),1:3);
    plot3(XYZ(1:2,1),XYZ(1:2,2),XYZ(1:2,3),'k')
end
sol_temp

```

```

sol_dL
k
nload=size(LOAD,1); i11=0;
for i1=1:nload
    if LOAD(i1,2)==1, i11=i11+1; load(i11,1:3)=[LOAD(i1,3),0,0]; y(i11)=i1;
    elseif LOAD(i1,2)==2, i11=i11+1; load(i11,1:3)=[0,LOAD(i1,3),0]; y(i11)=i1;
    elseif LOAD(i1,2)==3, i11=i11+1; load(i11,1:3)=[0,0,LOAD(i1,3)]; y(i11)=i1;
    end
end
if i11>=1,
    x=[1:i11];
    quiver3(LOAD(y,1)*6-6,[12; 12],[0; 0],load(x,1),load(x,2),load(x,3),'r')
end
%% end one extra elements

```

Appendix D: MATLAB Program – Material Distribution Topology Optimization

```
%***** Modified by Donald Harby for testing typical MMT Base Sides 2D***  
%%%%%% A 99 LINE TOPOLOGY OPTIMIZATION CODE BY OLE SIGMUND,  
JANUARY 2000 %%%  
%%%%%% CODE MODIFIED FOR INCREASED SPEED, September 2002, BY  
OLE SIGMUND %%%  
%***** Modified for MMT base 8-21-07 Donald Harby ***
```

```
function topo()  
clear all  
nelx=72;nely=24;volfrac=0.4;penal=2.5;rmin=1.1;
```

```
close all  
hold off
```

```
% INITIALIZE  
x(1:nely,1:nelx) = volfrac;
```

```
%**** Add fixed material and holes ***  
% ***** passive holes active fixed material **  
for ely=1:nely  
    for elx=1:nelx  
        active(ely,elx)=0;  
        if elx<=2  
            active(ely,elx)=1;  
            x(ely,elx)=1;  
        end  
        if elx>=nelx-1  
            active(ely,elx)=1;  
            x(ely,elx)=1;  
        end  
        if ely<=2  
            active(ely,elx)=1;  
            x(ely,elx)=1;  
        end  
        if ely>=nely-1  
            active(ely,elx)=1;  
            x(ely,elx)=1;  
        end  
    end  
end
```

```

end
%***** end my passive or active

loop = 0;
change = 1.;
% START ITERATION
% while change > 0.01
while loop < 60
    loop = loop + 1;
    xold = x;
    % FE-ANALYSIS
    [U]=FE(nelx,nely,x,penal);
    % OBJECTIVE FUNCTION AND SENSITIVITY ANALYSIS
    [KE] = lk;
    c = 0.;
    for ely = 1:nely
        for elx = 1:nelx
            n1 = (nely+1)*(elx-1)+ely;
            n2 = (nely+1)* elx +ely;
            dc(ely,elx)=0.;
            for i=1:2
                Ue = U([2*n1-1;2*n1; 2*n2-1;2*n2; 2*n2+1;2*n2+2; 2*n1+1;2*n1+2],i);
                c = c + x(ely,elx)^penal*Ue'*KE*Ue;
                dc(ely,elx) = dc(ely,elx)-penal*x(ely,elx)^(penal-1)*Ue'*KE*Ue;
            end
        end
    end
    % FILTERING OF SENSITIVITIES
    [dc] = check(nelx,nely,rmin,x,dc);
    % DESIGN UPDATE BY THE OPTIMALITY CRITERIA METHOD
    [x] = OC(nelx,nely,x,volfrac,dc,active);
    % PRINT RESULTS
    change = max(max(abs(x-xold)));
    disp([' It.: ' sprintf('%4i',loop) ' Obj.: ' sprintf('%10.4f',c) ...
        ' Vol.: ' sprintf('%6.3f',sum(sum(x))/(nelx*nely)) ...
        ' ch.: ' sprintf('%6.3f',change )])
    % PLOT DENSITIES
    colormap(gray); imagesc(-x); axis equal; axis tight; axis off; pause(1e-6);
end
%plot load vector
hold on
quiver3(72*2/6,0,0,0,10,0,'r')
quiver3(72*2/6-12,5,0,0,-1,0,.7,'g')

```

```

%%%%%%%%%%%%% OPTIMALITY CRITERIA
UPDATE %%%%%%%%%%%%%%
%%%%%%%%
function [xnew]=OC(nelx,nely,x,volfrac,dc,active)
l1 = 0; l2 = 100000; move = 0.2;
while (l2-l1 > 1e-4)
    lmid = 0.5*(l2+l1);
    xnew = max(0.001,max(x-move,min(1.,min(x+move,x.*sqrt(-dc./lmid)))));
    xnew(find(active))=1.0;
    if sum(sum(xnew)) - volfrac*nelx*nely > 0;
        l1 = lmid;
    else
        l2 = lmid;
    end
end

%%%%%%%%%%%%% MESH-INDEPENDENCY
FILTER %%%%%%%%%%%%%%
%%%%%%%%
function [dcn]=check(nelx,nely,rmin,x,dc)
dcn=zeros(nely,nelx);
for i = 1:nelx
    for j = 1:nely
        sum=0.0;
        for k = max(i-floor(rmin),1):min(i+floor(rmin),nelx)
            for l = max(j-floor(rmin),1):min(j+floor(rmin),nely)
                fac = rmin-sqrt((i-k)^2+(j-l)^2);
                sum = sum+max(0,fac);
                dcn(j,i) = dcn(j,i) + max(0,fac)*x(l,k)*dc(l,k);
            end
        end
        dcn(j,i) = dcn(j,i)/(x(j,i)*sum);
    end
end

%%%%%%%%%%%%% FE-
ANALYSIS %%%%%%%%%%%%%%
%%%%%%%%
function [U]=FE(nelx,nely,x,penal)
[KE] = lk;
K = sparse(2*(nelx+1)*(nely+1), 2*(nelx+1)*(nely+1));
F = sparse(2*(nely+1)*(nelx+1),2); U = zeros(2*(nely+1)*(nelx+1),2);
for elx = 1:nelx

```

```

for ely = 1:nely
    n1 = (nely+1)*(elx-1)+ely;
    n2 = (nely+1)* elx +ely;
    edof = [2*n1-1; 2*n1; 2*n2-1; 2*n2; 2*n2+1; 2*n2+2; 2*n1+1; 2*n1+2];
    K(edof,edof) = K(edof,edof) + x(ely,elx)^penal*KE;
end
end
% DEFINE LOADS AND SUPPORTS (HALF MBB-BEAM)
% F(2,1) = -1;
% fixeddofs = union([1:2*(nely+1)],[2*(nelx+1)*(nely+1)]);

%**** my forces and BC Donald Harby
mid_x=round(2*nelx/6);
F(2*(mid_x)*(nely+1)+2,1)=-1;
F(2*(mid_x-12)*(nely+1)+2,2)=.25;
fixeddofs=[2*(nely+1)-1 2*(nely+1) 2*(nelx+1)*(nely+1)-1 2*(nelx+1)*(nely+1)];
%*****

alldofs = [1:2*(nely+1)*(nelx+1)];
freedofs = setdiff(alldofs,fixeddofs);
% SOLVING
U(freedofs,:) = K(freedofs,freedofs) \ F(freedofs,:);
U(fixeddofs,:)= 0;
%%%%%%%%%%%%% ELEMENT STIFFNESS
MATRIX %%%%%%%%%%%%%%
%%%%%%%%%
function [KE]=lk
E = 1.;
nu = 0.3;
k=[ 1/2-nu/6  1/8+nu/8 -1/4-nu/12 -1/8+3*nu/8 ...
    -1/4+nu/12 -1/8-nu/8  nu/6  1/8-3*nu/8];
KE = E/(1-nu^2)*[ k(1) k(2) k(3) k(4) k(5) k(6) k(7) k(8)
    k(2) k(1) k(8) k(7) k(6) k(5) k(4) k(3)
    k(3) k(8) k(1) k(6) k(7) k(4) k(5) k(2)
    k(4) k(7) k(6) k(1) k(8) k(3) k(2) k(5)
    k(5) k(6) k(7) k(8) k(1) k(2) k(3) k(4)
    k(6) k(5) k(4) k(3) k(2) k(1) k(8) k(7)
    k(7) k(4) k(5) k(2) k(3) k(8) k(1) k(6)
    k(8) k(3) k(2) k(5) k(4) k(7) k(6) k(1)];
%
%%%%%%%%%%%%%
%%%%%%%%%
% This Matlab code was written by Ole Sigmund, Department of Solid %

```

```

% Mechanics, Technical University of Denmark, DK-2800 Lyngby,
Denmark.    %
% Please sent your comments to the author: sigmund@fam.dtu.dk    %
%                                     %
% The code is intended for educational purposes and theoretical details    %
% are discussed in the paper                                     %
% "A 99 line topology optimization code written in Matlab"    %
% by Ole Sigmund (2001), Structural and Multidisciplinary Optimization,    %
% Vol 21, pp. 120--127.                                     %
%                                     %
% The code as well as a postscript version of the paper can be    %
% downloaded from the web-site: http://www.topopt.dtu.dk    %
%                                     %
% Disclaimer:                                     %
% The author reserves all rights but does not guaranty that the code is    %
% free from errors. Furthermore, he shall not be liable in any event    %
% caused by the use of the program.                                     %
%%%%%%%%%%%%%%%%%%%%%%%%%%%%%%%%%%%%%%%%%%%%%%%%%%%%%%%%%%%%%%%%%%%%%%%%
%%%%%%%%%%%%%%%%%%%%%%%%%%%%%%%%%%%%%%%%%%%%%%%%%%%%%%%%%%%%%%%%%%%%%%%%

```


Appendix E: MATLAB Program PSO of MMT Base 3D

```
%*****Continous Constrained Optimization
% Test and generates the branches for the 3D case
% of a typical MMT Base structure
% Saves the data for NN testing
%-----
clear all
close all
global X b h d enac num_ele nn_save nu_sol nu_fea P T LOAD
LOAD=[5 2 100; 6 2 -1200;19 2 -1200;20 2 100];
nn_save=0;
nu_sol=0;
nu_fea=1;
b=36;
h=12;
d=12;
X=zeros(4,3);
X(2,2)=h; X(4,2)=h;
X(3,3)=d; X(4,3)=d;

enac=6; % number of elements across the top
% set the number of extra elements
num_ele=0;

%set optimazation options
% options =
optimset('LargeScale','off','DiffMaxChange',.5,'DiffMinChange',0.005,'Diagnostics',
'off','Display','off','TolFun',0.1,'TolCon',0.01,'TolX',0.05);
options =
optimset('LargeScale','off','DiffMaxChange',1,'DiffMinChange',0.005,'Diagnostics',
'off','Display','off','TolFun',2.0,'TolCon',0.01,'TolX',0.1);

%% optimize with no extra elements
LB = zeros(24,1);
UB = ones(24,1);
%test worst case for feasible solution
if mynonlin_cons_1(UB) <= 0
    nn_save=1;
    nu_sol=nu_sol+1;
    disp('foo')
    %          x0=mypso;
```

```

        x0=LB+.5;
%        options =
optimset('LargeScale','off','DiffMaxChange',.5,'DiffMinChange',0.005,'Diagnostics'
,'off','Display','off','TolFun',0.1,'TolCon',0.01,'TolX',0.05);
        [fx, fval, exitflag, output, lambda] =
fmincon('obj_3d_1',x0,[],[],[],[],LB,UB,'mynonlin_cons_1',options);
        nn_save=0;
end
%% end no extra elements

%% optimize with one extra elements
% set the number of extra elements
num_ele=1;
clear x0 UB LB;
LB = zeros(26,1);
UB = ones(26,1);
for xi=1:(enac+1)
    X(1,1)=0;
    for xj=1:(enac+1)

        %test worst case for feasible solution

        if mynonlin_cons_1(UB) <= 0
            nn_save=1;
            nu_sol=nu_sol+1;
            disp('foo2')
            %            x0=mypso;
            x0=LB+.5;
%            options =
optimset('LargeScale','off','DiffMaxChange',.5,'DiffMinChange',0.005,'Diagnostics'
,'off','Display','off','TolFun',0.1,'TolCon',0.01,'TolX',0.05);
            %[fx, fval, exitflag, output, lambda] =
fmincon('obj_3d_1',x0,[],[],[],[],LB,UB,'mynonlin_cons_1',options);

            nn_save=0;
            end

            X(1,1)=X(1,1)+b/enac;
        end
        X(2,1)=X(2,1)+b/enac;
    end
    X(1,1)=0;X(2,1)=0;
%% end one extra elements

```

```

%% optimize with two extra elements
% set the number of extra elements
num_ele=2;
clear x0 UB LB;
LB = zeros(28,1);
UB = ones(28,1);
for xi=1:(enac+1)
    X(1,1)=0;
    for xj=1:(enac+1)
        X(3,1)=0;
        for xii=1:(enac+1)
            X(4,1)=0;
            for xjj=1:(enac+1)

                %test worst case for feasible solution

                if mynonlin_cons_1(UB) <= 0
                    clear P T;
                    global P T
                    P=zeros(100,28);
                    T=zeros(100,14);
                    nu_fea=1;
                    nn_save=1;
                    nu_sol=nu_sol+1
                    x0=mypso(LB);
                    x0=x0';
                    mynonlin_cons_1(UB);
                    mynonlin_cons_1(LB);
                    %x0=LB+.5;
                    %
                    options =
optimset('LargeScale','off','DiffMaxChange',.5,'DiffMinChange',0.005,'Diagnostics'
,'off','Display','off','TolFun',0.1,'TolCon',0.01,'TolX',0.05);
                    [fx, fval, exitflag, output, lambda] =
fmincon('obj_3d_1',x0,[],[],[],LB,UB,'mynonlin_cons_1',options);
                    xtemp=[X(1,1) X(2,1) X(3,1) X(4,1)];
                    save(strcat('X',num2str(nu_sol)),'X','-ascii');
                    save(strcat('P',num2str(nu_sol)),'P','-ascii');
                    save(strcat('T',num2str(nu_sol)),'T','-ascii');
                    sol(nu_sol)=fval;
                    nn_save=0;
                end
            end
        end
    end
end

```

```

        X(4,1)=X(4,1)+b/enac;
    end
    X(3,1)=X(3,1)+b/enac;
end

    X(1,1)=X(1,1)+b/enac;
end
    X(2,1)=X(2,1)+b/enac;
end
X(1,1)=0;X(2,1)=0;X(3,1)=0;X(4,1)=0;
%save the solutions
save sol.txt sol -ascii;


%plot final topo.
[x, ielem]=mymesh;

nnode=size(x,1);% nnode=total number of nodes
nel=size(ielem,1);% nel=total number of elements
figure(1)
title('3D MMT BASE')
xlabel('X'), ylabel('Y'), zlabel('Z')
hold('on')
grid('on')
XYZ=zeros(nel,3);

for i = 1:nel;
    XYZ(1,1:3)=x(ielem(i,1),1:3);
    XYZ(2,1:3)=x(ielem(i,2),1:3);
    plot3(XYZ(1:2,1),XYZ(1:2,2),XYZ(1:2,3),'k')
end
LOAD([1 4],3)=LOAD([1 4],3)*6;
nload=size(LOAD,1); i11=0;
for i1=1:nload
    if LOAD(i1,2)==1, i11=i11+1; load(i11,1:3)=[LOAD(i1,3),0,0]; y(i11)=i1;
    elseif LOAD(i1,2)==2, i11=i11+1; load(i11,1:3)=[0,LOAD(i1,3),0]; y(i11)=i1;
    elseif LOAD(i1,2)==3, i11=i11+1; load(i11,1:3)=[0,0,LOAD(i1,3)]; y(i11)=i1;
    end
end
end
if i11>=1,

```

```

x=[1:i11];
quiver3([LOAD(1,1)*6-6;LOAD(2,1)*6-6;(LOAD(3,1)-15)*6;(LOAD(4,1)-
15)*6],[12; 12;12;12],[0; 0;12;12],load(x,1),load(x,2),load(x,3),'r')
end

```

```

function pbest=mypso(L)
% the pso for the 3D base
global X b h d enac num_ele nn_save nu_sol P T nu_fea
%pass the following to the function once it works
wmax=0.9;
wmin=0.4;
itmax=4;
errmax=.0001;
c1=1.5;
c2=1.5;
N=50;
D=size(L,1);

```

```

% for i=1:itmax
% W(i)=wmax-((wmax-wmin)/itmax)*i;
% end

```

```

i=1:itmax;
W=wmax-((wmax-wmin)/itmax)*i;

```

```

% Initialization of positions
a=0;
b=1;
x=a+(b-a)*rand(N,D,1);

```

```

for i=1:N
F(i,1)=myext_penalty(x(i,:));
end

```

```

[C,l]=min(abs(F(:,1)));
pB=C;
gB=pB;
XX(1,1)=l;
gbest(1,:)=x(l,:);
pbest=gbest;
for i=1:N
V=c1*rand*(pbest-x(i,:))+c2*rand*(gbest-x(i,:));

```

```

    x(i,:)=x(i,:)+V;
end

jj=0;
while jj<itmax

    for i=1:N
        x(i,:)=myclamped(x(i,:),0,1);

        F(i,1)=myext_penalty(x(i,:));
    end
    [C,l]=min(abs(F(:,1)));
    gbest(1,:)=x(l,:);
    gB=C;

    for i=1:N
        V=W(jj+1)*c1*rand*(pbest-x(i,:))+c2*rand*(gbest-x(i,:));
        x(i,:)=x(i,:)+V;
    end
    if gB<pB
        pB=gB;
        pbest=gbest;
    end

    jj=jj+1;
    %sol(jj,1:(D+1))=[pB pbest'];
end

function [c, ceq] = mynonlin_cons_1(L)
% this function take cross sectional data L2 and t
% and returns the deflection and natural freq of the
% structure
% ***** this is for the 3D case *****
global X b h d enac num_ele nn_save nu_sol P T nu_fea LOAD
%remove the following after testing
b=36;
h=12;
d=12;
enac=6;

nenode=2;% nenode = number of nodes/element
ndof=6;% ndof=number of degrees of freedom/node

```

```

%mesh the model
[x, ielem]=mymesh;
%get element properties
eleprop=myeleprop(L);

nnode=size(x,1);% nnode=total number of nodes
nel=size(ielem,1);% nel=total number of elements
%
%set BC and loads
BC=zeros(nnode,ndof); %zero=free 1=fixed
BC([enac+2 (enac+1)*2 3*enac+4 (enac+1)*4],1:6)=1;
%BC([enac+2 tot_ele+2],1:6)=1;
BC(1:nnode,3:5)=1;

% LOAD is now global
% LOAD=[4 2 75; 5 2 -700;18 2 -700;19 2 75];
F(1:nnode*ndof)=0;

XYZ=zeros(nel,3);
K=zeros(nnode*ndof,nnode*ndof);
M=zeros(nnode*ndof,nnode*ndof);

%element and cs data for book example delete for final
% use the Lsection program to replace
% Set up all the constants
E=30e6;
G=11.5e6;
rho=0.286;

%get element stiffness matrices then put in global stiffness matrix
% set the lumped mass matrix
for i = 1:nel;
    A=eleprop(i,1);
    ly=eleprop(i,2);
    lz=eleprop(i,3);
    J=eleprop(i,4);

    k=mystiff(E,G,A,ly,lz,J,x(ielem(i,1),1),x(ielem(i,1),2),x(ielem(i,1),3),x(ielem(i,2),1),
    x(ielem(i,2),2),x(ielem(i,2),3));

    m=mymass(rho,A,x(ielem(i,1),1),x(ielem(i,1),2),x(ielem(i,1),3),x(ielem(i,2),1),x(ielem(i,2),2),x(ielem(i,2),3));

```

```

    M=myassemble(M,m,ielem(i,1),ielem(i,2));
    K=myassemble(K,k,ielem(i,1),ielem(i,2));
end

% compute and assemble element load vector force vector
i2=1;i3=1;
for i = 1:nnode;%loop thru each node
    for i1=1:ndof;%loop thru each dof in the node
        if BC(i,i1) == 0;
            %set up book keeping for partition
            bk(i3)=i2;
            i3=i3+1;
        end
        i2=i2+1;
    end
end
% Insert forces into global force vector
for i=1:size(LOAD,1);
    F((LOAD(i,1)-1)*6+LOAD(i,2))=LOAD(i,3);
end
%partition the system of eq.
m=zeros(size(bk,2),size(bk,2));
k=zeros(size(bk,2),size(bk,2));
f(1:size(bk,2))=0;
for i=1:size(bk,2);
    for i1=1:size(bk,2);
        m(i,i1)=M(bk(i),bk(i1));
        k(i,i1)=K(bk(i),bk(i1));
    end
    f(i)=F(bk(i));
end
%

%solve for 1st natural frequency
w=eig(k,m);
w1=sqrt(abs(w(1)));

%solve for displacements
u=k\l'f';

%Setup Global Nodal Displacement Vector
U(1:nnode*ndof)=0;
for i=1:size(bk,2);

```



```

    U(bk(i))=u(i);
end

%calculate the global nodal force vector
F=K*U';

%set max deflection and natural freq.
md=0.005;mf=40;
% nonlinear inequality constraints returned as vector c

for i=1:(enac+1)
    ydisp(i)=U((i-1)*6+2);
    ydisp(i+(enac+1))=U(((i+(2*enac+3))-2)*6+2);
end

if nn_save==1
    P(nu_fea,:)=L';
    T(nu_fea,:)=ydisp;
    nu_fea=nu_fea+1;
end

c=max(abs(ydisp))-md;

% nonlinear equality constraints returned as vector ceq
ceq = []; % there are no nonlinear equality
           % constraints in this problem

% This function test the best topo branches
% Using discreet values for standard steel
% members it can use NN or FEA It can
% train NN using previous weights and bias
% of generate new.
% ***** CAution!!! it will take
% forever to solve using FEA weeks or months for
% simple problems !!! use the NN
clear all
close all
global X b h d enac num_ele nn_save nu_sol nu_fea P T LOAD
nn_save=0;
LOAD=[5 2 100; 6 2 -1200;19 2 -1200;20 2 100];

%** set hidden layer size factor
hls=1.5;

```

```

%*** get input from user
pretrain=input('pretrain NN? 1=yes 0=no');
useNN=input('use NN? 1=yes 0=no');

nu_sol=0;
nu_fea=1;
enac=6; % number of elements across the top
% set the number of extra elements
num_ele=2;

%load and sort the continuous sol. for each branch
load sol.txt -ascii;
[Y,I]=sort(sol);
sol_temp=10000;

j=1;
cpu_seconds=0;
while sol_temp>sol(j)
i=I(j);
p=load(strcat('P',num2str(i)),'-ascii');
t=load(strcat('T',num2str(i)),'-ascii');
topo=load(strcat('X',num2str(i)),'-ascii');
P=p';
T=t';
T=[T(2:6,:);T(9:13,:)];
X=topo
clear t p topo;

if useNN == 1 %*** test if NN *****
% ***** build NN and train *****
minP=min(P');
maxP=max(P');
PR=[minP',maxP'];
layer1=round(1.5*size(P,1));
layer2=round(layer1/2);
outlayer=size(T,1);
%net = newff(PR,[layer1 outlayer],{'logsig','tansig'},'traincgf');
net = newff(PR,[layer1 layer2 outlayer],{'tansig', 'logsig','purelin'},'trainrp');
%net.trainParam.mem_reduc=4;
net.trainParam.goal=1e-7;
net.trainParam.show=100;
net.trainParam.epochs=3000;

```

```

if pretrain > 0
% load previous NN weights and bias
    load -ascii pw1.txt;net.IW{1,1}=pw1;
    load -ascii pw2.txt;net.LW{2,1}=pw2;
    load -ascii pw3.txt;net.LW{3,2}=pw3;
    load -ascii pb1.txt;net.b{1,1}=pb1;
    load -ascii pb2.txt;net.b{2,1}=pb2;
    load -ascii pb3.txt;net.b{3,1}=pb3;
    net = newff(PR,[layer1 layer2 outlayer],{'tansig', 'logsig','purelin'},'trainrp');
    net.trainParam.goal=1e-10;
    net.trainParam.epochs=2000;
end %***** end pretrain *****
%***** train network *****
net=train(net,P,T);
pretrain=2;%***** use pretrained data for future test ***
%***** finish build and train the NN *****

close all
% save the weights and bias for later
    w1=net.IW{1,1};
    w2=net.LW{2,1};
    w3=net.LW{3,2};
    b1=net.b{1,1};
    b2=net.b{2,1};
    b3=net.b{3,1};
    save pw1.txt w1 -ascii;
    save pw2.txt w2 -ascii;
    save pw3.txt w3 -ascii;
    save pb1.txt b1 -ascii;
    save pb2.txt b2 -ascii;
    save pb3.txt b3 -ascii;
end %***** end NN test *****

%***** test each branch *****
k=0; cpu0=cputime;
for k1=1:3
    for k2=1:3
        for k3=1:3
            for k4=1:3
                for k5=1:3
                    for k6=1:3
                        for k7=1:3

```



```

        end
    end
end
end
end
end
end
end
end
j=j+1;
cpu1=cputime;cpu_seconds=cpu_seconds+(cpu1-cpu0)
end %end the while
%plot final topo.
X=dX
[x, ielem]=mymesh;

nnode=size(x,1);% nnode=total number of nodes
nel=size(ielem,1);% nel=total number of elements
figure(1)
title('3D MMT BASE')
xlabel('X'), ylabel('Y'), zlabel('Z')
hold('on')
grid('on')
XYZ=zeros(nel,3);

for i = 1:nel;
    XYZ(1,1:3)=x(ielem(i,1),1:3);
    XYZ(2,1:3)=x(ielem(i,2),1:3);
    plot3(XYZ(1:2,1),XYZ(1:2,2),XYZ(1:2,3),'k')
end
LOAD([1 4],3)=LOAD([1 4],3)*6;
nload=size(LOAD,1); i11=0;
for i1=1:nload
    if LOAD(i1,2)==1, i11=i11+1; load(i11,1:3)=[LOAD(i1,3),0,0]; y(i11)=i1;
    elseif LOAD(i1,2)==2, i11=i11+1; load(i11,1:3)=[0,LOAD(i1,3),0]; y(i11)=i1;
    elseif LOAD(i1,2)==3, i11=i11+1; load(i11,1:3)=[0,0,LOAD(i1,3)]; y(i11)=i1;
    end
end
if i11>=1,
    x=[1:i11];
    quiver3([LOAD(1,1)*6-6;LOAD(2,1)*6-6;(LOAD(3,1)-15)*6;(LOAD(4,1)-
15)*6],[12; 12;12;12],[0; 0;12;12],load(x,1),load(x,2),load(x,3),'r')
end

```

Appendix F: MATLAB Program Used to Generate AutoLISP Program Lspgen.m

```
global X b h d enac num_ele

%uncomment the following for testing
b=36;
h=12;
d=12;
num_ele=2;enac=6;

fid = fopen('exp.lsp','w');
X=[30 0 0;36 12 0;24 0 12;24 12 0];
cs=[3 1 3 1 3 1 3 1 3 2 2 3 2 3];
[x, ielem]=mymesh;
nnode=size(x,1);% nnode=total number of nodes
nel=size(ielem,1);% nel=total number of elements
j=1;jj=1;
for i=1:nel
    if i<=(enac*4)
        elecs=cs(j);
        jj=jj+1;
        if jj==enac+1;
            jj=1;
            j=j+1;
        end
    end
    if i>(enac*4)
        elecs=cs(j);
        if ((i>(enac*4)+8) & (i<=(enac*4)+10))
            elecs=1;
        else
            j=j+1;
        end
    end
end

x1=x(ielem(i,1),:);
x2=x(ielem(i,2),:);
fprintf(fid, '(setq pt1 \047(%s) pt2 \047(%s))\n', num2str(x1), num2str(x2));
fprintf(fid, '(command \"ucs\" \"n\" \"za\" pt1 pt2)\n');
fprintf(fid, '(command \"insert\" \"%s\" \"0,0,0\" \"\" \"\" \"\")\n', num2str(elecs));
fprintf(fid, '(vl-cmdf \"explode\" (entlast))\n');
```

```
    fprintf(fid,'(vl-cmdf \"extrude\" (entlast) \"\" (distance pt1 pt2) \"\")\n');  
    fprintf(fid,'(command \"ucs\" \"w\")\n\n');  
end  
fprintf(fid,'(command \"union\" \"all\" \"\")\n\n');  
fclose(fid);
```

Appendix G: Sample AutoLISP Code Generated from MATLAB Exp.lsp

```
(setq pt1 '(0 12 0) pt2 '(6 12 0))  
(command "ucs" "n" "za" pt1 pt2)  
(command "insert" "3" "0,0,0" "" "" "")  
(vl-cmdf "explode" (entlast))  
(vl-cmdf "extrude" (entlast) "" (distance pt1 pt2) "")  
(command "ucs" "w")
```

```
(setq pt1 '(6 12 0) pt2 '(12 12 0))  
(command "ucs" "n" "za" pt1 pt2)  
(command "insert" "3" "0,0,0" "" "" "")  
(vl-cmdf "explode" (entlast))  
(vl-cmdf "extrude" (entlast) "" (distance pt1 pt2) "")  
(command "ucs" "w")
```

```
(setq pt1 '(12 12 0) pt2 '(18 12 0))  
(command "ucs" "n" "za" pt1 pt2)  
(command "insert" "3" "0,0,0" "" "" "")  
(vl-cmdf "explode" (entlast))  
(vl-cmdf "extrude" (entlast) "" (distance pt1 pt2) "")  
(command "ucs" "w")
```

```
(setq pt1 '(18 12 0) pt2 '(24 12 0))  
(command "ucs" "n" "za" pt1 pt2)  
(command "insert" "3" "0,0,0" "" "" "")  
(vl-cmdf "explode" (entlast))  
(vl-cmdf "extrude" (entlast) "" (distance pt1 pt2) "")  
(command "ucs" "w")
```

```
(setq pt1 '(24 12 0) pt2 '(30 12 0))  
(command "ucs" "n" "za" pt1 pt2)  
(command "insert" "3" "0,0,0" "" "" "")  
(vl-cmdf "explode" (entlast))  
(vl-cmdf "extrude" (entlast) "" (distance pt1 pt2) "")  
(command "ucs" "w")
```

```
(setq pt1 '(30 12 0) pt2 '(36 12 0))  
(command "ucs" "n" "za" pt1 pt2)  
(command "insert" "3" "0,0,0" "" "" "")  
(vl-cmdf "explode" (entlast))
```



```
(vl-cmdf "extrude" (entlast) "" (distance pt1 pt2) "")  
(command "ucs" "w")
```

```
(setq pt1 '(0 0 0) pt2 '(6 0 0))  
(command "ucs" "n" "za" pt1 pt2)  
(command "insert" "1" "0,0,0" "" "" "")  
(vl-cmdf "explode" (entlast))  
(vl-cmdf "extrude" (entlast) "" (distance pt1 pt2) "")  
(command "ucs" "w")
```

```
(setq pt1 '(6 0 0) pt2 '(12 0 0))  
(command "ucs" "n" "za" pt1 pt2)  
(command "insert" "1" "0,0,0" "" "" "")  
(vl-cmdf "explode" (entlast))  
(vl-cmdf "extrude" (entlast) "" (distance pt1 pt2) "")  
(command "ucs" "w")
```

```
(setq pt1 '(12 0 0) pt2 '(18 0 0))  
(command "ucs" "n" "za" pt1 pt2)  
(command "insert" "1" "0,0,0" "" "" "")  
(vl-cmdf "explode" (entlast))  
(vl-cmdf "extrude" (entlast) "" (distance pt1 pt2) "")  
(command "ucs" "w")
```

```
(setq pt1 '(18 0 0) pt2 '(24 0 0))  
(command "ucs" "n" "za" pt1 pt2)  
(command "insert" "1" "0,0,0" "" "" "")  
(vl-cmdf "explode" (entlast))  
(vl-cmdf "extrude" (entlast) "" (distance pt1 pt2) "")  
(command "ucs" "w")
```

```
(setq pt1 '(24 0 0) pt2 '(30 0 0))  
(command "ucs" "n" "za" pt1 pt2)  
(command "insert" "1" "0,0,0" "" "" "")  
(vl-cmdf "explode" (entlast))  
(vl-cmdf "extrude" (entlast) "" (distance pt1 pt2) "")  
(command "ucs" "w")
```

```
(setq pt1 '(30 0 0) pt2 '(36 0 0))  
(command "ucs" "n" "za" pt1 pt2)  
(command "insert" "1" "0,0,0" "" "" "")  
(vl-cmdf "explode" (entlast))  
(vl-cmdf "extrude" (entlast) "" (distance pt1 pt2) "")
```

```
(command "ucs" "w")
```

```
(setq pt1 '(0 12 12) pt2 '(6 12 12))  
(command "ucs" "n" "za" pt1 pt2)  
(command "insert" "3" "0,0,0" "" "" "")  
(vl-cmdf "explode" (entlast))  
(vl-cmdf "extrude" (entlast) "" (distance pt1 pt2) "")  
(command "ucs" "w")
```

```
(setq pt1 '(6 12 12) pt2 '(12 12 12))  
(command "ucs" "n" "za" pt1 pt2)  
(command "insert" "3" "0,0,0" "" "" "")  
(vl-cmdf "explode" (entlast))  
(vl-cmdf "extrude" (entlast) "" (distance pt1 pt2) "")  
(command "ucs" "w")
```

```
(setq pt1 '(12 12 12) pt2 '(18 12 12))  
(command "ucs" "n" "za" pt1 pt2)  
(command "insert" "3" "0,0,0" "" "" "")  
(vl-cmdf "explode" (entlast))  
(vl-cmdf "extrude" (entlast) "" (distance pt1 pt2) "")  
(command "ucs" "w")
```

```
(setq pt1 '(18 12 12) pt2 '(24 12 12))  
(command "ucs" "n" "za" pt1 pt2)  
(command "insert" "3" "0,0,0" "" "" "")  
(vl-cmdf "explode" (entlast))  
(vl-cmdf "extrude" (entlast) "" (distance pt1 pt2) "")  
(command "ucs" "w")
```

```
(setq pt1 '(24 12 12) pt2 '(30 12 12))  
(command "ucs" "n" "za" pt1 pt2)  
(command "insert" "3" "0,0,0" "" "" "")  
(vl-cmdf "explode" (entlast))  
(vl-cmdf "extrude" (entlast) "" (distance pt1 pt2) "")  
(command "ucs" "w")
```

```
(setq pt1 '(30 12 12) pt2 '(36 12 12))  
(command "ucs" "n" "za" pt1 pt2)  
(command "insert" "3" "0,0,0" "" "" "")  
(vl-cmdf "explode" (entlast))  
(vl-cmdf "extrude" (entlast) "" (distance pt1 pt2) "")  
(command "ucs" "w")
```

```
(setq pt1 '(0 0 12) pt2 '(6 0 12))
(command "ucs" "n" "za" pt1 pt2)
(command "insert" "1" "0,0,0" "" "" "")
(vl-cmdf "explode" (entlast))
(vl-cmdf "extrude" (entlast) "" (distance pt1 pt2) "")
(command "ucs" "w")
```

```
(setq pt1 '(6 0 12) pt2 '(12 0 12))
(command "ucs" "n" "za" pt1 pt2)
(command "insert" "1" "0,0,0" "" "" "")
(vl-cmdf "explode" (entlast))
(vl-cmdf "extrude" (entlast) "" (distance pt1 pt2) "")
(command "ucs" "w")
```

```
(setq pt1 '(12 0 12) pt2 '(18 0 12))
(command "ucs" "n" "za" pt1 pt2)
(command "insert" "1" "0,0,0" "" "" "")
(vl-cmdf "explode" (entlast))
(vl-cmdf "extrude" (entlast) "" (distance pt1 pt2) "")
(command "ucs" "w")
```

```
(setq pt1 '(18 0 12) pt2 '(24 0 12))
(command "ucs" "n" "za" pt1 pt2)
(command "insert" "1" "0,0,0" "" "" "")
(vl-cmdf "explode" (entlast))
(vl-cmdf "extrude" (entlast) "" (distance pt1 pt2) "")
(command "ucs" "w")
```

```
(setq pt1 '(24 0 12) pt2 '(30 0 12))
(command "ucs" "n" "za" pt1 pt2)
(command "insert" "1" "0,0,0" "" "" "")
(vl-cmdf "explode" (entlast))
(vl-cmdf "extrude" (entlast) "" (distance pt1 pt2) "")
(command "ucs" "w")
```

```
(setq pt1 '(30 0 12) pt2 '(36 0 12))
(command "ucs" "n" "za" pt1 pt2)
(command "insert" "1" "0,0,0" "" "" "")
(vl-cmdf "explode" (entlast))
(vl-cmdf "extrude" (entlast) "" (distance pt1 pt2) "")
(command "ucs" "w")
```

```
(setq pt1 '(0 12 0) pt2 '(0 0 0))
(command "ucs" "n" "za" pt1 pt2)
(command "insert" "3" "0,0,0" "" "" "")
(vl-cmdf "explode" (entlast))
(vl-cmdf "extrude" (entlast) "" (distance pt1 pt2) "")
(command "ucs" "w")
```

```
(setq pt1 '(36 12 0) pt2 '(36 0 0))
(command "ucs" "n" "za" pt1 pt2)
(command "insert" "1" "0,0,0" "" "" "")
(vl-cmdf "explode" (entlast))
(vl-cmdf "extrude" (entlast) "" (distance pt1 pt2) "")
(command "ucs" "w")
```

```
(setq pt1 '(0 12 12) pt2 '(0 0 12))
(command "ucs" "n" "za" pt1 pt2)
(command "insert" "3" "0,0,0" "" "" "")
(vl-cmdf "explode" (entlast))
(vl-cmdf "extrude" (entlast) "" (distance pt1 pt2) "")
(command "ucs" "w")
```

```
(setq pt1 '(36 12 12) pt2 '(36 0 12))
(command "ucs" "n" "za" pt1 pt2)
(command "insert" "1" "0,0,0" "" "" "")
(vl-cmdf "explode" (entlast))
(vl-cmdf "extrude" (entlast) "" (distance pt1 pt2) "")
(command "ucs" "w")
```

```
(setq pt1 '(0 12 0) pt2 '(0 12 12))
(command "ucs" "n" "za" pt1 pt2)
(command "insert" "3" "0,0,0" "" "" "")
(vl-cmdf "explode" (entlast))
(vl-cmdf "extrude" (entlast) "" (distance pt1 pt2) "")
(command "ucs" "w")
```

```
(setq pt1 '(0 0 0) pt2 '(0 0 12))
(command "ucs" "n" "za" pt1 pt2)
(command "insert" "2" "0,0,0" "" "" "")
(vl-cmdf "explode" (entlast))
(vl-cmdf "extrude" (entlast) "" (distance pt1 pt2) "")
(command "ucs" "w")
```

```
(setq pt1 '(36 12 0) pt2 '(36 12 12))
```

```
(command "ucs" "n" "za" pt1 pt2)
(command "insert" "2" "0,0,0" "" "" "")
(vl-cmdf "explode" (entlast))
(vl-cmdf "extrude" (entlast) "" (distance pt1 pt2) "")
(command "ucs" "w")
```

```
(setq pt1 '(36 0 0) pt2 '(36 0 12))
(command "ucs" "n" "za" pt1 pt2)
(command "insert" "3" "0,0,0" "" "" "")
(vl-cmdf "explode" (entlast))
(vl-cmdf "extrude" (entlast) "" (distance pt1 pt2) "")
(command "ucs" "w")
```

```
(setq pt1 '(18 12 0) pt2 '(18 0 12))
(command "ucs" "n" "za" pt1 pt2)
(command "insert" "1" "0,0,0" "" "" "")
(vl-cmdf "explode" (entlast))
(vl-cmdf "extrude" (entlast) "" (distance pt1 pt2) "")
(command "ucs" "w")
```

```
(setq pt1 '(18 0 0) pt2 '(18 12 12))
(command "ucs" "n" "za" pt1 pt2)
(command "insert" "1" "0,0,0" "" "" "")
(vl-cmdf "explode" (entlast))
(vl-cmdf "extrude" (entlast) "" (distance pt1 pt2) "")
(command "ucs" "w")
```

```
(setq pt1 '(30 12 0) pt2 '(36 0 0))
(command "ucs" "n" "za" pt1 pt2)
(command "insert" "2" "0,0,0" "" "" "")
(vl-cmdf "explode" (entlast))
(vl-cmdf "extrude" (entlast) "" (distance pt1 pt2) "")
(command "ucs" "w")
```

```
(setq pt1 '(24 12 12) pt2 '(24 0 12))
(command "ucs" "n" "za" pt1 pt2)
(command "insert" "3" "0,0,0" "" "" "")
(vl-cmdf "explode" (entlast))
(vl-cmdf "extrude" (entlast) "" (distance pt1 pt2) "")
(command "ucs" "w")
```

```
(command "union" "all" "")
```

VITA

Donald Harby was born on January 13, 1967, in St. Louis, MO. After graduating from Wellsville-Middletown High School in Wellsville, MO in 1985, he received a B.S. in Aeronautical Engineering from St. Louis University in 1991. He worked as a carpenter and construction manager from 1991 to 1993.

In the fall of 1993, he worked as an electrical engineering technician for the department of Agricultural Engineering at the University of Missouri – Columbia. In 1993 he also started to pursue graduate studies in engineering at the University of Missouri – Columbia. He received his M.S. degree in Agricultural/Biological Engineering in 2002.

From 1995 to 1999 he worked as a mechanical design engineer for Midwayusa and Battenfeld Technologies in Columbia, MO. He worked as an instructor for Linn State Technical College from 1999 to 2006 at the advanced technology center (ATC) in Mexico, MO. While at Linn State Technical College he helped start the ATC and helped develop three new associate of applied science degree programs.

In the fall of 2003, he entered in the Ph.D. program at the University of Missouri – Columbia under Dr. Yuyi Lin. He received the GAANN fellowship in Mechanical Engineering in 2003.

In the fall of 2006, he was appointed assistant professor at the University of Central Missouri. He is currently program coordinator of all engineering technology programs at the University of Central Missouri. In the spring of 2007 he was awarded, as principle investigator, a grant with a total budget of over \$750,000 from the Society of Manufacturing Engineers. The grant will be used to create an advanced manufacturing research center at the University of Central Missouri.

Accepted Publications:

Harby, D., Polastri, P., and Chakapoing, C., “A New Approach to Teaching Programmable Logic Controllers” *ASEE Annual Conference and Exposition*, June 2007, Honolulu, HI

Naylor, J.B., R.L. Kallenbach, D.W. Harby, and D.J. England., Automated harvester reduces labor for sampling pastures. Abst. #26010 In *Agronomy Abstracts*. ASA, 2006, Madison, WI.

Lin, Y., Harby, D., and Brown, D. “Dynamic Modeling and Experimental Verification of Helical Spring with Variable Pitch”, *15th International*

Mechanisms and Machine Science Conference, Aug. 2006, Yin Chuan, China

Lin, Y. and Harby, D. "Web-based Tools and Course Materials for Teaching Capstone Design Internationally", *Proceedings ASEE Annual Conference and Exposition*, June 2006, Chicago, IL

Harby, D. and Lin, Y. "A New Approach to Modular Machine Tool Control System Design", *3rd SME Int. Conf. On Manufacturing Education*, June 2005, San Luis Obispo, CA

Lin, Y., Harby, D., Jang, D., and Ye, Z. "Capstone Design Education in Globalization Environment", *3rd SME Int. Conf. On Manufacturing Education*, June 2005, San Luis Obispo, CA

Lin, Y. and Harby, D. "Problems and Solutions in Internationalizing Capstone Design", *Proceedings ASEE Annual Conference and Exposition*, June 2005, Portland, OE

Lin, Y., Harby, D., Cai, X., and Walker, M. "Experimental Study of Dynamic Performance for Helical Spring with Variable Pitch", *14th Chinese National Mechanism Conference*, July 2004, Chongqing, China

Lin, Y., Harby, D., Jang, D., and Zheng, W., "Teaching Capstone Design in the Globalization Environment", *Proceedings ASEE Annual Conference and Exposition*, June 2004, Salt Lake City, UT

Lin, Y., Harby, D., Zhen, W., and Jang, D., "Internationalizing the Capstone Design Course", *ASEE Proceedings 38th Midwest Section Meeting*, Sept. 2003, Rolla, MO

Cai, X., Harby, D., and Lin, Y., "Design Perturbation for Improving Manufacturability and Performance", *Proceeding of 20th Annual Conference of Midwest Chinese American Science and Technology Association*, 2003, St. Louis, MO

Lin, Y., Zhang, Y., and Harby, D., "Development of a Digital Case Library for Mechanical Design Education", *Proceedings of Capstone Design Forum*, 2003, Seoul, Korea

THESES

"Implementation of a Real-Time Statistical Process Controller", Masters Thesis, Advisor, Professor Jinglu Tan